NASA TECHNICAL MEMORANDUM

NASA TM X-62,361

NASA TM X-62,361

PERTURBATION SOLUTIONS FOR THE INFLUENCE OF FORWARD FLIGHT ON HELICOPTER ROTOR FLAPPING STABILITY

Wayne Johnson

Ames Research Center
and
U.S. Army Air Mobility R&D Laboratory
Moffett Field, Calif. 94035

August 1974

CONTENTS

PERTURBATION SOLUTIONS FOR THE INFLUENCE OF FORWARD FLIGHT ON HELICOPTER ROTOR FLAPPING STABILITY

By Wayne Johnson*

U. S. Army Air Mobility R&D Laboratory
Moffett Field, Calif., 94035

SUMMARY

The stability of the flapping motion of a helicopter rotor blade in forward flight is investigated, using a perturbation technique which gives analytic expressions for the eigenvalues, including the influence of the periodic aerodynamic forces in forward flight. The perturbation solutions are based on small advance ratio μ (the ratio of the helicopter forward speed to the rotor tip speed). The results are valid to approximately $\mu = 0.5$, which covers the forward speed range of most helicopters. The rotor configurations considered are a single, independent blade; a teetering rotor; a gimballed rotor with three, four, and five or more blades; and a rotor with N independent blades. The eigenvalues of a constant coefficient approximation to the flapping equation are obtained by an expansion in μ, and are compared with the perturbation solution including the periodic coefficients. The constant coefficient approximation with the equations and degrees of freedom in the nonrotating frame represents the flap dynamic reasonably well for the lower frequency modes, although it cannot, of course, be completely correct. The transfer function of the rotor flap response to sinusoidal pitch input is examined, as an alternative to the eigenvalues as a representation of the dynamic characteristics of the flap motion.

INTRODUCTION

The fundamental motion of helicopter rotor blade is flapping motion: first mode out of plane (vertical) displacement from the plane of rotation of the rotor. For an articulated rotor this motion is rigid body rotation of the blade about a hinge at or near the center of rotation. For a cantilever rotor it is elastic bending motion, primarily about flexibility at the blade root. Due to the high centrifugal forces on the blade, the mode shape for first mode bending of a blade with cantilever root restraint is nearly the same as for the rigid body flap motion of a hinged blade; it is the difference in the natural frequencies of the cantilever and articulated blades; that is, of primary significance for the flap dynamics. This flapping motion of the rotor

---

*Research Scientist, Large-Scale Aerodynamics Branch, NASA-Ames Research Center.

has a basic role in helicopter stability and control, blade loads, vibration, and in most other areas of helicopter behavior. An important aspect of helicopter rotor flapping dynamics is the dynamic stability of the motion in forward flight. Besides the question of high speed stability, this topic also is of interest for its implications on the decay of transient motions of the blade, for example, in response to control inputs or aerodynamic gusts. Any significant degradation of the blade stability and response to control due to forward speed will have important effects on all aspects of the helicopter behavior.

In hover (zero forward speed), the aerodynamic forces on the rotor blade provide the flap motion with high damping, hence, good stability and fast response. The motion of the blade in hover is describable by constant coefficient linear differential equations, which may be analyzed to obtain the dynamic behavior by the standard methods of linear system theory. In forward flight however, the aerodynamic forces on the blade introduce time varying - specifically, periodic around the rotor azimuth - coefficients into the linear differential equations describing the flap motion. These periodic coefficients are due to the once-per-revolution variation of the free stream velocity seen by the rotating blade when the helicopter has forward speed. Systems described by periodic coefficient equations require a considerably more involved analysis in order to investigate their stability and response to control. Appendix A discusses the behavior characteristic of periodic coefficient systems, and presents some of the results of the mat' ematical theory of such systems. Often a direct numerical integration of the equations of motion is used as either the most or the only practical solution method; the mathematical theory of periodic coefficient equations has also been used for the analysis of rotor dynamics in forward flight.

The flapping stability of a rotor in forward flight has been investigated in a number of publications (refs. 1-20). The primary reason for the frequent reexamination of this one problem is the search for a satisfactory technique for the treatment of the influence of the periodic coefficients in the differential equations, for even to determine the stability of such an equation is a much more difficult mathematical problem than with constant coefficients. Usually the flap stability has been determined by numerically integrating the equations of motion, and then using the results of Floquet theory to find the eigenvalues (roots) from the transient solution over one period (refs. 2, 4, 5, 7, 10, 12, 13, and 18; the references usually describe the mathematical theory required for the method). There have also been a number of solutions using the methods of perturbation theory (refs. 3, 6, 9, 14-17), using an analog computer to solve the equation (refs. 8, 11, and 20), and a solution using the classical methods of the analysis of Hill's equation (ref. 1). The reverse flow region of the rotor is important in very high speed forward flight, and several investigations have considered the aerodynamics of reverse flow and its impact on the flapping stability (refs. 5, 7, 8, 11, 12, 14, 15, and 19). Pitch/flap coupling of the blade motion is another import factor which has been treated (refs. 2, 3, 8, 12, 14, 15, and 17). A number of the studies have extended the stability analysis by adding other degrees of freedom besides rigid flapping to the blade motion description: flapwise elastic bending of the blade (refs. 4, 5), blade torsion (refs. 5, 9, 11),

blade lag motion (refs. 10, 16), or the flap motion of the other blades of the rotor (ref. 13). There is, however, still work that may be done with just the problem of flapping stability, particularly since most of these studies have only presented numerical results.

This report investigates the effect of forward speed on the helicopter rotor flapping stability and response to control. A solution for the stability is obtained by a perturbation technique which is reasonably straightforward, and which provides analytic expressions for the eigenvalues of the flap motion. The solution method is direct enough so that it is possible to consider here a number of rotor configurations, in addition to the problem of a single independent blade which is the subject of most of the literature. The perturbation method to be used here is known as the method of multiple time scales. It is described briefly in Appendix B, but in fact the method is best discussed by example, of which there will be several here. For more information on the mathematics of this perturbation technique and others, the reader is directed to reference 21 (and to ref. 14, which discusses the techniques specifically in the context of the problem of rotor flapping stability). For the speed range of most helicopters, the advance ratio μ (the ratio of the helicopter forward speed to the rotor tip speed) is a small parameter; a maximum of $\mu = 0.4$ to 0.5 may be assumed. Therefore, a perturbation solution based on small μ may be expected to be applicable over the entire range of interest for most helicopters. Most of the present work will be concerned with the small μ results, although the stability at high μ (around 1.0 to 2.5) will be briefly discussed. For the range of speed involving small advance ratio, $\mu = 0.0$ to 0.5 or so, a perturbation solution to order μ^2 is satisfactory. It is therefore possible to neglect the effects of the reverse flow region on the rotor (since they are of higher order than μ^2 - see ref. 8), which results in a considerable simplification of the aerodynamic forces which must be considered.

With the great difficulties involved in the mathematical analysis of periodic coefficient differential equations, it is natural to consider the use of a constant coefficient approximation to the equations describing the system. That is, the periodic coefficients are replaced by their average values, so the equations of motion are reduced to constant coefficient equations which may be easily analyzed by the standard techniques. The validity and applicability of the constant coefficient approximation to several of the rotor configurations considered here will be investigated. An expansion of the eigenvalues for small μ will be found, for comparison with the perturbation solutions including the periodic coefficients.

The following topics will be considered in this report. First, the stability of the flap motion of an independent blade will be investigated; that is, the case of a rotor with a fixed shaft, so that the motion of any one blade is independent of that of the other blades of the rotor. A perturbation solution (for small μ) will be found for the influence of forward flight on the eigenvalues. This analysis will be followed by a summary, which will collect the results for the eigenvalues. The behavior of these results will be discussed, and examples given of their application. Next the flap stability of a teetering rotor will be investigated, followed by a summary and

discussion of the results. Then a gimballed rotor will be considered, for the cases of three, four, and five or more blades. The description and behavior in the nonrotating frame of a rotor with N independent blades will be given; it is more appropriate to make the constant coefficient approximation in the nonrotating frame since some of the influence of the rotating periodic coefficients is retained. Next, the constant coefficient approximation in the rotating and nonrotating frames will be considered, and the results compared with the solution including the periodic coefficient influence. Then the transfer function, that is, the response of the flap motion to sinusoidal control inputs, will be investigated, including the influence of the periodic aerodynamic forces in forward flight. The transfer function is an alternative to the eigenvalues as a representation of the dynamic characteristics of the system. Finally, some of the previous work with this problem will be discussed.

NOMENCLATURE

A	constant in the order μ solution for β
C_1, C_2	constants for the 1/rev critical region
D	secular equation parameter, defining the root behavior near the critical regions
H	transfer function
i	$\sqrt{-1}$
K_p	pitch/flap feedback gain, $K_p = \tan \delta_3$
m	blade index, $m = 1, \ldots, N$
$M_{\dot{\beta}}$	flap moment due to flapping velocity $\dot{\beta}$
M_β	flap moment due to flapping displacement β
M_θ	flap moment due to pitch control θ
N	number of blades
r	blade radial station
R	blade radius
β	blade flap degree of freedom
$\beta_0, \beta_1, \beta_2, \ldots$	coefficients in expansion of β as series in μ
β_{1c}	rotor tip path plane pitch degree of freedom

β_{1s}	rotor tip path plane roll degree of freedom
β_0	rotor coning mode degree of freedom
$\vec{\beta}$	vector of β_{1c},β_{1s} degrees of freedom
γ	lock number of the blade
$\gamma_0,\gamma_1,\gamma_2,\ldots$	coefficients in expansion of γ as series in μ
δ_3	pitch/flap coupling parameter
$\Delta(\omega)$	denominator of the hover transfer function
$\Delta\gamma$	$\gamma - \gamma_0$
ρ	air density
η	blade flap mode shape
θ	blade pitch control
λ	eigenvalue
λ_0	order 1 eigenvalue (the hover limit)
μ	advance ratio, helicopter forward speed divided by rotor tip speed
μ_{corner}	μ at boundary of critical region
μ_1,μ_2	corner μ for 1/rev critical region
ν	blade flap natural frequency (rotating, per rev)
ψ	blade azimuth angle; nondimensional time variable
$\psi_0,\psi_1,\psi_2,\ldots$	time scales, $\psi_n = \mu^n\psi$
ψ_m	azimuth angle of the mth blade
ω	frequency
Ω	rotor rotational speed
$\bar{(\ )}$	complex conjugate; for the transfer functions, magnitude of the input and response
$\dot{(\ )}$	time derivative (when dimensionless, the derivative with respect to ψ)

The equations and parameters used in this analysis are dimensionless, based on the air density ρ, the rotor rotation speed Ω, and the rotor radius R.

PERTURBATION SOLUTION FOR HELICOPTER ROTOR FLAPPING STABILITY

Equation of Motion

Consider the first mode flap motion of a single blade of a helicopter rotor. The rotor shaft is fixed so there is no coupling of the blades through the shaft or control system. Then each blade is independent of the motion of the other blades. The equation describing the flap motion in the rotating frame is

$$\ddot{\beta} + \nu^2\beta = \gamma\left[M_{\dot{\beta}}\dot{\beta} + M_{\beta}\beta + M_{\theta}(\theta - K_p\beta)\right] \tag{1}$$

This is the equation for small perturbations of the flap motion from a trim state. Only blade pitch control (also a perturbation from the trim state, that is, cyclic and collective control as required for the given thrust and forward speed) is included as an input. The degree of freedom representing the perturbed flap motion is β. For an articulated rotor β is the angle of rotation of the blade about the flap hinge. In general, (i.e., for a cantilever rotor, or an articulated blade with flap hinge offset) the blade out of plane deflection is $\beta\eta$, where $\eta(r)$ is the mode shape of first mode flapping, normalized to unity at the tip (at $r = 1$). The blade pitch control perturbation is θ; it is input by the control system, as rigid pitch motion of the blade about a feathering axis at the blade root. So θ is the pitch change of the blade all along its span. The dot denotes the derivative with respect to the blade azimuth angle ψ, which is the nondimensional time variable.

The first term on the left-hand side of equation (1), $\ddot{\beta}$, is the flapping inertia. The second term, $\nu^2\beta$, is the flap spring, which has structural and centrifugal contributions. The parameter ν is the rotating natural frequency of the flap motion (per rev since frequencies are nondimensionalized by Ω). For an articulated blade, that is, a flap hinge with no offset or spring restrain, $\nu = 1$; this is entirely the centrifugal stiffening. A blade with structural restraint (cantilever root, or a hinge spring), or with the flap hinge offset from the center of rotation, has $\nu > 1$; $\nu = 1.1$ to 1.15 is typical of a cantilever rotor, and $\nu = 1.03$ to 1.05 for an articulated rotor with hinge offset. The right-hand side of equation (1) is composed of the aerodynamic flap moments, due to the flapping velocity and displacement, and the blade pitch control. Mechanical pitch/flap coupling is included, that is, feedback control of the form $\Delta\theta = -K_p\beta$. This feedback is usually accomplished (for articulated rotors) by mechanical arrangement of the flap hinge and pitch form equivalent to rotation of the flap hinge by the angle δ_3, so $K_p = \tan\delta_3$. Positive K_p (i.e., $\delta_3 > 0$) is negative feedback, which introduces a positive aerodynamic spring into the flap equation through the coefficient M_θ.

The factor γ is the rotor Lock number, defined as $\gamma = \rho a c R^4 / I_b$ (where ρ is the air density, a is the blade section lift-curve slope, c is the blade chord, R the rotor radius, and I_b is the moment of inertia of the flap motion). The Lock number represents the ratio of the aerodynamic forces to the inertia forces on the blade; γ typically has values from 6 to 10 for current helicopters. The left-hand side of equation (1) is the blade aerodynamic flap moments due to flapping and pitch control. Neglecting reverse flow, and assuming the mode shape is $\eta = r$, then the aerodynamic moments are

$$\left.\begin{aligned} M_{\dot\beta} &= -\left(\frac{1}{8} + \frac{1}{6}\mu \sin\psi\right) \\ M_{\beta} &= -\mu \cos\psi\left(\frac{1}{6} + \frac{1}{4}\mu \sin\psi\right) \\ M_{\theta} &= \frac{1}{8} + \frac{1}{3}\mu \sin\psi + \frac{1}{4}(\mu \sin\psi)^2 \end{aligned}\right\} \qquad (2)$$

where μ is the rotor advance ratio, the ratio of the helicopter forward speed to the rotor tip speed; for current helicopters, the advance ratio at maximum forward speed is typically between 0.3 and 0.5. The neglect of reverse flow is valid to about $\mu = 0.5$, for reverse flow adds order μ^4 terms to the harmonics of the flap moments. Hence, neglecting reverse flow is consistent with the present small μ perturbation analysis, which will be carried to order μ^2.

The equation of motion then, substituting for the flap moments and dropping the pitch control forcing terms to obtain the homogeneous equation, becomes

$$\ddot\beta + \left(\frac{\gamma}{8} + \frac{\gamma}{6}\mu \sin\psi\right)\dot\beta + \left\{\nu^2 + \mu \cos\psi\left(\frac{\gamma}{6} + \frac{\gamma}{4}\mu \sin\psi\right) + K_p\left[\frac{\gamma}{8} + \frac{\gamma}{3}\mu \sin\psi + \frac{\gamma}{4}(\mu \sin\psi)^2\right]\right\}\beta = 0 \qquad (3)$$

The derivation of this equation may be found in the literature, for example in reference 8, which also considers the reverse flow aerodynamics. The only parameters are the flap natural frequency ν, which is always 1 or slightly above; the pitch/flap coupling K_p, which is frequently zero for helicopter main rotors; the Lock number γ, a measure of the relative strength of the aerodynamic forces on the blade; and the forward speed μ. For the hover limit, $\mu = 0$, equation (3) reduces to a constant coefficient linear differential equation. For forward flight, μ introduces periodic coefficients into the differential equation. The stability of a system is defined by its eigenvalues, or roots; there are two for this second-order equation. The stability of the flap motion will be examined for the case of small advance ratio, by means of a perturbation technique to handle the influence of the periodic coefficients due to forward flight.

Hover

In the hover limit, $\mu = 0$, the equation reduces to

$$\ddot{\beta} + \frac{\gamma}{8}\dot{\beta} + \left(\nu^2 + K_p \frac{\gamma}{8}\right)\beta = 0 \tag{4}$$

The eigenvalues λ of this constant coefficient differential equation are obtained from the characteristic equation

$$\lambda^2 + \frac{\gamma}{8}\lambda + \nu^2 + K_p \frac{\gamma}{8} = 0$$

which has the solution

$$\lambda = -\frac{\gamma}{16} \pm i\sqrt{\nu^2 + \frac{\gamma}{8}K_p - \left(\frac{\gamma}{16}\right)^2} \tag{5}$$

These roots are usually complex conjugate pair, that is, the radicand is positive. For that case, the two roots lie on a circular arc in the λ plane, with center at $\mathrm{Re}\lambda = -K_p$ and radius $\sqrt{\nu^2 + K_p^2}$, so the circle goes through the imaginary axis at $\pm i\nu$. The real part of the roots is given by γ only, $\mathrm{Re}\lambda = -\gamma/16$, which then determines the location of the two roots on this arc. The root locus for varying γ then consists of the portion of this circle to the left of the imaginary axis (since γ is positive), plus the real axis from $-\infty$ to $-K_p$. At $\gamma = 0$ the roots are at $\lambda = \pm i\nu$ on the imaginary axis. For $\gamma \to \infty$ the roots approach $\lambda = -\infty$ and $\lambda = -K_p$ (which notice is the center of the circle). The γ locus intercepts the real axis at $\lambda = -K_p - \sqrt{\nu^2 + K_p^2}$ (the center of the circle plus its radius), when $\gamma/16 = K_p + \sqrt{\nu^2 + K_p^2}$. For γ still larger there are two real roots, that is, the radicand of equation (5) is negative; for smaller γ the roots are a complex conjugate pair. For $K_p = 0$ this intercept occurs at $\gamma/16 = \nu$, hence at γ approximately 16, which is quite large for current helicopters. Negative pitch/flap coupling K_p (positive feedback) is required for the intercept to occur at more usual values of γ.

With two real roots, the branch of the locus going to $\lambda = -K_p$ will go into the right half plane - become unstable - if $K_p < 0$. This root is on the real axis, so passes through the origin ($\lambda = 0$) to go into the right half plane. That is, a static instability, or divergence, occurring due to the net spring rate being negative. The stability boundary is crossed at $\gamma/16 = -\nu^2/K_p$, and the flap motion is divergence unstable for larger γ. This may better be viewed as a limit of K_p:

$$K_p > -\frac{\nu^2}{\frac{\gamma}{8}} \tag{6}$$

required for stability. At this boundary, the other root is at $\lambda = \nu^2/K_p$ (hence stable, since $K_p < 0$).

Hover root locations which will be of particular interest are those where the frequency is near a multiple of ½/rev. The hover root has a frequency of ½/rev for $\gamma/16 = K_p + \sqrt{\nu^2 + K_p^2} - (1/4)$. For $K_p = 0$ or small, this means γ approximately 14, so the hover root frequency is above ½/rev usually. The hover root has a frequency 1/rev for $\gamma/16 = K_p + \sqrt{\nu^2 + K_p^2} - 1$. For $K_p = 0$ or small, this means γ must be small. Since $\nu \geq 1$, there is only one crossing of $\mathrm{Im}\lambda = 1$ or ½/rev by the γ locus (except for the case $\nu = 1$, when the locus starts at $\mathrm{Im}\lambda = 1$ for $\gamma = 0$, and will have a second crossing if $K_p > 0$).

The natural frequency of the flap motion is $\omega_n^2 = \nu^2 + (\gamma/8)K_p$. This is mainly given by the structural and centrifugal stiffening, that is, by the frequency ν; it depends on γ only as it influences the effectiveness of pitch/flap coupling. Negative pitch/flap feedback, $K_p > 0$, adds a positive aerodynamic spring and so increases the effective flap spring rate. Notive that $\omega_n = 0$ gives the criterion for divergence of the flap motion. The damping ratio is $\zeta = (\gamma/16)/\omega_n$. Hence, the flap motion is very heavily damped in hover, with ζ typically 50 percent critical damping, due to the high aerodynamic damping.

Expansion in μ

Consider a perturbation solution for the stability in forward flight at small μ. Using the method of multiple time scales (as described in Appendix B), the behavior of the system is examined for ψ of the order 1, μ^{-1}, μ^{-2}, etc.; that is, let $\psi_0 = \psi$, $\psi_1 = \mu\psi$, $\psi_2 = \mu^2\psi$, ... Then the time derivative is

$$\frac{\partial}{\partial\psi} = \frac{\partial}{\partial\psi_0} + \mu\frac{\partial}{\partial\psi_1} + \mu^2\frac{\partial}{\partial\psi_2} + \cdots$$

Expand β as a series in μ, each term depending on all the time scales ψ_n:

$$\beta = \beta_0(\psi_0, \psi_1, \psi_2, \ldots) + \mu\beta_1(\psi_0, \psi_1, \ldots) + \cdots$$

and also expand the parameter γ as a series in μ:

$$\gamma = \gamma_0 + \mu\gamma_1 + \mu^2\gamma_2 + \cdots$$

This expansion of γ is a way of quantifying when γ is near certain critical values; that is, if γ_0 is some critical value, and $\gamma_1 = (\gamma - \gamma_0)/\mu$ is order 1, then γ is order μ near γ_0. The quantity γ is still the parameter given, hence this decomposition into γ_0, γ_1, γ_2, . . . changes with μ.

Now β, $d/d\psi$, and γ are all expanded as series in μ. These expansions are substituted into equation (3), and all terms of the same order in μ

collected, assuming that all the coefficients in the expansion are of the same order. A fundamental assumption of the method of multiple time scales is that the β_n must all be the same order for all the time scales ψ_n. All the terms of like order in μ are collected and separately set to zero, to obtain the equation that starts the analysis at each order.

Order 1 Results

The order 1 terms of equation (3) give

$$\frac{\partial^2 \beta_0}{\partial \psi_0^2} + \frac{\gamma_0}{8} \frac{\partial \beta_0}{\partial \psi_0} + \left(\nu^2 + K_p \frac{\gamma_0}{8} \right) \beta_0 = 0 \tag{7}$$

The solution of this equation is

$$\beta_0 = \mathrm{Re}\left[\beta_{01}(\psi_1, \psi_2, \ldots) e^{\lambda_0 \psi_0} \right] \tag{8}$$

where the root λ_0 is

$$\lambda_0 = -\frac{\gamma_0}{16} + i \sqrt{\nu^2 + \frac{\gamma_0}{8} K_p - \left(\frac{\gamma_0}{16} \right)^2} \tag{9}$$

The convention will be followed that λ_0 is the root with positive frequency; the other root is the conjugate $\bar{\lambda}_0$. Then to order 1 the equation of motion, and so the roots, are just the hover limit. Since β_0 is a function of all the time scales, equation (7) is a partial differential equation, which determines β_0 as a function of ψ_0 only. Thus, β_{01} still depends on ψ_1, ψ_2, etc.

Order μ Results

The order μ equation is

$$\left[\frac{\partial^2 \beta_1}{\partial \psi_0^2} + \frac{\gamma_0}{8} \frac{\partial \beta_1}{\partial \psi_0} + \left(\nu^2 + K_p \frac{\gamma_0}{8} \right) \beta_1 \right] = 2 \frac{\partial^2 \beta_0}{\partial \psi_0 \, \partial \psi_1} + \frac{\gamma_0}{8} \frac{\partial \beta_0}{\partial \psi_1} + \left(\frac{\gamma_1}{8} + \frac{\gamma_0}{6} \mu \sin \psi_0 \right) \frac{\partial \beta_0}{\partial \psi_0} + \left(\frac{\gamma_0}{6} \cos \psi_0 + \frac{\gamma_1}{8} K_p + \frac{\gamma_0}{3} K_p \sin \psi_0 \right) \beta_0 \tag{10}$$

This is a differential equation for $\beta_1(\psi_0)$, forced by the order 1 solution $\beta_0(\psi_0)$; substituting for β_0, it becomes

$$-\left[\frac{\partial^2\beta_1}{\partial\psi_0^2} + \frac{\gamma_0}{8}\frac{\partial\beta_1}{\partial\psi_0} + \left(\nu^2 + K_p\frac{\gamma_0}{8}\right)\beta_1\right]$$

$$= \left[\left(2\lambda_0 + \frac{\gamma_0}{8}\right)\frac{\partial\beta_{01}}{\partial\psi_1} + \frac{\gamma_1}{8}(\lambda_0 + K_p)\beta_{01}\right]e^{\lambda_0\psi_0}$$

$$+ \frac{\gamma_0}{12}\left[1 - i(\lambda_0 + 2K_p)\right]\beta_{01}e^{(\lambda_0+i)\psi_0}$$

$$+ \frac{\gamma_0}{12}\left[1 + i(\lambda_0 + 2K_p)\right]\beta_{01}e^{(\lambda_0-i)\psi_0}$$

$$+ \text{conjugate} \qquad (11)$$

The right-hand side has a term of the form $A_1e^{\lambda_0\psi_0}$ due to the β_0 solution, where A_1 is independent of ψ_0. But the left-hand side is the same as the order 1 equation (eq. (7)), so it has the same homogeneous solution $e^{\lambda_0\psi_0}$. Then the solution for β_1 is of the form

$$\beta_1 = \text{Re}\left(\beta_{11}e^{\lambda_0\psi_0} - \frac{A_1}{2\lambda_0 + \frac{\gamma_0}{8}}\psi_0e^{\lambda_0\psi_0} + \ldots\right) \qquad (12)$$

The forcing of equation (10) by its own homogeneous solution produces the second term in β_1, which is order ψ_0 compared to the solution for β_0. So as ψ_0 increases, β_1 will become arbitrarily large compared to β_0, which violates the assumption that all the terms β_n in the expansion of β are the same order. This situation can only be avoided if the secular term A_1, the coefficient of the homogeneous solution forcing equation (10), is identically zero.

Assume for now that $\bar{\lambda}_0 \pm i \neq \lambda_0$; then the periodic coefficients do not contribute to the secular term of equation (10). Setting the secular term to zero gives a differential equation for $\beta_{01}(\psi_1)$:

$$\left(2\lambda_0 + \frac{\gamma_0}{8}\right)\frac{\partial\beta_{01}}{\partial\psi_1} + \frac{\gamma_1}{8}(\lambda_0 + K_p)\beta_{01} = 0 \qquad (13)$$

or

$$\frac{\partial\beta_{01}}{\partial\psi_1} - \lambda_1\beta_{01} = 0 \qquad (14)$$

where

$$\lambda_1 = - \frac{\frac{\gamma_1}{8} (\lambda_0 + K_p)}{2i \mathrm{Im}\lambda_0}$$

The solution of this equation is $\beta_{01} = \beta_{02}(\psi_2, \ldots) e^{\lambda_1 \psi_1}$, so the solution for β so far is

$$\beta = \mathrm{Re}\left[\beta_{02}(\psi_2, \ldots) e^{\lambda_0 \psi_0 + \lambda_1 \psi_1}\right] + O(\mu) \tag{15}$$

The eigenvalue to order μ is then

$$\lambda = \lambda_0 + \mu\lambda_1 = - \frac{\gamma}{16} + i \sqrt{\nu^2 + \frac{\gamma}{8} K_p - \left(\frac{\gamma}{16}\right)^2} \tag{16}$$

That is, λ_1 is just an order μ perturbation of the hover root, due to the order μ expansion of γ. To order μ then, the eigenvalue remains just the hover value, with no influence of forward flight at all.

The assumption that $\overline{\lambda}_0 \pm i \neq \lambda_0$ means that $\mathrm{Im}\lambda_0 \neq \frac{1}{2}$/rev. This requirement then is that the hover root λ should not have a frequency near $\frac{1}{2}$/rev; "near" means being able to write the hover root as λ_0 plus an increment, such that when λ_0 has a frequency of $\frac{1}{2}$/rev, $\lambda - \lambda_0$ is order μ small. As μ increases then, the distance from $\frac{1}{2}$/rev which considered "near" increases. The analysis will return to the case $\mathrm{Im}\lambda_0 = \frac{1}{2}$/rev later.

With the secular term removed, equation (10) becomes

$$\frac{\partial^2 \beta_1}{\partial \psi_0^2} + \frac{\gamma_0}{8} \frac{\partial \beta_1}{\partial \psi_0} + \left(\nu^2 + K_p \frac{\gamma_0}{8}\right) \beta_1$$

$$= - \frac{\gamma_0}{12} \left[1 - i(\lambda_0 + 2K_p)\right] \beta_{01} e^{(\lambda_0 + i)\psi_0}$$

$$- \frac{\gamma_0}{12} \left[1 + i(\lambda_0 + 2K_p)\right] \beta_{01} e^{(\lambda_0 - i)\psi_0}$$

$$+ \text{conjugate} \tag{17}$$

The solution of this equation is

$$\beta_1 = \mathrm{Re}\left\{\beta_{11}(\psi_1) e^{\lambda_0 \psi_0} + \frac{\gamma_0}{12} \beta_{01} \left[A_+ e^{(\lambda_0 + i)\psi_0} + A_- e^{(\lambda_0 - i)\psi_0}\right]\right\} \tag{18}$$

where

$$A_{\pm} = \frac{1 \mp i(\lambda_0 + 2Kp)}{\pm 2Im\lambda_0 + 1}$$

The second term is the particular solution, which with the secular term dropped is now the same order as β_0. This completes the solution to order μ; the solution so far is $\beta_0(\psi_0,\psi_1)$ and $\beta_1(\psi_0)$.

Order μ^2 Results

The order μ^2 equation is

$$-\left[\frac{\partial^2\beta_2}{\partial\psi_0^2} + \frac{\gamma_0}{8}\frac{\partial\beta_2}{\partial\psi_0} + \left(\nu^2 + K_p\frac{\gamma_0}{8}\right)\beta_2\right]$$

$$= 2\frac{\partial^2\beta_1}{\partial\psi_0\,\partial\psi_1} + \frac{\gamma_0}{8}\frac{\partial\beta_1}{\partial\psi_1} + \left(\frac{\gamma_1}{8} + \frac{\gamma_0}{6}\sin\psi_0\right)\frac{\partial\beta_1}{\partial\psi_0}$$

$$+ \left(\frac{\gamma_0}{6}\cos\psi_0 + K_p\frac{\gamma_1}{8} + K_p\frac{\gamma_0}{3}\sin\psi_0\right)\beta_1$$

$$+ \frac{\partial^2\beta_0}{\partial\psi_1^2} + 2\frac{\partial^2\beta_0}{\partial\psi_0\,\partial\psi_2} + \frac{\gamma_0}{8}\frac{\partial\beta_0}{\partial\psi_2} + \left(\frac{\gamma_1}{8} + \frac{\gamma_0}{6}\sin\psi_0\right)\frac{\partial\beta_0}{\partial\psi_1} + \left(\frac{\gamma_2}{8} + \frac{\gamma_1}{6}\sin\psi_0\right)\frac{\partial\beta_0}{\partial\psi_0}$$

$$+ \left[\frac{\gamma_1}{6}\cos\psi_0 + \frac{\gamma_0}{8}\sin 2\psi_0 + K_p\left(\frac{\gamma_2}{8} + \frac{\gamma_4}{8} + \frac{\gamma_1}{3}\sin\psi_0 - \frac{\gamma_0}{8}\cos 2\psi_0\right)\right]\beta_0 \tag{19}$$

The solutions to order μ for β_0 and β_1 are substituted into this equation, and the coefficient of the homogeneous solution $e^{\lambda_0\psi_0}$ - that is, the secular term - are collected. Assume for now that $\bar{\lambda}_0 \pm 2i \neq \lambda_0$, that is, $Im\lambda_0 \neq 1/rev$; it has already been assumed that the hover frequency is not near $\frac{1}{2}/rev$. Then the secular term is

$$-\left(\frac{\partial\beta_{11}}{\partial\psi_1} - \lambda_1\beta_{11}\right) = \left\{\frac{\partial\beta_{02}}{\partial\psi_2} + \left[-\lambda_2 + \frac{Kp\frac{\gamma_4}{8} + \left(\frac{\gamma_0}{12}\right)^2 i(\lambda_0 + 2Kp)(A_+ - A_-)}{2iIm\lambda_0}\right]\beta_{02}\right\}e^{\lambda_1\psi_1} \tag{20}$$

where λ_2 is the order μ^2 term in the expansion of the hover root:

$$\lambda_0 + \mu\lambda_1 + \mu^2\lambda_2 = -\frac{\gamma}{16} + i\sqrt{\nu^2 + \frac{\gamma}{8}Kp - \left(\frac{\gamma}{16}\right)^2} + O(\mu^3) \tag{21}$$

Regarding this as a differential equation for $\beta_{11}(\psi_1)$, it is forced by *its* own homogeneous solution $e^{\lambda_1 \psi_1}$. Setting the secular term of equation (20) (i.e., the entire right-hand side) to zero gives an equation for $\beta_{02}(\psi_2)$:

$$\frac{\partial \beta_{02}}{\partial \psi_2} + \left[-\lambda_2 + \frac{K_p \frac{\gamma_0}{8} + \left(\frac{\gamma_0}{12}\right)^2 i(\lambda_0 + 2K_p)(A_+ - A_-)}{2i\,\mathrm{Im}\lambda_0} \right] \beta_{02} = 0 \qquad (22)$$

Thus, the eigenvalue to order μ^2 is

$$\lambda = \lambda_0 + \mu\lambda_1 + \mu^2 \left[\lambda_2 - \frac{K_p \frac{\gamma_0}{8} + \left(\frac{\gamma_0}{12}\right)^2 i(\lambda_0 + 2K_p)(A_+ - A_-)}{2i\,\mathrm{Im}\lambda_0} \right]$$

$$= \lambda_{\text{hover}} + \frac{\mu^2 i}{2\,\mathrm{Im}\lambda_0} \left[K_p \frac{\gamma_0}{8} + \left(\frac{\gamma_0}{12}\right)^2 \frac{2\left(\nu^2 - \frac{\gamma_0}{8} K_p + 4K_p^2\right)}{1 - (2\,\mathrm{Im}\lambda_0)^2} \right] \qquad (23)$$

or to order μ^2 this is

$$\lambda = -\frac{\gamma}{16} \pm i \sqrt{\nu^2 + (1+\mu^2)\frac{\gamma}{8} K_p - \left(\frac{\gamma}{16}\right)^2 \left[1 + \mu^2 \frac{8}{9} \frac{\nu^2 - \frac{\gamma}{8} K_p + 4K_p^2}{\nu^2 + \frac{\gamma}{8} K_p - \left(\frac{\gamma}{16}\right)^2 - \frac{1}{4}} \right]} \qquad (24)$$

Then to order μ^2 - and for γ and ν such that the hover frequency is away from ½/rev and 1/rev - the influence of forward flight on the eigenvalues is simply a small (order μ^2) change in the frequency. The first effect in the frequency just corrects the $(\gamma/8)K_p$ spring term to account for the increase of the mean of $K_p M_\theta$ with μ. The second effect of μ is entirely due to the periodic coefficients. This order μ^2 change in the frequency is in fact quite small for μ out to 0.5 or so, as the examples below will show. There is no influence of forward flight at all on the damping of the root.

This expression for the eigenvalue was derived assuming that the hover roots are a complex conjugate pair; it may be shown, however, that the same expression is valid for γ large enough that the two roots are real, that is, when the radicand is negative. A point of particular interest is where one branch of the locus on the real axis crosses into the right half plane, that is, the divergence stability boundary. The criterion for this boundary is that $\lambda = 0$, which from equation (24) gives

$$\nu^2 + (1+\mu^2)\frac{\gamma}{8} K_p = \left(\frac{\gamma}{16}\right)^2 \mu^2 \frac{8}{9} \frac{\nu^2 - \frac{\gamma}{8} K_p + 4K_p^2}{\nu^2 + \frac{\gamma}{8} K_p - \left(\frac{\gamma}{16}\right)^2 - \frac{1}{4}}$$

or since $-(\gamma/8)K_p$ is an order μ^2 distance from ν^2, the criterion on K_p for stability is

$$(1 + \mu^2)\frac{\gamma}{8}K_p > -\nu^2\left[1 + \mu^2\frac{16}{9}\frac{\left(\frac{\gamma}{16}\right)^2 + \frac{\nu^2}{2}}{\left(\frac{\gamma}{16}\right)^2 + \frac{1}{4}}\right] \tag{25}$$

The μ effect on the right-hand side (the periodic coefficients) dominates that on the left-hand side (the average of K_pM_θ). So the critical value of negative K_p, beyond which the locus lies in the right half plane, is actually increased by μ; the hover criterion on K_p is then conservative in forward flight. That is the opposite conclusion as would have been reached considering just the averaged coefficients. In any case, however, the influence of forward flight is only order μ^2 small.

Equation (24) also gives the effects of μ on the boundary between where there are two real roots, and where the roots are conjugate pairs. This boundary is given by $\mathrm{Im}\lambda = 0$, which to order μ^2 is

$$\frac{\gamma}{16} = \left(K_p + \sqrt{\nu^2 + K_p^2}\right)\left[1 + \mu^2\frac{\frac{16}{9}\nu^2\left(-K_p + \sqrt{\nu^2 + K_p^2}\right) - K_p}{\sqrt{\nu^2 + K_p^2}}\right] \tag{26}$$

For $K_p = 0$ this reduces to simply

$$\frac{\gamma}{16} = \nu\left(1 + \mu^2\frac{16}{9}\nu^2\right) \tag{27}$$

Near ½/rev Frequency

Now return to the case when the hover root frequency is near ½/rev. If $\mathrm{Im}\lambda_0 = 1/2$, then $\bar{\lambda}_0 + i = \lambda_0$ and the periodic coefficients contribute to the order μ secular term. The criterion $\mathrm{Im}\lambda_0 = 1/2$ means

$$\frac{\gamma_0}{16} = K_p + \sqrt{\nu^2 + K_p^2 - \frac{1}{4}}\,.$$

Since $\gamma = \gamma_0 + \mu\gamma_1 + \ldots$, that means γ must be such that $\gamma - \gamma_0$ is order μ small. The order 1 root is then $\lambda_0 = -(\gamma_0/16) + (i/2)$, and the order μ secular term is now

$$\left(2\lambda_0 + \frac{\gamma_0}{8}\right)\frac{\partial\beta_{01}}{\partial\psi_1} + \frac{\gamma_1}{8}(\lambda_0 + K_p)\beta_{01} + \frac{\gamma_0}{12}\left[1 - i(\bar{\lambda}_0 + 2K_p)\right]\bar{\beta}_{01} = 0$$

or

$$\frac{\partial \beta_{01}}{\partial \psi_1} - \lambda_1 \beta_{01} + \left(\frac{\gamma_0^2}{192} - \frac{\gamma_0}{6} K_p - \frac{\gamma_0}{24} i \right) \bar{\beta}_{01} = 0 \tag{28}$$

where here, since $\mathrm{Im}\lambda_0 = 1/2$, the order μ expansion of the hover root is

$$\lambda_1 = - \frac{\gamma_1}{16} - i \frac{\gamma_1}{8} \left(\frac{\gamma_0}{16} - K_p \right).$$

The $\bar{\beta}_{01}$ term is the periodic coefficient contribution to the secular term. The solution of an equation of this form is given in Appendix C. The solution for β_{01} depends on the quantity

$$\begin{aligned} D^2 &= (\mathrm{Im}\lambda_1)^2 - \left[\left(\frac{\gamma_0^2}{192} - \frac{\gamma_0}{6} K_p \right)^2 + \left(\frac{\gamma_0}{24} \right)^2 \right] \\ &= \left[\frac{\gamma_1}{8} \left(\frac{\gamma_0}{16} - K_p \right) \right]^2 - \left(\frac{\gamma_0}{12} \right)^2 \left(\nu^2 - \frac{\gamma_0}{8} K_p + 4 K_p^2 \right) \end{aligned} \tag{29}$$

Now if $D^2 > 0$, the solution for β_{01} has terms with time behavior like

$$e^{-(\mathrm{Re}\lambda_1 \pm iD)\psi_1} = e^{-\mu(\gamma_1/16)\psi \pm i\mu D\psi}$$

and then β_0 has terms like

$$\beta_{01} e^{\lambda_0 \psi_0} \sim e^{-(\gamma/16)\psi \pm i\psi \left[(1/2) + \mu D \right]}$$

The damping is unchanged, and there is an order μ change in the frequency, due to the periodic coefficients when the hover frequency is near ½/rev. If $D^2 < 0$, then β_{01} has terms like

$$e^{-(\mathrm{Re}\lambda_1 \pm D)\psi_1} = e^{\left[-\mu(\gamma_1/16) \pm \mu D \right]\psi}$$

and then β_0 has terms like

$$\beta_{01} e^{\lambda_0 \psi_0} \sim e^{\left[-(\gamma/16) \pm \mu D \right]\psi + (i/2)\psi}$$

There is an order μ change in the damping, both more and less stable, while the frequency remains fixed at ½/rev.

The influence of μ on the roots near ½/rev frequency then is first an order μ change in the frequency towards ½/rev, with the damping at the hover value. When the roots reach ½/rev, the frequency remains fixed while there is an order μ change in the damping. One root is stabilized, the locus moving to the left on the λ plane, but the other is destabilized, it moves to the right. This type of behavior of the roots is characteristic of periodic systems (as discussed in Appendix A). Indeed it appears here due to the contributions of the periodic coefficients to the order μ secular equation when the hover frequency is near ½/rev. There is in this case a *critical region*, inside of which a change in the flap damping occurs. For many problems with periodic coefficients, the system is unstable inside such a region. In this case, however, the hover damping, $\mathrm{Re}\lambda = -\gamma/16$, is quite large; and the change in the damping is only $\pm\mu D$, hence, order μ small compared to the hover damping. So the critical region is a region of stability degradation rather than instability (for small μ, i.e.).

The boundary of the critical region is given by $D^2 = 0$, or

$$\left(\frac{\gamma_0}{16} - K_p\right)\frac{\gamma_1}{8} = \pm\frac{\gamma_0}{12}\sqrt{\nu^2 - \frac{\gamma_0}{8}K_p + 4K_p^2} \tag{30}$$

Since $\gamma = \gamma_0 + \mu\gamma_1$, write $\gamma = \gamma_0 + \Delta\gamma$ where γ is the value such that the hover root is at ½/rev. Then if the hover frequency with γ is near ½/rev, $\Delta\gamma = \gamma - \gamma_0$ must be order μ small. The boundary of the critical region is then

$$\left(\frac{\gamma_0}{16} - K_p\right)\frac{\Delta\gamma}{16} = \pm\mu\frac{\gamma_0}{24}\sqrt{\nu^2 - \frac{\gamma_0}{8}K_p + 4K_p^2} \tag{31}$$

Considering the μ root locus, then the critical region boundary is the value of μ for which the locus reaches ½/rev frequency, and is just about to encounter the stability change at ½/rev frequency. From the behavior of the μ root locus, this boundary value will be denoted μ_{corner}, where then

$$\mu_{corner} = \frac{\pm\frac{\Delta\gamma}{16}\left(\frac{\gamma_0}{16} - K_p\right)}{\frac{\gamma_0}{24}\sqrt{\nu^2 - \frac{\gamma_0}{8}K_p + 4K_p^2}} \tag{32}$$

For $K_p = 0$ this reduces to $\mu_{corner} = \pm(\Delta\gamma/16)(3/2\nu)$. In general, this equation gives the boundary of the critical region on the $\gamma - \mu$ plane. The eigenvalues are

$$\lambda = \lambda_0 + \mu \mathrm{Re}\lambda_1 - i\mu D$$

$$= -\frac{\gamma}{16} + \frac{i}{2} - i\mu\sqrt{\left(\frac{\gamma_1}{16}\right)^2 4\left(\frac{\gamma_0}{16} - K_p\right)^2 - \left(\frac{\gamma_0}{12}\right)^2\left(\nu^2 - \frac{\gamma_0}{8}K_p + 4K_p^2\right)} \qquad (33)$$

which may be written

$$\lambda = -\frac{\gamma}{16} + \frac{i}{2} - i\frac{\Delta\gamma}{16} 2\left(\frac{\gamma_0}{16} - K_p\right)\sqrt{1 - \left(\frac{\mu}{\mu_{corner}}\right)^2} \qquad (34)$$

For $\mu = 0$, this reduces to

$$\lambda = -\frac{\gamma}{16} + \frac{i}{2} - i\frac{\Delta\gamma}{16} 2\left(\frac{\gamma_0}{16} - K_p\right),$$

which is just an order μ (i.e., order $\Delta\gamma$) expansion of the hover root from ½/rev frequency at γ_0.

Near 1/rev Frequency

Consider now the case with the hover root frequency near 1/rev. With $\mathrm{Im}\lambda_0 = 1$, then $\bar{\lambda}_0 + 2i = \lambda_0$, so the periodic coefficients contribute to the order μ^2 secular term. The criterion $\mathrm{Im}\lambda_0 = 1$ means $\gamma_0/16 = K_p + \sqrt{\nu^2 + K_p^2 - 1}$, and the order 1 root is then $\lambda_0 = -(\gamma_0/16) + i$. For this case $\mathrm{Im}\lambda_0 \neq 1/2$, so the order μ results are applicable; then the root to order μ is known (i.e., $\lambda = \lambda_0 + \mu\lambda_1$), and now the order μ^2 influence is sought. The secular term of equation (19) becomes, for $\mathrm{Im}\lambda_0 = 1$:

$$-\left(\frac{\partial\beta_{11}}{\partial\psi_1} - \lambda_1\beta_{11}\right) = \left\{\frac{\partial\beta_{02}}{\partial\psi_2} + \left[-\lambda_2 + \left(\frac{\gamma_0}{6}\right)^2 \frac{i}{12}\left(\nu^2 - \frac{\gamma_0}{8}K_p + 4K_p^2\right) - K_p\frac{\gamma_0}{16}i\right]\beta_{02}\right\}e^{\lambda_1\psi_1}$$

$$+ \left\{\frac{1}{2i}\left(\frac{\gamma_0}{12}\right)^2\left[2 - i(\bar{\lambda}_0 + 2K_p)\right]\bar{A}_- - \frac{\gamma_0}{32}(1 - iK_p)\right\}\bar{\beta}_{02}e^{\bar{\lambda}_1\psi_1} \qquad (35)$$

The $\bar{\beta}_{02}$ term is the contribution of the periodic coefficients to the secular term when $\mathrm{Im}\lambda_0 = 1$. The secular term of *this* equation is the coefficient of $e^{\lambda_1 \psi_1}$, hence, it is exactly as before (eq. (24)) - giving the same result for the eigenvalues to order μ^2 - unless $\bar{\lambda}_1 = \lambda_1$. In that case, which requires that λ_1 be real, the entire right-hand side is the secular term of equation (35), including the $\bar{\beta}_{02}$ term. Since

$$\lambda_1 = -\frac{\gamma_1}{16} + i\frac{\gamma_1}{16}\left(-\frac{\gamma_0}{16} + K_p\right),$$

requiring $\mathrm{Im}\lambda_1 = 0$ means that $\gamma_1 = 0$; and so $\lambda_1 = 0$ in fact. For the periodic coefficients to contribute to the order μ^2 secular term requires then that $\gamma = \gamma_0 + \mu^2\gamma_2 + \ldots$, that is, γ must be such that $\gamma - \gamma_0$ is order μ^2 small; this quantifies what "near" 1/rev frequency means. For a given μ then the hover frequency must be closer to the critical value than was required for the ½/rev region. The effect of forward flight near 1/rev frequency is smaller than near ½/rev, only order μ^2 compared to order μ for the latter.

With $\gamma_1 = 0$, the secular term of equation (35) becomes

$$\frac{\partial \beta_{02}}{\partial \psi_2} + \left[-i\frac{\gamma_2}{16}(\lambda_0 + K_p) + \left(\frac{\gamma_0}{6}\right)^2 \frac{i}{12}\left(\nu^2 - \frac{\gamma_0}{8}K_p + 4K_p{}^2\right) - K_p\frac{\gamma_0}{16}i\right]\beta_{02}$$

$$+ \left[-\frac{\gamma_0}{32} + iK_p\frac{\gamma_0}{32} - i\frac{1}{8}\left(\frac{\gamma_0}{6}\right)^2\left(-\frac{\gamma_0}{16} + 2K_p\right)\left(-\frac{\gamma_0}{16} + 2K_p + i\right)\right]\bar{\beta}_{02} = 0 \qquad (36)$$

The solution for β_{02} depends on the quantity D (see Appendix C) given by

$$D^2 = \left[\left(\frac{\gamma_0}{16} - K_p\right)\frac{\gamma_2}{16} + \left(\frac{\gamma_0}{6}\right)^2 \frac{\nu^2 - \frac{\gamma_0}{8}K_p + 4K_p{}^2}{12} - K_p\frac{\gamma_0}{16}\right]^2$$

$$- \left(\frac{\gamma_0}{32}\right)^2\left\{\left[1 + \frac{\gamma_0}{9}\left(\frac{\gamma_0}{16} - 2K_p\right)\right]^2 + \left[K_p - \frac{\gamma_0}{9}\left(\frac{\gamma_0}{16} - 2K_p\right)^2\right]^2\right\} \qquad (37)$$

The behavior of the roots is similar to that near ½/rev, except that all changes due to forward flight are here order μ^2. There is a critical region, inside which there is an order μ^2 change in the damping of the flap motion. For small μ, the damping is the same as the hover root while there is an order μ^2 change in the frequency, towards 1/rev. At the boundary of the critical region the root reaches 1/rev frequency; and for still larger μ,

inside the critical region, the frequency is fixed at 1/rev while there is an order μ^2 change in the damping, one root becoming more stable and the other less.

The boundary of the critical region is given by $D^2 = 0$. Since $\gamma = \gamma_0 + \mu^2\gamma_2 + \ldots$, write $\gamma = \gamma_0 + \Delta\gamma$ where γ_0 is the value such that the hover root is at 1/rev. Then, if the hover frequency with γ is near 1/rev, $\Delta\gamma = \gamma - \gamma_0$ must be order μ^2 small. The critical region boundary may then be written

$$\left(\frac{\gamma_0}{16} - K_p\right)\frac{\Delta\gamma}{16} = \mu^2(C_1 \pm C_2) \tag{38}$$

where

$$C_1 = -\left(\frac{\gamma_0}{6}\right)^2 \frac{\nu^2 - \frac{\gamma_0}{8}K_p + 4K_p^2}{12} + K_p\frac{\gamma_0}{16}$$

$$= -\frac{16}{27}(\nu^2 - 1)^2 - \frac{16}{27}\left(\frac{\gamma_0}{16}\right)^2 + K_p\frac{\gamma_0}{16} \tag{39}$$

$$C_2 = \frac{\gamma_0}{32}\sqrt{\left[1 + \frac{\gamma_0}{9}\left(\frac{\gamma_0}{16} - 2K_p\right)\right]^2 + \left[K_p - \frac{\gamma_0}{9}\left(\frac{\gamma_0}{16} - 2K_p\right)^2\right]^2}$$

$$= \frac{\gamma_0}{32}\sqrt{\left[1 + \frac{16}{9}(\nu^2 - 1)\right]^2 + \left[K_p - \frac{16}{9}(\nu^2 - 1)\left(\frac{\gamma_0}{16} - 2K_p\right)\right]^2} \tag{40}$$

Then the μ root locus reaches the critical region boundary at $\mu_{corner} = \mu_1$ or μ_2, where

$$\mu_1^2, \mu_2^2 = \frac{\left(\frac{\gamma_0}{16} - K_p\right)\frac{\Delta\gamma}{16}}{C_1 \pm C_2} \tag{41}$$

For $K_p = 0$, this becomes

$$\mu_1^2, \mu_2^2 = \frac{\frac{\Delta\gamma}{16}}{-\frac{16}{27}\nu^2\sqrt{\nu^2 - 1} \pm \frac{1}{2}\sqrt{1 + \frac{32}{9}(\nu^2 - 1) + \frac{256}{81}\nu^2(\nu^2 - 1)^2}} \tag{42}$$

The eigenvalues are now

$$\lambda = \lambda_0 + \mu^2 \mathrm{Re}\lambda_2 - i\mu^2 D$$

$$= -\frac{\gamma}{16} + i - i\mu^2 \sqrt{\left[\frac{\gamma_2}{16}\left(\frac{\gamma_1}{16} - K_p\right) - C_1\right]^2 - C_2{}^2}$$

$$= -\frac{\gamma}{16} + i - i\,\frac{\Delta\gamma}{16}\left(\frac{\gamma_0}{16} - K_p\right)\sqrt{\left(1 - \frac{\mu^2}{\mu_1{}^2}\right)\left(1 - \frac{\mu^2}{\mu_2{}^2}\right)} \qquad (43)$$

For $\mu = 0$, this reduces to simply an order $\Delta\psi$ (order μ^2) expansion of the hover root from 1/rev at γ_0.

Summary, and Discussion of the Results

This section summarizes the results of the perturbation solution for the influence of forward flight on the helicopter rotor blade flapping stability. The expressions for the eigenvalues are collected from the analysis above. The behavior of the roots is discussed, in terms of the μ root loci and the critical regions on the γ - μ plane. These results are for the shaft-fixed stability of an individual rotor blade.

Hover.- The hover limit, $\mu = 0$, has the eigenvalues

$$\lambda = -\frac{\gamma}{16} \pm i\sqrt{\nu^2 + \frac{\gamma}{8} K_p - \left(\frac{\gamma}{16}\right)^2} \qquad (44)$$

These roots are usually a complex conjugate pair, located at $\mathrm{Re}\lambda = -\gamma/16$ on the circular arc with radius $\sqrt{\nu^2 + K_p{}^2}$ and center at $\lambda = -K_p$. Forward flight, $\mu > 0$, introduces periodic aerodynamic forces into the dynamics, which radically influences the behavior of the eigenvalues and the analysis technique required to obtain them. A perturbation method based on small μ has been used to obtain explicit expressions for the roots when $\mu > 0$, including the effects of the periodic coefficients. It is an order μ^2 analysis (consistent with the neglect of the reverse flow region effects), which is valid to approximately $\mu = 0.5$.

Forward flight, away from critical regions.- When the hover root frequency is not too close to a multiple of ½/rev, the roots to order μ^2 are

$$\lambda = -\frac{\gamma}{16} \pm i\sqrt{\nu^2 + (1+\mu^2)\,\frac{\gamma}{8} K_p - \left(\frac{\gamma}{16}\right)^2 \left[1 + \mu^2\,\frac{\frac{8}{9}\,\nu^2 - \frac{\gamma}{8} K_p + 4K_p{}^2}{\nu^2 + \frac{\gamma}{8} K_p - \left(\frac{\gamma}{16}\right)^2 - \frac{1}{4}}\right]} \qquad (45)$$

There is only an order μ^2 change in the frequency, which is quite small even up to $\mu = 0.5$. This expression applies in particular when there are two real roots, that is, when γ is large enough so the radicand is negative, so it gives the criterion for divergence instability, including the influence of forward flight. The divergence boundary is given by where one branch of the locus on the real axis goes through the origin into the right half plane. The boundary criterion is then $\lambda = 0$, for which equation (45) gives the criterion for divergence stability as

$$(1 + \mu^2)\frac{\gamma}{8} K_p > -\nu^2\left[1 + \mu\,\frac{16}{9}\,\frac{\left(\frac{\gamma}{16}\right)^2 + \frac{\nu^2}{2}}{\left(\frac{\gamma}{16}\right)^2 + \frac{1}{4}}\right] \tag{46}$$

This is a limit on the pitch/flap feedback allowed; the divergence instability occurs when K_p is sufficiently large negative (positive feedback). A constant coefficient approximation to the equation of motion, using the average of the coefficients, includes only the effect of the mean of M_θ on the left-hand side of equation (46); that is, a conservative approximation for this case.

Forward flight, near ½/rev frequency.- It is characteristic of a system with periodic coefficients that for certain values of the parameters there occurs a degradation of the stability. Typically this occurs where the basic eigenvalue - here the hover root - has a frequency corresponding to a multiple of one half the fundamental frequency of the equation coefficients. Specifically, consider when the frequency of the hover root of the flap motion is near ½/rev. There occurs then an order μ influence of forward flight. When the frequency is near ½/rev, equation (45) is no longer valid for λ, and the following result must be used instead. Let γ_0 be the value of γ for which the hover root would (with the given ν and K_p) have a frequency exactly ½/rev; that is, $\gamma_0/16 = K_p + \sqrt{\nu^2 + K_p^2 - (1/4)}$. Write $\Delta\gamma = \gamma - \gamma_0$. Then, if $\Delta\gamma/16$ is order μ small, the eigenvalue is given by

$$\lambda = -\frac{\gamma}{16} + \frac{i}{2} - i\,\frac{\Delta\gamma}{16}\,2\left(\frac{\gamma_0}{16} - K_p\right)\sqrt{1 - \left(\frac{\mu}{\mu_{corner}}\right)^2} \tag{47}$$

where

$$\mu_{corner} = \frac{\frac{\Delta\gamma}{16}\left(\frac{\gamma_0}{16} - K_p\right)}{\frac{\gamma_0}{24}\sqrt{\nu^2 - \frac{\gamma_0}{8}K_p + 4K_p^2}} \tag{48}$$

The subscript "corner" refers to the behavior of the μ root locus on the λ plane, as discussed below; it is the boundary of the critical region. For $K_p = 0$ this result reduces to $\gamma_0/16 = \sqrt{\nu^2 - 1/4}$, and $\mu_{corner} = (\Delta\gamma/16)(3/2\nu)$ for the boundary.

This solution exhibits the following behavior. If $\mu < \mu_{corner}$, there is an order μ change in the frequency, toward ½/rev, while the real part of the root remains fixed at the hover value of $-\gamma/16$. At $\mu = \mu_{corner}$ the roots reach $Im\lambda = ½/rev$. For $\mu > \mu_{corner}$ the frequency remains fixed at ½/rev while there is an order μ change in the damping; $Re\lambda$ is increased for one root and decreased for the other. This behavior of the locus near $Im\lambda = ½/rev$ is characteristic of periodic systems (Appendix A). While there is a stability degradation if μ is large enough (greater than μ_{corner}, which decreases with $\Delta\gamma$, i.e., as the hover root approaches ½/rev), the reduction in damping is order μ small. The hover damping, $Re\lambda = -\gamma/16$, is quite large for usual values of γ, and so stability is maintained for small μ, even with the influence of the periodic coefficients.

Forward flight, near 1/rev frequency.- Similar behavior is exhibited when the hover root frequency is near 1/rev. Let $\Delta\gamma = \gamma - \gamma_0$, where now γ_0 is the value of γ for which the hover root (with the given ν and K_p) is exactly at 1/rev, that is, $\gamma_0/16 = K_p + \sqrt{\nu^2 + K_p^2 - 1}$. Then if $\Delta\gamma/16$ is order small the roots are given by

$$\lambda = -\frac{\gamma}{16} + i - i\,\frac{\Delta\gamma}{16}\left(\frac{\gamma_0}{16} - K_p\right)\Big/\sqrt{\left(1 - \frac{\mu^2}{\mu_1^2}\right)\left(1 - \frac{\mu^2}{\mu_2^2}\right)} \tag{49}$$

where the corner μ are

$$\mu_1^2, \mu_2^2 = \frac{\frac{\Delta\gamma}{16}\left(\frac{\gamma_0}{16} - K_p\right)}{C_1 \pm C_2} \tag{50}$$

Expressions for C_1 and C_2 are given above (eqs. (39) and (40)), along with the results for the limit $K_p = 0$. The behavior of the μ loci is like that near ½/rev, except that here all changes are only order μ^2. For small μ there is an order μ^2 change in the frequency, toward 1/rev, while there is no change in the real part from the hover value. For $\mu = \mu_1$ or μ_2 (only one will be real) the roots reach $Im\lambda = 1/rev$, the critical region boundary. For still larger μ, the frequency is fixed at 1/rev while there is an increase of the real part of one root and a decrease of the other. The stability degradation is only order μ^2 small, so again the flap motion will remain stable for small μ and reasonable γ.

Comparisons with numerical solutions for the flap roots (from calculations by the author, and from the literature, e.g., ref. 12) indicate that the perturbation solution to order μ^2 is accurate to about $\mu = 0.5$. This solution then covers the range of interest for most helicopters.

Root loci for forward flight.- Typical μ root loci are shown in figure 1, for several cases of ν and γ. The cases considered are: (a) $\nu = 1$

and $\gamma = 10$; (b) $\nu = 1.1$ and $\gamma = 6$; and (c) $\nu = 1$ and $\gamma = 6$. The pitch/flap feedback $K_p = 0$ for all three cases. Then the hover roots, $\mu = 0$, are located on a circle with radius ν and center at the origin. Case (a) is a typical articulated blade; with the large γ and $\nu = 1$, the hover frequency is well below 1/rev. Hence, with $\mu > 0$ the locus encounters the ½/rev critical region. Case (b) is a typical cantilever blade (i.e., a hingeless rotor); with $\nu > 1$ and a lower γ, the hover frequency is above 1/rev. Hence, the locus encounters the 1/rev critical region. Case (c) is an example of the behavior when the hover frequency is away from any multiple of ½/rev. So the only influence of μ is a very small - order μ^2 - change in the frequency. The loci shown in figure 1 thus cover all the cases of away from the critical regions, near ½/rev, and near 1/rev. They illustrate the form and magnitude of the influence of forward flight. Specifically, the behavior in the critical regions at ½/rev and 1/rev frequencies is shown; and the large - order μ - effect of the ½/rev region, and the quite small effect away from all critical regions may be seen.

$\gamma - \mu$ *plane.*- The eigenvalues depend primarily on γ and μ, so the above results may be presented as contours of constant $\mathrm{Re}\lambda$ and the constant $\mathrm{Im}\lambda$ on the $\gamma - \mu$ plane. This is the presentation found in much of the literature. Such plots are shown in figures 2 to 5 for $K_p = 0$ and $\nu = 1$, 1.05, 1.1, and 1.15, respectively; and for $\nu = 1$ and $K_p = 0.1$ in figure 6. They are based on the perturbation solution given here. The expressions for the critical region boundaries in terms of the corner μ for the μ root loci may be rearranged, to give the boundary in terms of γ for a given value of μ. Writing $\gamma = \gamma_0 + \Delta\gamma$, the two real root region boundary is

$$\frac{\Delta\gamma}{16} = \mu^2 \frac{\gamma_0}{16} \frac{\frac{16}{9}\nu^2\left(-K_p + \sqrt{\nu^2 + K_p^2}\right) + K_p}{\sqrt{\nu^2 + K_p^2}} \tag{51}$$

where $\gamma_0/16 = K_p + \sqrt{\nu^2 + K_p^2}$. The ½/rev critical region boundary is

$$\frac{\Delta\gamma}{16} = \pm\mu \frac{\frac{\gamma_0}{24}\sqrt{\nu^2 - \frac{\gamma_0}{8}K_p + 4K_p^2}}{\frac{\gamma_0}{16} - K_p} \tag{52}$$

where $\gamma_0/16 = K_p + \sqrt{\nu^2 + K_p^2 - 1/4}$. And the 1/rev critical region boundary is

$$\frac{\Delta\gamma}{16} = \mu^2 \frac{C_1 \pm C_2}{\frac{\gamma_0}{16} - K_p} \tag{53}$$

where $\gamma_0/16 = K_p + \sqrt{\nu^2 + K_p^2 - 1}$, and the constants C_1 and C_2 are given above (eqs. (39) and (40)). This expression shows that C_1 gives the offset

of the 1/rev critical region boundary from γ_0, and C_2 gives the width of the region; the ½/rev region has no offset to order μ, so is symmetrical in $\Delta\gamma$ about γ_0. For $K_p = 0$ these boundaries reduce to

$$\frac{\Delta\gamma}{16} = \mu^2 \frac{16}{9} \nu^3 \qquad \text{with} \quad \frac{\gamma_0}{16} = \nu \tag{54}$$

$$\frac{\Delta\gamma}{16} = \pm\mu \frac{2}{3} \nu \qquad \text{with} \quad \frac{\gamma_0}{16} = \sqrt{\nu^2 - \frac{1}{4}} \tag{55}$$

$$\frac{\Delta\gamma}{16} = \mu^2 \left[-\frac{16}{27} \nu^2 \sqrt{\nu^2 - 1} \pm \frac{1}{2} \sqrt{1 + \frac{32}{9}(\nu^2 - 1) + \frac{256}{81} \nu^2 (\nu^2 - 1)^2} \right]$$

$$\text{with} \quad \frac{\gamma_0}{16} = \sqrt{\nu^2 - 1} \tag{56}$$

respectively. The boundaries in figures 2 to 6 were constructed using these expressions. Only the critical region and real root boundaries are shown here, but expressions for constant $\mathrm{Re}\lambda$ and $\mathrm{Im}\lambda$ may also be obtained from the perturbation solutions. The presentations of the γ - μ plane results given in the literature usually include the $\mathrm{Re}\lambda$ contours at least (since only numerical results are usually available, the γ - μ plane is the most efficient way to indicate the stability trends with γ and μ variations).

No instabilities are encountered on the γ - μ plane, for the range of parameters shown. A divergence (static) instability is encountered at high γ if $K_p < 0$, and an instability in the critical region (usually the 1/rev region first) is encountered for much higher μ (around 2). The critical regions, combinations of γ and μ where the frequency is fixed at ½ or 1/rev, are the principle effect of the periodic coefficients. Notice they encompass more and more of the γ range as μ increases, that is, as the periodic coefficients increase. The two real root region ($\mathrm{Im}\lambda = 0$, i.e., two roots on the $\mathrm{Re}\lambda$ axis) is due to γ being large enough so the flap motion has super-critical damping; while it is influenced by the periodic coefficients, it is not the same type of phenomenon as the critical regions (the roots for this case are given by the same expression as for two complex roots away from the critical regions).

A horizontal line on the γ - μ plane is a line of constant γ, hence, the variation of $\mathrm{Re}\lambda$ and $\mathrm{Im}\lambda$ as such a line is traversed gives the root locus for varying μ. For example, consider the μ locus for case (a) above, $\nu = 1$ and $\gamma = 10$; the $\gamma = 10$ line is indicated on figure 2. As μ increases from zero, the line remains parallel to $\mathrm{Re}\lambda$ = constant lines, so $\mathrm{Re}\lambda$ remains fixed at the hover value. The $\mathrm{Im}\lambda$ = ½/rev critical region comes closer to the horizontal line, indicating that the frequency of the root approaches ½/rev. At the corner μ, the locus crosses into the ½/rev region.

For higher μ the locus is in the critical region, so the frequency remains fixed at ½/rev while for each point in the region there will be two values of Reλ, one more and one less stable than the hover root. The constant γ lines for cases (b) and (c) are also shown in figures 2 and 4; the behavior of the γ - μ plane along these lines may be compared to the μ loci shown in figure 1.

Figure 7 shows the γ - μ plane for $\nu = 1$ and $K_p = 0$, from a perturbation solution equivalent to the present one but including the order μ^2 correction to the ½/rev critical region boundary. That solution, from reference 6, gives the ½/rev boundary as

$$\frac{\Delta\gamma}{16} = \pm\mu \frac{2}{3} + \mu^2 \frac{10}{9\sqrt{3}} \tag{55a}$$

to order μ^2. Figure 7 may be compared to figure 2, which is based on the present solution, hence, only to order μ in the ½/rev region. While the order μ^2 influence is not negligible for $\mu = 0.5$ or so, the major effects of forward flight are contained in the order μ solution. The results of reference 6 are discussed further below.

High μ behavior.- For μ larger than 0.5 or so, a numerical method must be used to calculate the eigenvalues of the flap motion. It is also necessary then to include the reverse flow effect in the aerodynamic flap moments. At very high μ (above 3 to 4, say) a perturbation solution based on an expansion in μ^{-1} is possible (ref. 14). Such a solution is of less use than the small μ solution, at least for current helicopters; it does, however, give some insight into the high μ behavior (refs. 14 and 15). For μ around 1, only numerical solutions are possible, unless some other parameter is used for the perturbation variable (such as γ, as in ref. 14).

At $\mu = 2.2$ or so - the exact value depends on ν, γ, and K_p, but there is not much variation for the range of parameters of current helicopters - a flapping instability is encountered. It occurs in the 1/rev critical region, the root being destabilized by the periodic coefficient influence crossing the imaginary axis into the right half plane. The γ - μ plane for $\nu = 1$ and $K_p = 0$, with μ out to 2.5, is shown in figure 8; this plot is a composite of the results available in the literature. Figures 2 and 7 give the γ - μ plane for the same ν and K_p, but for μ to 0.5 only. The behavior of the critical region boundaries at high μ, and the high μ instability in the 1/rev region are shown. The high μ behavior of the μ root loci in figure 1 may also be inferred from figure 8.

For case (c), $\nu = 1.1$ and $\gamma = 6$, the μ locus enters the 1/rev critical region at small μ. The locus remains in that region, one root moving to the left and the other to the right, until the latter branch becomes unstable (crosses the imaginary axis into the right half plane) at high μ. For case (b), $\nu = 1$ and $\gamma = 6$, the locus shows a decrease in frequency up to $\mu = 0.5$. But at somewhat higher μ the loci turn around and the frequency begins to increase, for at about $\mu = 1.1$ the roots encounter the 1/rev

critical region - see the $\gamma = 6$ line in figure 8. In the 1/rev critical region for higher μ, one branch of the locus is destabilized, until an instability is encountered at about $\mu = 2.35$.

For case (a), $\nu = 1$ and $\gamma = 10$, the μ loci also encounter the high μ instability in the 1/rev critical region, so first the roots must get from the ½/rev region to the 1/rev region (see the $\gamma = 10$ line in figure 8). As μ increases above 0.5, the loci in the ½/rev region eventually turn around, the real parts of the two branches then approaching each other instead of diverging. At μ about 1.55 the roots get back to the hover value of damping, and then break away from the ½/rev region. The frequency of the roots increases toward 1/rev then, while the damping is fixed; that is, the roots are complex conjugates again. When the roots reach 1/rev they enter the 1/rev critical region. The transition from ½/rev to 1/rev frequency occurs very quickly, during a very small μ increase, because the corridor between the two critical regions is very narrow at this point (fig. 8). In the 1/rev critical region for higher μ, one branch of the locus is destabilized then, and eventually a flapping instability is encountered at about $\mu = 2.25$.

N-BLADED ROTOR EQUATIONS OF MOTION

Consider a rotor with N independent blades, with no coupling by shaft motion and only the excitation due to the blade pitch control. The flap motion of the rotor is described by a set of N equations, each of the form of equation (3):

$$\ddot{\beta}^{(m)} + \left(\frac{\gamma}{8} + \frac{\gamma}{6}\mu \sin\psi_m\right)\dot{\beta}^{(m)} + \left\{\nu^2 + \mu \cos\psi_m\left(\frac{\gamma}{6} + \frac{\gamma}{4}\mu \sin\psi_m\right)\right.$$

$$\left. + K_p\left[\frac{\gamma}{8} + \frac{\gamma}{3}\mu \sin\psi_m + \frac{\gamma}{4}(\mu \sin\psi_m)^2\right]\right\}\beta^{(m)}$$

$$= \left[\frac{\gamma}{8} + \frac{\gamma}{3}\mu \sin\psi_m + \frac{\gamma}{4}(\mu \sin\psi_m)^2\right]\theta^{(m)} \qquad (57)$$

where $\beta^{(m)}$ is the flap degree of freedom for the mth blade, $m = 1, \ldots, N$. The azimuth location of the mth blade is $\psi_m = \psi + m\Delta\psi$, $\Delta\psi = 2\pi/N$.

For a teetering or gimballed rotor, the blades do not act independently, so the rotor motion is not described by these equations. They may be used, however, to derive the appropriate equations of motion.

TEETERING ROTOR

Equation of Motion

Consider a teetering rotor: a two-bladed rotor with a single flap hinge at the center of rotation. The two blades are not independent then, rather the rotor flaps as a whole, one blade up and one down. The equation of motion must be obtained from equilibrium of moments on the entire rotor rather than on individual blades. The coning motion of the rotor - both blades up or both down at the same time - is reacted by the structural restraint at the blade root. That is, it is a cantilever mode type of motion, for a very stiff blade, so with a very high frequency. In the teetering motion, however, the blade acts like a hinged rotor, usually, in fact, with no hub spring at all so the flap natural frequency $\nu = 1/\text{rev}$ (although the general case of $\nu \geq 1$ will be considered). Consequently, the coning motion of the rotor will be neglected as a higher frequency motion, and only the teetering degree of freedom considered.

Let β be the degree of freedom for the rotor teetering motion, so $\beta^{(2)} = \beta$ and $\beta^{(1)} = -\beta$. Equilibrium of flap moments on the entire rotor is given by half the difference between the $\beta^{(2)}$ and $\beta^{(1)}$ equations of motion. Then, the equation of motion for the teetering rotor flap motion is

$$\ddot{\beta} + \frac{\gamma}{8}\dot{\beta} + \left[\nu^2 + \frac{\gamma}{8}\mu^2 \sin 2\psi + K_p\left(\frac{\gamma}{8} + \frac{\gamma}{8}\mu^2 - \frac{\gamma}{8}\mu^2 \cos 2\psi\right)\right]\beta = 0 \qquad (58)$$

Notice that all 1/rev harmonics drop from the coefficients of β, because with the teetering motion the rotor has a period of only π with respect to the aerodynamic environment. As a consequence, all the order μ terms have dropped, leaving only the order μ^2 influence of forward flight on the coefficients of the flap equation.

Hover

For the hover limit $\mu = 0$, the roots are as before (for independent blades):

$$\lambda = -\frac{\gamma}{16} \pm i\sqrt{\nu^2 + \frac{\gamma}{8}K_p - \left(\frac{\gamma}{16}\right)^2} \qquad (59)$$

Expansion in μ^2

Only order μ^2 terms appear in the flap equation, so an expansion in μ^2 is used now:

$$\frac{\partial}{\partial \psi} = \frac{\partial}{\partial \psi_0} + \mu^2 \frac{\partial}{\partial \psi_2} + \ldots$$

$$\beta = \beta_0 + \mu^2 \beta_2 + \ldots$$

$$\gamma = \gamma_0 + \mu^2 \gamma_2 + \ldots$$

Order 1 Results

This is the hover limit again:

$$\frac{\partial^2 \beta_0}{\partial \psi_0^2} + \frac{\gamma_0}{8} \frac{\partial \beta_0}{\partial \psi_0} + \left(\nu^2 + K_p \frac{\gamma_0}{8} \right) \beta_0 = 0 \tag{60}$$

with solution

$$\beta_0 = \mathrm{Re}\left[\beta_{02}(\psi_2, \ldots) e^{\lambda_0 \psi_0} \right] \tag{61}$$

where the order 1 eigenvalue is

$$\lambda_0 = -\frac{\gamma_0}{16} + i \sqrt{\nu^2 + \frac{\gamma_0}{8} K_p - \left(\frac{\gamma_0}{16} \right)^2} \tag{62}$$

Order μ^2 Results

The order μ^2 equation is

$$- \left[\frac{\partial^2 \beta_2}{\partial \psi_0^2} + \frac{\gamma_0}{8}\frac{\partial \beta_2}{\partial \psi_0} + \left(\nu^2 + K_p \frac{\gamma_0}{8}\right)\beta_2\right]$$

$$= 2\frac{\partial^2 \beta_0}{\partial \psi_0 \partial \psi_2} + \frac{\gamma_0}{8}\frac{\partial \beta_0}{\partial \psi_2} + \frac{\gamma_2}{8}\frac{\partial \beta_0}{\partial \psi_0}$$

$$+ \left(\frac{\gamma_0}{8}\sin 2\psi_0 + K_p \frac{\gamma_2}{8} + K_p \frac{\gamma_0}{8} - K_p \frac{\gamma_0}{8}\cos 2\psi_0\right)\beta_0$$

$$= \left\{\left(2\lambda_0 + \frac{\gamma_0}{8}\right)\frac{\partial \beta_{02}}{\partial \psi_2} + \left[\frac{\gamma_2}{8}(\lambda_0 + K_p) + \frac{\gamma_0}{8}K_p\right]\beta_{02}\right\}e^{\lambda_0 \psi_0}$$

$$+ \frac{\gamma_0}{16}(-i - K_p)\beta_{02}e^{(\lambda_0+2i)\psi_0}$$

$$+ \frac{\gamma_0}{16}(i - K_p)\beta_{02}e^{(\lambda_0-2i)\psi_0}$$

$$+ \text{conjugate} \qquad (63)$$

Assuming that $\overline{\lambda}_0 + 2i \neq \lambda_0$, that is, $\mathrm{Im}\lambda_0 \neq 1/\mathrm{rev}$, then the secular term is

$$\left(2\lambda_0 + \frac{\gamma_0}{8}\right)\frac{\partial \beta_{02}}{\partial \psi_2} + \left[\frac{\gamma_2}{8}(\lambda_0 + K_p) + \frac{\gamma_0}{8}K_p\right]\beta_{02} = 0$$

or

$$\frac{\partial \beta_{02}}{\partial \psi_2} - \lambda_2 \beta_{02} = 0 \qquad (64)$$

where

$$\lambda_2 = -\frac{\frac{\gamma_0}{8}(\lambda_0 + K_p) + \frac{\gamma_0}{8}K_p}{2i\,\mathrm{Im}\lambda_0}$$

The solution is

$$\beta_{02} = \beta_{04}(\psi_4, \ldots)e^{\lambda_2 \psi_2} \qquad (65)$$

So

$$\beta = \mathrm{Re}\left(\beta_{04} e^{\lambda_0 \psi_0 + \lambda_2 \psi_2}\right) + O(\mu^2) \tag{66}$$

Then, for $\mathrm{Im}\lambda_0 \neq 1$, the eigenvalue to order μ^2 is

$$\lambda = \lambda_0 + \mu^2 \lambda_2$$

$$= -\frac{\gamma}{16} \pm i \sqrt{\nu^2 + (1 + \mu^2)\frac{\gamma}{8} K_p - \left(\frac{\gamma}{16}\right)^2} \tag{67}$$

The only influence of forward flight on the eigenvalues of the teetering rotor is then the increase in the mean of $K_p M_\theta$ (to order μ^2, and for $\mathrm{Im}\lambda_0 \neq 1$). This result is substantially simpler than for the independent blade, with much less influence of the periodic coefficients. The difference is the result of the internal cancelling of the 1/rev, order μ flap moments for the teetering rotor. In fact, if $K_p = 0$ there is no order μ^2 influence on the roots at all, they remain at the hover values; if $K_p > 0$ there is an order μ^2 increase in the frequency, due to the increased effectiveness of K_p acting through M_θ.

The divergence criterion ($\lambda = 0$), becomes now, for stability

$$(1 + \mu^2)\frac{\gamma}{8} K_p > -\nu^2 \tag{68}$$

This is a stricter requirement on K_p than for the independent blade (i.e., the boundary is reached at a negative K_p of smaller magnitude), but the difference is only order μ^2. The two real root boundary ($\mathrm{Im}\lambda = 0$) is

$$\frac{\gamma}{16} = \left(K_p + \sqrt{\nu^2 + K_p^2}\right)\left(1 + \mu^2 \frac{K_p}{\sqrt{\nu^2 + K_p^2}}\right) \tag{69}$$

or for $K_p = 0$, $\gamma/16 = \nu$.

Near 1/rev Frequency

Return now to the case $\bar{\lambda}_0 + 2i = \lambda_0$, that is, $\mathrm{Im}\lambda_0 = 1$, the hover frequency near 1/rev. This means $\gamma_0/16 = K_p + \sqrt{\nu^2 + K_p^2} - 1$, and the order 1 root is $\lambda_0 = -(\gamma_0/16) + i$. Now the periodic coefficients contribute to the secular term, to give

$$\frac{\partial \beta_{02}}{\partial \psi_2} - \lambda_2 \beta_{02} + i \frac{\gamma_0}{32} (i + K_p) \bar{\beta}_{02} = 0 \tag{70}$$

where since $\mathrm{Im}\lambda_0 = 1$,

$$\lambda_2 = - \frac{\gamma_2}{16} + i \left[\frac{\gamma_2}{16} \left(- \frac{\gamma_0}{16} + K_p \right) + \frac{\gamma_0}{16} K_p \right] .$$

The solution depends on

$$D^2 = \left[\frac{\gamma_2}{16} \left(- \frac{\gamma_0}{16} + K_p \right) + K_p \frac{\gamma_0}{16} \right]^2 - \left(\frac{\gamma_0}{32} \right)^2 (1 + K_p^2) \tag{71}$$

The critical region boundary is given by $D^2 = 0$, or writing $\gamma = \gamma_0 + \Delta\gamma$, with $\Delta\gamma$ order μ^2 small:

$$\frac{\Delta\gamma}{16} \left(\frac{\gamma_0}{16} - K_p \right) = \mu^2 \left(K_p \frac{\gamma_0}{16} \pm \frac{\gamma_0}{32} \sqrt{1 + K_p^2} \right) \tag{72}$$

In terms of the μ locus, this gives the corner μ:

$$\mu_1^2, \mu_2^2 = \frac{\frac{\Delta\gamma}{16} \left(\frac{\gamma_0}{16} - K_p \right)}{K_p \frac{\gamma_0}{16} \pm \frac{\gamma_0}{32} \sqrt{1 + K_p^2}} \tag{73}$$

This expression is similar to that for the 1/rev region boundary of the independent blade (eq. (41)), but with

$$\left. \begin{aligned} C_1 &= K_p \frac{\gamma_0}{16} \\ C_2 &= \frac{\gamma_0}{32} \sqrt{1 + K_p^2} \end{aligned} \right\} \tag{74}$$

that is, with considerably less influence of the periodic coefficients. The eigenvalue is

$$\lambda = \lambda_0 + \mu^2 \mathrm{Re}\lambda_2 - i\mu^2 D$$

$$= -\frac{\gamma}{16} + i - i\frac{\Delta\gamma}{16}\left(\frac{\gamma_0}{16} - K_p\right)\sqrt{\left(1 - \frac{\mu^2}{\mu_1{}^2}\right)\left(1 - \frac{\mu^2}{\mu_2{}^2}\right)} \qquad (75)$$

which is identical to the independent blade result (eq. (43)), except that the corner μ have different values. For $K_p = 0$, the criterion $\mathrm{Im}\lambda_0 = 1$ reduces to $\gamma_0/16 = \sqrt{\nu^2 - 1}$, the 1/rev boundary is $\mu_1{}^2, \mu_2{}^2 = \pm 2(\Delta\gamma/16)$, and the eigenvalue reduces to

$$\lambda = -\frac{\gamma}{16} + i - i\sqrt{\nu^2 - 1}\sqrt{\left(\frac{\Delta\gamma}{16}\right)^2 - \frac{\mu^4}{4}} \qquad (76)$$

For $\nu = 1$ (and $K_p = 0$) this is the same boundary as for the independent blade. For $\nu > 1$, the critical region has a smaller width, and is not offset ($C_1 = 0$ still, since $K_p = 0$).

Summary

The influence of forward flight on the teetering rotor differs from that on the individual blade principally in that: there is no ½/rev critical region at all; and the periodic coefficient influence is much simpler. Away from the 1/rev region, the roots are given by

$$\lambda = -\frac{\gamma}{16} \pm i\sqrt{\nu^2 + (1 + \mu^2)\frac{\gamma}{8}K_p - \left(\frac{\gamma}{16}\right)^2} \qquad (77)$$

including the forward flight influence to order μ^2. The corresponding criterion for divergence stability is

$$(1 + \mu^2)\frac{\gamma}{8}K_p > -\nu^2 \qquad (78)$$

There is no ½/rev critical region, so this expression holds also when the hover frequency is near ½/rev. A critical region is encountered only if the hover frequency is near 1/rev. That is, if $\Delta\gamma = \gamma - \gamma_0$ is order μ^2 small, where $\gamma_0/16 = K_p + \sqrt{\nu^2 + K_p{}^2 - 1}$, then the roots are

$$\lambda = -\frac{\gamma}{16} + i - i\frac{\Delta\gamma}{16}\left(\frac{\gamma_0}{16} - K_p\right)\sqrt{\left(1 - \frac{\mu^2}{\mu_1{}^2}\right)\left(1 - \frac{\mu^2}{\mu_2{}^2}\right)} \qquad (79)$$

where the corner μ are

$$\mu_1^2, \mu_2^2 = \frac{\frac{\Delta\gamma}{16}\left(\frac{\gamma_0}{16} - K_p\right)}{C_1 \pm C_2} \tag{80}$$

and the constants C_1 and C_2 are given above (eq. (74)). For $K_p = 0$, this reduces to $\mu^2_{corner} = \pm 2(\Delta\gamma/16)$.

The $\gamma - \mu$ plane boundaries are, writing $\gamma = \gamma_0 + \Delta\gamma$, for the two real root region

$$\frac{\Delta\gamma}{16} = \mu^2 \frac{\gamma_0}{16} \frac{K_p}{\sqrt{\nu^2 + K_p^2}} \tag{81}$$

where $\gamma_0/16 = K_p + \sqrt{\nu^2 + K_p^2}$; and for the 1/rev critical region

$$\frac{\Delta\gamma}{16} = \mu^2 \frac{K_p \frac{\gamma_0}{16} \pm \frac{\gamma_0}{32}\sqrt{1 + K_p^2}}{\frac{\gamma_0}{16} - K_p} \tag{82}$$

where $\gamma_0/16 = K_p + \sqrt{\nu^2 + K_p^2 - 1}$. For $K_p = 0$ these boundaries reduce to

$$\frac{\Delta\gamma}{16} = 0 \qquad \text{with} \quad \frac{\gamma_0}{16} = \nu \tag{83}$$

$$\frac{\Delta\gamma}{16} = \pm \frac{1}{2}\mu^2 \qquad \text{with} \quad \frac{\gamma_0}{16} = \sqrt{\nu^2 - 1} \tag{84}$$

respectively. These results may be compared with the $\gamma - \mu$ plane boundaries of the independent blade, as illustrated in figures 2 to 6. For $K_p = 0$, the two real root boundary is now a constant γ line, that is, a horizontal line; there is no ½/rev region at all; and the 1/rev region is the same when $\nu = 1$, but narrower and not offset ($C_1 = 0$) when $\nu > 1$.

Consider the μ root loci of the teetering rotor. When $K_p = 0$, as in figure 1 for the independent blade, then for case (a) with $\nu = 1$ and $\gamma = 10$, and case (b) with $\nu = 1$ and $\gamma = 6$ - that is, away from the 1/rev critical region - there is no effect of μ at all to order μ^2. The locus remains at the hover value. For case (c) with $\nu = 1.1$ and $\gamma = 6$, that is, near 1/rev, the behavior is basically the same as for the independent blade. However, the critical region is narrower now, and not offset, resulting in a higher value for μ_{corner} (0.407 compared to 0.286 for the independent blade). Notice that if the hover root frequency were below 1/rev, then μ_{corner} would probably decrease because of the absence of the critical region offset with the teetering rotor; this is best seen on the $\gamma - \mu$ plane, as in figure 4.

There is then considerably less influence of the periodic aerodynamic forces on the teetering rotor flap stability, as compared to the independent blade. This is the result of the internal cancelling of all the 1/rev, order μ flap moments. Specifically, there is no ½/rev critical region, because of the absence of 1/rev harmonics in the coefficients; the 1/rev critical region is narrower, in general, and not offset if $K_P = 0$; and there is less influence of μ on the two real root boundary. If $K_P = 0$, the two real root boundary does not change at all with μ; this corresponds to the absence of a ½/rev critical region, which for the independent blade pushes the 0/rev boundary up (as in figure 2).

In fact, unless the frequency of the hover root is near 1/rev - and the 1/rev critical region is quite narrow, being only order μ^2 wide - then using a constant coefficient approximation gives exactly the correct eigenvalues to order μ^2. That is, if the periodic coefficients in equation (58) are simply dropped - and they are the reason for all this perturbation analysis - then the only effect of μ retained is the increase of the mean of M_θ by the factor $(1 + \mu^2)$; but that is the only effect that appears in the correct roots for the teetering rotor anyway. This suggests that such a constant coefficient approximation may be an adequate representation for the teetering rotor flapping dynamics (if the frequency of the root is kept away from 1/rev).

GIMBALLED ROTOR, THREE BLADES

Equations of Motion

Consider a gimballed rotor: three or more blades attached to a hub with cantilever root restraint, and the hub to the rotor shaft by a universal joint. The possibility of a hub spring is included, so $\nu \geq 1$ is allowed still. The blades do not move independently now, rather the entire rotor moves as a whole about the gimbal bearings. There are two degrees of freedom describing the rotor flap motion: longitudinal tip path plane tilt β_{1C} and lateral tip path plane tilt β_{1S}. The variables describe the rotor motion in the nonrotating frame; β_{1C} is defined positive for tilt forward, and β_{1S} is positive for tilt toward the retreating side. All other modes of motion of the rotor blades - such as the coning motion - are reacted by the cantilever root stiffness, so will be neglected as higher frequency motions.

The flap motion of the mth blade is given now by

$$\beta^{(m)} = \beta_{1C} \cos \psi_m + \beta_{1S} \sin \psi_m \tag{85}$$

The equations of motion for the gimballed rotor tip path plane tilt are obtained from equilibrium of the pitch and roll moments on the hub. The equations may be obtained from the flap moment equilibrium for the mth blade (eq. (57)) by the operators

$$\frac{2}{N}\sum_{m=1}^{N}(\ .\ .\ .)\cos\psi_m,\quad \frac{2}{N}\sum_{m=1}^{N}(\ .\ .\ .)\sin\psi_m \tag{86}$$

The result of the summation operation depends on N when, as here, the equations have periodic coefficients. For a three bladed gimballed rotor, N = 3, the result is

$$\begin{pmatrix}\beta_{1c}\\ \beta_{1s}\end{pmatrix}'' + \begin{bmatrix}\frac{\gamma}{8} + \mu\frac{\gamma}{12}\sin 3\psi & 2 - \mu\frac{\gamma}{12}\cos 3\psi\\ -2 - \mu\frac{\gamma}{12}\cos 3\psi & \frac{\gamma}{8} - \mu\frac{\gamma}{12}\sin 3\psi\end{bmatrix}\begin{pmatrix}\beta_{1c}\\ \beta_{1s}\end{pmatrix}'$$

$$+ \begin{bmatrix}\nu^2 - 1 + \mu\frac{\gamma}{6}\cos 3\psi & \frac{\gamma}{8}\left(1 + \frac{\mu^2}{2}\right) + \mu\frac{\gamma}{6}\sin 3\psi\\ -\frac{\gamma}{8}\left(1 - \frac{\mu^2}{2}\right) + \mu\frac{\gamma}{6}\sin 3\psi & \nu^2 - 1 - \mu\frac{\gamma}{6}\cos 3\psi\end{bmatrix}\begin{pmatrix}\beta_{1c}\\ \beta_{1s}\end{pmatrix}$$

$$= \begin{bmatrix}\frac{\gamma}{8}\left(1 + \frac{\mu^2}{2}\right) + \mu\frac{\gamma}{6}\sin 3\psi & -\mu\frac{\gamma}{6}\cos 3\psi\\ -\mu\frac{\gamma}{6}\cos 3\psi & \frac{\gamma}{8}\left(1 + \frac{3}{2}\mu^2\right) - \mu\frac{\gamma}{6}\sin 3\psi\end{bmatrix}\begin{pmatrix}\theta_{1c} - K_p\beta_{1c}\\ \theta_{1s} - K_p\beta_{1s}\end{pmatrix} \tag{87}$$

The cases of N = 4 and N $\geq$ 5 will be considered in later sections. The notation

$$\vec{\beta} = \begin{pmatrix}\beta_{1c}\\ \beta_{1s}\end{pmatrix}$$

will be used for the degrees of freedom.

Hover

In the hover limit, $\mu = 0$, the differential equation is

$$\ddot{\vec{\beta}} + \begin{bmatrix}\frac{\gamma}{8} & 2\\ -2 & \frac{\gamma}{8}\end{bmatrix}\dot{\vec{\beta}} + \begin{bmatrix}\nu^2 - 1 + K_p\frac{\gamma}{8} & \frac{\gamma}{8}\\ -\frac{\gamma}{8} & \nu^2 - 1 + K_p\frac{\gamma}{8}\end{bmatrix}\vec{\beta} = 0 \tag{88}$$

The characteristic equation is

$$\left(\lambda^2 + \frac{\gamma}{8}\lambda + \nu^2 - 1 + K_p\frac{\gamma}{8}\right)^2 + \left(2\lambda + \frac{\gamma}{8}\right)^2 = 0 \tag{89}$$

which has the solutions $\lambda = \lambda_0 \pm i$ and their conjugates, where

$$\lambda_0 = -\frac{\gamma}{16} + i\sqrt{\nu^2 + \frac{\gamma}{8}K_p - \left(\frac{\gamma}{16}\right)^2} \tag{90}$$

is the rotating hover root. So the hover roots for the gimbal degrees of freedom, which are in the nonrotating frame, are just the rotating roots ±1/rev frequency due to the transfer from rotating to nonrotating coordinates. This hover result $\lambda_{NR} = \lambda_R \pm i$ is true for any number of blades, in fact. In forward flight the result is not this simple because the blades of a gimballed rotor are not independent.

There are two degrees of freedom, hence, a total of four eigenvalues. There is a high frequency mode with roots $\lambda_0 + i$ and its conjugate, that is, at frequency $\mathrm{Im}\lambda_0 + 1/\mathrm{rev}$; and a low frequency mode with roots $\lambda_0 \quad i$ and its conjugate, that is, at frequency $\mathrm{Im}\lambda_0 - 1/\mathrm{rev}$. The correspondence between the rotating and nonrotating regions is then as follows:

Rotating frequency	Nonrotating frequency
0/rev	1/rev
½/rev	½ and 3/2/rev
1/rev	0 and 2/rev

The 0/rev rotating frequency means two real roots; it includes the case of divergence instability. The regions, boundaries, and behavior of the roots will be discussed in terms of the *rotating* frequencies, so that the results may be compared with those of the single blade analysis.

The eigenvectors for the roots $\lambda_0 \pm i$ are

$$\begin{pmatrix}\beta_{1c}\\ \beta_{1s}\end{pmatrix} = \begin{pmatrix}\pm i\\ 1\end{pmatrix} \tag{91}$$

that is, $\beta_{1c}/\beta_{1s} = \pm i$; this corresponds to a wobbling or whirling motion of the tip path plane.

Expansion in μ

Let

$$\frac{\partial}{\partial\psi} = \frac{\partial}{\partial\psi_0} + \mu\frac{\partial}{\partial\psi_1} + \mu^2\frac{\partial}{\partial\psi_2} + \cdots$$

$$\vec{\beta} = \vec{\beta}_0 + \mu\vec{\beta}_1 + \mu^2\vec{\beta}_2 + \cdots$$

$$\gamma = \gamma_0 + \mu\gamma_1 + \mu^2\gamma_2 + \cdots$$

Order 1 Results

The order 1 equation is just the hover limit as usual:

$$\frac{\partial^2\vec{\beta}_0}{\partial\psi_0^2} + \begin{bmatrix} \frac{\gamma_0}{8} & 2 \\ -2 & \frac{\gamma_0}{8} \end{bmatrix}\frac{\partial\vec{\beta}_0}{\partial\psi_0} + \begin{bmatrix} \nu^2 - 1 + K_p\frac{\gamma_0}{8} & \frac{\gamma_0}{8} \\ -\frac{\gamma_0}{8} & \nu^2 - 1 + K_p\frac{\gamma_0}{8} \end{bmatrix}\vec{\beta}_0 = 0 \qquad (92)$$

The order 1 eigenvalues are then $\lambda = \lambda_0 \pm i$ and the conjugates, where

$$\lambda_0 = -\frac{\gamma_0}{16} + i\sqrt{\nu^2 + \frac{\gamma_0}{8}K_p - \left(\frac{\gamma_0}{16}\right)^2} \qquad (93)$$

is the order 1 rotating hover root. The corresponding eigenvectors are $\beta_{1c}/\beta_{1s} = \pm i$, so the solution for $\vec{\beta}_0$ is

$$\vec{\beta}_0 = \mathrm{Re}\left[\beta_{01+}\begin{pmatrix} i \\ 1 \end{pmatrix}e^{(\lambda_0+i)\psi_0} + \beta_{01-}\begin{pmatrix} -i \\ 1 \end{pmatrix}e^{(\lambda_0-i)\psi_0}\right] \qquad (94)$$

The first term (subscript +) is the high frequency mode, the second (subscript -) the low frequency mode; $\beta_{01\pm}$ are complex functions of the higher time scales ψ_1, ψ_2, etc.

Order μ Results

The order μ equation is

$$
-\left\{\frac{\partial^2\vec{\beta}_1}{\partial\psi_0^2}+\begin{bmatrix}\frac{\gamma_0}{8} & 2\\ -2 & \frac{\gamma_0}{8}\end{bmatrix}\frac{\partial\vec{\beta}_1}{\partial\psi_0}+\begin{bmatrix}\nu^2-1+Kp\frac{\gamma_0}{8} & \frac{\gamma_0}{8}\\ -\frac{\gamma_0}{8} & \nu^2-1+Kp\frac{\gamma_0}{8}\end{bmatrix}\vec{\beta}_1\right\}
$$

$$
=2\frac{\partial^2\vec{\beta}_0}{\partial\psi_0\,\partial\psi_1}+\begin{bmatrix}\frac{\gamma_0}{8} & 2\\ -2 & \frac{\gamma_0}{8}\end{bmatrix}\frac{\partial\vec{\beta}_0}{\partial\psi_1}+\begin{bmatrix}\frac{\gamma_1}{8}+\frac{\gamma_0}{12}\sin 3\psi_0 & -\frac{\gamma_0}{12}\cos 3\psi_0\\ -\frac{\gamma_0}{12}\cos 3\psi_0 & \frac{\gamma_1}{8}-\frac{\gamma_0}{12}\sin 3\psi_0\end{bmatrix}\frac{\partial\vec{\beta}_0}{\partial\psi_0}
$$

$$
+\begin{bmatrix}\frac{\gamma_0}{6}\cos 3\psi_0+Kp\frac{\gamma_1}{8}+Kp\frac{\gamma_0}{6}\sin 3\psi_0 & \frac{\gamma_1}{8}+\frac{\gamma_0}{6}\sin 3\psi_0-Kp\frac{\gamma_0}{6}\cos 3\psi_0\\ -\frac{\gamma_1}{8}+\frac{\gamma_0}{6}\sin 3\psi_0-Kp\frac{\gamma_0}{6}\cos 3\psi_0 & -\frac{\gamma_0}{6}\cos 3\psi_0+Kp\frac{\gamma_1}{8}-Kp\frac{\gamma_0}{6}\sin 3\psi_0\end{bmatrix}\vec{\beta}_0
$$

$$
=\left[\left(2\lambda_0+\frac{\gamma_0}{8}\right)\frac{\partial\beta_{01+}}{\partial\psi_1}+\frac{\gamma_1}{8}(\lambda_0+Kp)\beta_{01+}\right]\begin{pmatrix}i\\1\end{pmatrix}e^{(\lambda_0+i)\psi_0}
$$

$$
-i\frac{\gamma_0}{12}(\lambda_0-i+2Kp)\beta_{01+}\begin{pmatrix}-i\\1\end{pmatrix}e^{(\lambda_0-2i)\psi_0}
$$

$$
+\left[\left(2\lambda_0+\frac{\gamma_0}{8}\right)\frac{\partial\beta_{01-}}{\partial\psi_1}+\frac{\gamma_1}{8}(\lambda_0+Kp)\beta_{01-}\right]\begin{pmatrix}-i\\1\end{pmatrix}e^{(\lambda_0-i)\psi_0}
$$

$$
+i\frac{\gamma_0}{12}(\lambda_0+i+2Kp)\beta_{01-}\begin{pmatrix}i\\1\end{pmatrix}e^{(\lambda_0+2i)\psi_0}
$$

$$
+\text{ conjugate} \qquad (95)
$$

The secular terms are the coefficients of the homogeneous solution

$$
\begin{pmatrix}\pm i\\1\end{pmatrix}e^{(\lambda_0\pm i)\psi_0}
$$

on the right-hand side of equation (95). Notice there are two homogeneous solutions now (really four, including the complex conjugates), as in equation (94), and the coefficients of each must be set to zero. The resulting equations give the order μ corrections to the roots for the high and low frequency modes.

Assuming for now that $\mathrm{Im}\lambda_0 \neq \frac{1}{2}$/rev, then the secular terms are

$$\left(2\lambda_0 + \frac{\gamma_0}{8}\right)\frac{\partial \beta_{01\pm}}{\partial \psi_1} + \frac{\gamma_1}{8}(\lambda_0 + K_p)\beta_{01\pm} = 0$$

or

$$\frac{\partial \beta_{01\pm}}{\partial \psi_1} - \lambda_1 \beta_{01\pm} = 0 \tag{96}$$

where

$$\lambda_1 = -\frac{\frac{\gamma_1}{8}(\lambda_0 + K_p)}{2i\mathrm{Im}\lambda_0}$$

The solution is $\beta_{01\pm} = \beta_{02\pm}(\psi_2, \ldots)e^{\lambda_1 \psi_1}$, so the solution for $\vec{\beta}_0$ is

$$\vec{\beta}_0 = \mathrm{Re}\left[\beta_{02+}\begin{pmatrix} i \\ 1 \end{pmatrix} e^{(\lambda_0+i)\psi_0+\lambda_1\psi_1} + \beta_{02-}\begin{pmatrix} -i \\ 1 \end{pmatrix} e^{(\lambda_0-i)\psi_0+\lambda_1\psi_1}\right] \tag{97}$$

Hence, the eigenvalues to order μ are

$$\begin{aligned} \lambda &= \lambda_0 \pm i + \mu\lambda_1 \\ &= -\frac{\gamma}{16} + i\sqrt{\nu^2 + \frac{\gamma}{8}K_p - \left(\frac{\gamma}{16}\right)^2} \pm i \end{aligned} \tag{98}$$

which is just the rotating hover root $\pm i$ still. With the secular terms set to zero, the solution of equation (95) is

$$\begin{aligned} \vec{\beta}_1 = \mathrm{Re}\Bigg[&\beta_{11+}\begin{pmatrix} i \\ 1 \end{pmatrix} e^{(\lambda_0+i)\psi_0} + \beta_{11-}\begin{pmatrix} -i \\ 1 \end{pmatrix} e^{(\lambda_0-i)\psi_0} \\ &+ A_+\beta_{01+}\begin{pmatrix} -i \\ 1 \end{pmatrix} e^{(\lambda_0-2i)\psi_0} + A_-\beta_{01-}\begin{pmatrix} i \\ 1 \end{pmatrix} e^{(\lambda_0+2i)\psi_0}\Bigg] \end{aligned} \tag{99}$$

where

$$A_\pm = -\frac{\gamma_0}{12}\frac{(\lambda_0 + 2K_p \mp i)(\mp i)}{\pm 2\mathrm{Im}\lambda_0 - 1}$$

which completes the solution to order μ.

Order μ^2 Results

The order μ^2 equation is

$$
-\left\{\frac{\partial^2\vec{\beta}_2}{\partial\psi_0^2}+\begin{bmatrix}\frac{\gamma_0}{8} & 2\\ -2 & \frac{\gamma_0}{8}\end{bmatrix}\frac{\partial\vec{\beta}_2}{\partial\psi_0}+\begin{bmatrix}\nu^2-1+\frac{\gamma_0}{8}K_p & \frac{\gamma_0}{8}\\ -\frac{\gamma_0}{8} & \nu^2-1+\frac{\gamma_0}{8}K_p\end{bmatrix}\vec{\beta}_2\right\}
$$

$$
=2\frac{\partial^2\vec{\beta}_1}{\partial\psi_0\,\partial\psi_1}+\begin{bmatrix}\frac{\gamma_0}{8} & 2\\ -2 & \frac{\gamma_0}{8}\end{bmatrix}\frac{\partial\vec{\beta}_1}{\partial\psi_1}+\begin{bmatrix}\frac{\gamma_1}{8}+\frac{\gamma_0}{12}\sin 3\psi_0 & -\frac{\gamma_0}{12}\cos 3\psi_0\\ -\frac{\gamma_0}{12}\cos 3\psi_0 & \frac{\gamma_1}{8}-\frac{\gamma_0}{12}\sin 3\psi_0\end{bmatrix}\frac{\partial\vec{\beta}_1}{\partial\psi_0}
$$

$$
+\begin{bmatrix}\frac{\gamma_0}{6}\cos 3\psi_0+K_p\frac{\gamma_1}{8}+K_p\frac{\gamma_0}{6}\sin 3\psi_0 & \frac{\gamma_1}{8}+\frac{\gamma_0}{6}\sin 3\psi_0-K_p\frac{\gamma_0}{6}\cos 3\psi_0\\ -\frac{\gamma_1}{8}+\frac{\gamma_0}{6}\sin 3\psi_0-K_p\frac{\gamma_0}{6}\cos 3\psi_0 & -\frac{\gamma_0}{6}\cos 3\psi_0+K_p\frac{\gamma_1}{8}-K_p\frac{\gamma_0}{6}\sin 3\psi_0\end{bmatrix}\vec{\beta}_1
$$

$$
+\frac{\partial^2\vec{\beta}_0}{\partial\psi_1^2}+2\frac{\partial^2\vec{\beta}_0}{\partial\psi_0\,\partial\psi_2}+\begin{bmatrix}\frac{\gamma_0}{8} & 2\\ -2 & \frac{\gamma_0}{8}\end{bmatrix}\frac{\partial\vec{\beta}_0}{\partial\psi_2}+\begin{bmatrix}\frac{\gamma_1}{8}+\frac{\gamma_0}{12}\sin 3\psi_0 & -\frac{\gamma_0}{12}\cos 3\psi_0\\ -\frac{\gamma_0}{12}\cos 3\psi_0 & \frac{\gamma_1}{8}-\frac{\gamma_0}{12}\sin 3\psi_0\end{bmatrix}\frac{\partial\vec{\beta}_0}{\partial\psi_1}
$$

$$
+\begin{bmatrix}\frac{\gamma_2}{8}+\frac{\gamma_1}{12}\sin 3\psi_0 & -\frac{\gamma_1}{12}\cos 3\psi_0\\ -\frac{\gamma_1}{12}\cos 3\psi_0 & \frac{\gamma_2}{8}-\frac{\gamma_1}{12}\sin 3\psi_0\end{bmatrix}\frac{\partial\vec{\beta}_0}{\partial\psi_0}+\begin{bmatrix}\frac{\gamma_2}{8}K_p+\frac{\gamma_0}{16}K_p & \frac{\gamma_2}{8}+\frac{\gamma_0}{16}\\ -\frac{\gamma_2}{8}+\frac{\gamma_0}{16} & K_p\frac{\gamma_2}{8}+K_p3\frac{\gamma_0}{16}\end{bmatrix}\vec{\beta}_0
$$

$$
+\begin{bmatrix}\frac{\gamma_1}{6}\cos 3\psi_0+K_p\frac{\gamma_1}{6}\sin 3\psi_0 & \frac{\gamma_1}{6}\sin 3\psi_0-K_p\frac{\gamma_1}{6}\cos 3\psi_0\\ \frac{\gamma_1}{6}\sin 3\psi_0-K_p\frac{\gamma_1}{6}\cos 3\psi_0 & -\frac{\gamma_1}{6}\cos 3\psi_0-K_p\frac{\gamma_1}{6}\sin 3\psi_0\end{bmatrix}\vec{\beta}_0
$$

$$
\begin{aligned}
= &\left\{\left(2\lambda_0 + \frac{\gamma_0}{8}\right)\frac{\partial \beta_{11+}}{\partial \psi_1} + \frac{\gamma_1}{8}(\lambda_0 + K_p)\beta_{11+} + \left(2\lambda_0 + \frac{\gamma_0}{8}\right)\frac{\partial \beta_{01+}}{\partial \psi_2}\right.\\
&+ \frac{\partial^2 \beta_{01+}}{\partial \psi_1^{\,2}} + \frac{\gamma_1}{8}\frac{\partial \beta_{01+}}{\partial \psi_1} + \left[\frac{\gamma_2}{8}(\lambda_0 + K_p) + \frac{\gamma_0}{8}K_p + \frac{\gamma_0}{12}(\lambda_0 + 2K_p)iA_+\right]\beta_{01+}\Bigg\}\binom{i}{1}e^{(\lambda_0+i)\psi_0}\\
&+ \left[\frac{\gamma_0}{16}(i + K_p)\beta_{01+}\right]\binom{-i}{1}e^{(\lambda_0+i)\psi_0}\\
&+ \left\{\frac{\gamma_0}{12}(-i)(\lambda_0 + 2K_p - i)\beta_{11+} + \left[\frac{\gamma_0}{12}(-i) + \left(2\lambda_0 + \frac{\gamma_0}{8} - 2i\right)A_+\right]\frac{\partial \beta_{01+}}{\partial \psi_1}\right.\\
&\left.+ \left[\frac{\gamma_1}{12}(-i)(\lambda_0 + 2K_p - i) + \frac{\gamma_1}{8}(\lambda_0 + K_p - i)A_+\right]\beta_{01+}\right\}\binom{-i}{1}e^{(\lambda_0-2i)\psi_0}\\
&+ \left\{\left(2\lambda_0 + \frac{\gamma_0}{8}\right)\frac{\partial \beta_{11-}}{\partial \psi_1} + \frac{\gamma_1}{8}(\lambda_0 + K_p)\beta_{11-} + \left(2\lambda_0 + \frac{\gamma_0}{8}\right)\frac{\partial \beta_{01-}}{\partial \psi_2} + \frac{\partial^2 \beta_{01-}}{\partial \psi_1^{\,2}}\right.\\
&\left.+ \frac{\gamma_1}{8}\frac{\partial \beta_{01-}}{\partial \psi_1} + \left[\frac{\gamma_2}{8}(\lambda_0 + K_p) + \frac{\gamma_0}{8}K_p + \frac{\gamma_0}{8}(\lambda_0 + 2K_p)(-i)A_-\right]\beta_{01-}\right\}\binom{-i}{1}e^{(\lambda_0-i)\psi_0}\\
&+ \left[\frac{\gamma_0}{16}(-i + K_p)\beta_{01-}\right]\binom{i}{1}e^{(\lambda_0-i)\psi_0}\\
&+ \left\{\frac{\gamma_0}{12}i(\lambda_0 + 2K_p + i)\beta_{11-} + \left[\frac{\gamma_0}{12}i + \left(2\lambda_0 + \frac{\gamma_0}{8} + 2i\right)A_-\right]\frac{\partial \beta_{01-}}{\partial \psi_1}\right.\\
&\left.+ \left[\frac{\gamma_1}{12}i(\lambda_0 + 2K_p + i) + \frac{\gamma_1}{8}(\lambda_0 + K_p + i)A_-\right]\beta_{01-}\right\}\binom{i}{1}e^{(\lambda_0+2i)\psi_0}
\end{aligned}
\tag{100}
$$

+ conjugate

Assuming that $\mathrm{Im}\lambda_0 \neq 1$, the secular term is

$$\left(\frac{\partial \beta_{11\pm}}{\partial \psi_1} - \lambda_1 \beta_{11\pm}\right)$$

$$= \left\{\frac{\partial \beta_{02\pm}}{\partial \psi_2} + \left[-\lambda_2 + \frac{\frac{\gamma_0}{8} Kp + \frac{\gamma_0}{12}(\lambda_0 + 2Kp)(\pm i)A_\pm}{2iIm\lambda_0}\right]\beta_{02\pm}\right\} e^{\lambda_1 \psi_1} \qquad (101)$$

and the secular term of this is

$$\frac{\partial \beta_{02\pm}}{\partial \psi_2} + \left[-\lambda_2 + \frac{\frac{\gamma_0}{8} Kp + \frac{\gamma_0}{12}(\lambda_0 + 2Kp)(\pm i)A_\pm}{2iIm\lambda_0}\right]\beta_{02\pm} = 0 \qquad (102)$$

It follows that the eigenvalues to order μ^2 are

$$\lambda = \pm i + \lambda_0 + \mu\lambda_1 + \mu^2\left[\lambda_2 + i\,\frac{\frac{\gamma_0}{8} Kp + \frac{\gamma_0}{12}(\lambda_0 + 2Kp)(\pm i)A_\pm}{2Im\lambda_0}\right]$$

$$= \pm i - \frac{\gamma}{16} + i\sqrt{\nu^2 + (1+\mu^2)\frac{\gamma}{8} Kp - \left(\frac{\gamma}{16}\right)^2} + \mu^2 i\,\frac{\frac{\gamma_0}{12}(\lambda_0 + 2Kp)(\pm i)A_\pm}{2Im\lambda_0} \qquad (103)$$

Which may be reduced to

$$\lambda = \pm i\left\{1 + \mu^2\left(\frac{\gamma}{24}\right)^2\left[2 - \frac{\nu^2 - \frac{\gamma}{8} Kp + 4Kp^2}{\nu^2 + \frac{\gamma}{8} Kp - \left(\frac{\gamma}{16}\right)^2 - \frac{1}{4}}\right]\right\}$$

$$- \frac{\gamma}{16} + i\left\{\nu^2 + (1+\mu^2)\frac{\gamma}{8} Kp - \left(\frac{\gamma}{16}\right)^2\left[1 + \mu^2\,\frac{4}{9}\,\frac{\nu^2 - \frac{\gamma}{8} Kp + 4Kp^2}{\nu^2 + \frac{\gamma}{8} Kp - \left(\frac{\gamma}{16}\right)^2 - \frac{1}{4}}\right]\right.$$

$$\left. \pm i\mu^2\left(\frac{\gamma}{12}\right)^2\left(\frac{\gamma}{16} - 2Kp\right)\right\}^{1/2} \qquad (104)$$

and the conjugates.

Although derived here on the basis of complex roots, it may be demonstrated that this expression is also valid when γ is large enough so that the rotating hover roots lie on the real axis. This single composite expression then is valid for all cases except when the hover root frequency is near ½ or 1/rev. This result has some of the effects that have been seen for

the independent blade: the factor $(1 + \mu^2)$ correcting for the increase in the mean of $K_p M_\theta$ appears as usual, and the second order μ^2 term in the radicand is like the corresponding term for the independent blade (eq. (24)), although half the magnitude. There are also now some order μ^2 effects that give quite new behavior, however. There is an order μ^2 change in the $\pm i$ shift of the nonrotating roots. Secondly, the last order μ^2 term in the radicand produces, for the case of complex roots (i.e., as written), an order μ^2 change in the damping: an increase in the damping of the high frequency mode, and a decrease for the low frequency mode. This is quite different from the behavior seen so far, where the damping has always remained fixed at the hover value $-\gamma/16$ when the roots are outside the critical regions. For the case of the rotating roots being real (i.e., bringing the i inside the radicand) there is an order μ^2 change in the frequency of the roots: the more stable root going to higher frequency, and the less stable root to lower frequency. These new effects will be seen again when the constant coefficient approximation is considered; a discussion of their origin will be put off to that time, since that is a problem of more general interest. The present discussion will concentrate on outline the behavior of the eigenvalues produced by these new terms.

Consider the order μ^2 influence of forward flight on the divergence boundary. When the rotating hover roots are real - the divergence boundary being a special case of that - the last term in the radicand of equation (104) produces an order μ^2 change in the frequency. Hence

$$\mathrm{Re}\lambda = -\frac{\gamma}{16} \pm \left\{ \left(\frac{\gamma}{16}\right)^2 \left[1 + \mu^2 \frac{4}{9} \frac{\nu^2 - \frac{\gamma}{8} K_p + 4K_p^2}{\nu^2 + \frac{\gamma}{8} K_p - \left(\frac{\gamma}{16}\right)^2 - \frac{1}{4}} \right] - \nu^2 - (1 + \mu^2) \frac{\gamma}{8} K_p \right\}^{1/2}$$

Setting $\mathrm{Re}\lambda = 0$ for the divergence boundary, there follows the criterion for divergence stability:

$$(1 + \mu^2) \frac{\gamma}{8} K_p > -\nu^2 \left[1 + \mu^2 \frac{8}{9} \frac{\left(\frac{\gamma}{16}\right)^2 + \frac{\nu^2}{2}}{\left(\frac{\gamma}{16}\right)^2 + \frac{1}{4}} \right] \qquad (105)$$

The order μ^2 influence on the right-hand side is just half the result for the independent blade, so the criterion on negative K_p is more strict in this case. The difference is only order μ^2, however. In the nonrotating frame, this divergence instability occurs at a frequency order μ^2 above 1/rev.

Consider now the behavior of the roots of the three-bladed gimballed rotor near the boundary for two real roots (rotating). Recall the result for the hover roots of individual blades, in the rotating frame; figure 9(a) illustrates the behavior, for variations in γ. For $\gamma/16 = K_p + \sqrt{\nu^2 + K_p^2}$, the two roots meet at the real axis, and then for larger γ they proceed in opposite directions along the real axis. The transformation to the

nonrotating frame simply shifts this behavior by $\pm i$, so that the above behavior occurs at ± 1/rev instead of on the real axis. The hover roots of individual blades, will in the nonrotating frame thus have the behavior shown in figure 9(b). This is also the behavior of the hover roots of the three-bladed gimballed rotor, for γ near the rotating real root boundary. This should not be confused with the behavior of roots near a critical region; it occurs here at ± 1/rev because of the transformation to the nonrotating frame. The critical region behavior involves two roots, one at positive frequency and one at negative frequency, which after crossing the critical region boundary proceed in opposite directions on the λ plane. The behavior near the real root boundary involves four roots, two of which meet at 1/rev and two at -1/rev; hence, the roots occur as complex conjugate pairs always.

In forward flight ($\mu > 0$) the behavior of the roots for individual blades in the rotating frame is the same as that of the hover roots (i.e., as shown in fig. 9(a)), just with an order μ^2 shift. Since the blades are independent, the transformation to the nonrotating frame can only shift the locus by $\pm i$ in forward flight as it did in hover; so figure 9(b) presents the behavior of the roots of individual blades in the nonrotating frame for forward flight as well as for hover. The three-bladed gimballed rotor, however, exhibits different behavior near the real root boundary in forward flight. Instead of the two roots meeting and then proceeding in opposite directions at 1/rev frequency, the two branches of the loci only pass close to each other as illustrated in figure 9(c). That is, as μ increases, the locus intersection pulls apart. In terms of the γ locus at a given $\mu > 0$, as the branches approach 1/rev there is a $\pm$ order μ^2 change in the damping (with a corresponding change in the conjugate roots, so this is not critical region behavior); eventually the roots transition to more like the two real root behavior (at 1/rev frequency nonrotating), but with a $\pm$ order μ^2 difference in the frequency. Such behavior is, in fact, typical of the dynamics of coupled degrees of freedom; the root loci do not cross, but rather only pass close to one another, pulling farther apart as the coupling increases (in this case, as μ increases). The source of this behavior is the last term in the radicand of equation (104) for λ. There is, in addition, the order μ^2 change in the $\pm i$ term of equation (104), so all this occurs really at not quite ± 1/rev.

It follows then, that when $\mu > 0$ the three-bladed gimballed rotor does not have a definite real root boundary. Rather there is a gradual transition from primarily complex root behavior to primarily real root behavior. Examine now the locus in the neighborhood of the real root boundary. Write $\gamma = \gamma_0 + \mu^2\gamma_2$ where $\gamma_0 = K_p + \sqrt{\nu^2 + K_p^2}$, so γ is order μ^2 from the hover real root boundary. Look at the root near the 1/rev frequency, and near the $-\gamma/16$ real part; that is, let $\Delta\lambda$ be defined by

$$\lambda = i\left\{1 + \mu^2 \frac{16}{9}\left[\frac{1}{2}\left(\frac{\gamma_0}{16}\right)^2 + \nu^4\right]\right\} - \frac{\gamma}{16} + \Delta\lambda \qquad (106)$$

Then, from equation (104),

$$\Delta\lambda = \mu\sqrt{\frac{\gamma_2}{8}\left(\frac{\gamma_0}{16} - K_p\right) - \frac{\gamma_0}{8}K_p - \frac{16}{9}\nu^4 - i\,\frac{\gamma_0}{9}\nu^2} \tag{107}$$

This may be separated into real and imaginary parts:

$$(Re\Delta\lambda)^2 - (Im\Delta\lambda)^2 = \mu^2\left[\frac{\gamma_2}{8}\left(\frac{\gamma_0}{16} - K_p\right) - \frac{\gamma_0}{8}K_p - \frac{16}{9}\nu^4\right] \tag{108}$$

$$(Re\Delta\lambda)(Im\Delta\lambda) = -\frac{1}{2}\mu^2\,\frac{\gamma_0}{9}\nu^2 \tag{109}$$

The last equation shows that the locus on the $\Delta\lambda$ plane (i.e., on the λ plane, but with a shifted origin) is a hyperbola. The point of closest approach of the two branches occurs at

$$Re\Delta\lambda = -Im\Delta\lambda = \pm\mu\sqrt{\frac{\gamma_0}{18}}\,\nu \tag{110}$$

and the minimum separation of the branches is there

$$2|\Delta\lambda|_{min} = \mu\,\frac{8}{3}\sqrt{\frac{\gamma_0}{16}}\,\nu \tag{111}$$

The separation of the branches then is order μ. This point of closest approach may be taken as the definition of the real root boundary for this case. With $Re\Delta\lambda = -Im\Delta\lambda$, equation (108) then gives the boundary as

$$\frac{\gamma_2}{16} = \frac{\frac{8}{9}\frac{\gamma_0}{16}\left(\frac{\gamma_0}{16} - 2K_p\right)\nu^2 + \frac{\gamma_0}{16}K_p}{\frac{\gamma_0}{16} - K_p}$$

or

$$\frac{\gamma}{16} = \frac{\gamma_0}{16}\left[1 + \mu^2\,\frac{\frac{8}{9}\nu^2\left(-K_p + \sqrt{\nu^2 + K_p^2}\right) + K_p}{\sqrt{\nu^2 + K_p^2}}\right] \tag{112}$$

For $K_p = 0$ this reduces to $\gamma/16 = \nu\left[1 + \mu^2(8/9)\nu^2\right]$. Notice that this is the same as would be obtained if the last term in the radicand of λ (eq. (104)) - which is causing all this behavior - were simply ignored. Setting the radicand to zero without this term gives exactly the above boundary. The boundary obtained is similar in behavior to that of the individual blades; but again the second order μ^2 in the radicand of equation (104) has only half the magnitude. Hence, the $\Delta\gamma$ of the boundary for $K_p = 0$, for example, is only half as large as for the independent blade.

Near ½/rev Frequency

Consider now the case $\mathrm{Im}\lambda_0 = 1/2$, when the nonrotating roots are at 3/2/rev and -½/rev frequency. The order μ secular equation for β_{01-} is unchanged for this case, hence, the low frequency mode (λ_0 - i) does not have a critical region when the rotating frequency is near ½/rev. The order μ root is the same as equation (98) then, that is, there is no forward flight influence on the lower frequency root to order μ when $\mathrm{Im}\lambda_0 = 1/2$. The secular equation for β_{01+} is, however, changed for this case, and so the high frequency mode does encounter the ½/rev critical region. The complete rotor behavior is given, of course, by both the low and high frequency modes taken together; when the high frequency roots encounter the ½/rev region, the entire rotor does, even though only two of the four roots participate in the critical region behavior.

When $\mathrm{Im}\lambda_0 = 1/2$, the order μ secular term for β_{01+} is

$$\frac{\partial \beta_{01+}}{\partial \psi_1} - \lambda_1 \beta_{01+} + \frac{\gamma_0}{12}\left(-\frac{\gamma_0}{16} + 2K_p + \frac{i}{2}\right)\bar{\beta}_{01+} = 0 \tag{113}$$

so

$$D^2 = \left[\frac{\gamma_1}{8}\left(\frac{\gamma_0}{16} - K_p\right)\right]^2 - \left(\frac{\gamma_0}{12}\right)^2\left(\nu^2 - \frac{\gamma_0}{8}K_p + 4K_p{}^2\right) \tag{114}$$

This is the same secular equation and D^2 as for the ½/rev critical region of the independent blade. It follows then that the root behavior is the same as that solution, specifically the expressions for the critical region boundary, and for λ near the region (eq. (32) and (34)) are applicable here as well - adding i to λ to transform it to the high frequency mode in the nonrotating frame.

Near 1/rev Frequency

Consider the case $\mathrm{Im}\lambda_0 = 1$, so the nonrotating roots are a 0 and 2/rev. The order μ analysis is applicable, since $\mathrm{Im}\lambda_0 \neq 1/2$, and the order μ^2 analysis is correct for the high frequency mode even when $\mathrm{Im}\lambda_0 = 1$. Hence, the high frequency roots (near 2/rev frequency in the nonrotating frame) are given by the same expression as for the roots away from the critical regions (eq. (104)). The low frequency mode, however, (near 0/rev nonrotating) has an additional term in the order μ^2 secular term when $\mathrm{Im}\lambda_0 = 1$; instead of equation (101), β_{11-} is now given by

$$-\left[\left(2\lambda_0 + \frac{\gamma_0}{8}\right)\frac{\partial\beta_{11-}}{\partial\psi_1} + \frac{\gamma_1}{8}(\lambda_0 + K_p)\beta_{11-}\right]$$

$$= \left\{\left(2\lambda_0 + \frac{\gamma_0}{8}\right)\frac{\partial\beta_{02-}}{\partial\psi_2} + \left[\lambda_1^2 + \frac{\gamma_1}{8}\lambda_1 + \frac{\gamma_2}{8}(\lambda_0 + K_p) + \frac{\gamma_0}{8}K_p\right.\right.$$

$$\left.\left. + \frac{\gamma_0}{12}(\lambda_0 + 2K_p)(-i)A_-\right]\beta_{02-}\right\}e^{\lambda_1\psi_1}$$

$$+ \left[\frac{\gamma_0}{16}(i + K_p)\bar{\beta}_{02-}\right]e^{\bar{\lambda}_1\psi_1} \qquad (115)$$

Unless λ_1 is real, so $\bar{\lambda}_1 = \lambda_1$, the secular equation for $\beta_{02-}(\psi_2)$ is the same as before, however. Then, equation (104) holds for the lower frequency mode also, except when the frequency is order μ^2 from 1/rev (rotating). Requiring λ_1 be real means $\gamma_1 = 0$; the secular term of equation (115) is then

$$\frac{\partial\beta_{02-}}{\partial\psi_2} + \left[-\lambda_2 - i\frac{\gamma_0}{16}K_p + \left(\frac{\gamma_0}{12}\right)^2\frac{i}{2} + \frac{1}{2}\left(\frac{\gamma_0}{12}\right)^2\left(-\frac{\gamma_0}{16} + 2K_p\right)\right.$$

$$\left. -i\left(\frac{\gamma_0}{12}\right)^2\frac{\nu^2 - \frac{\gamma_0}{8}K_p + 4K_p^2}{6}\right]\beta_{02-} + \frac{\gamma_0}{32}(1 - iK_p)\bar{\beta}_{02-} = 0 \qquad (116)$$

So

$$D^2 = \left[\left(\frac{\gamma_0}{16} - K_p\right)\frac{\gamma_2}{16} + \frac{1}{2}\left(\frac{\gamma_0}{12}\right)^2 + \left(\frac{\gamma_0}{6}\right)^2\frac{\nu^2 - \frac{\gamma_0}{8}K_p + 4K_p^2}{24} - K_p\frac{\gamma_0}{16}\right]^2 - \left(\frac{\gamma_0}{32}\right)^2(1 + K_p^2) \qquad (117)$$

which has similarities to the results for both the individual blade and the teetering rotor. The boundary of the critical region is defined by $D^2 = 0$; letting $\gamma = \gamma_0 + \Delta\gamma$ with $\Delta\gamma$ order μ^2 small, then the boundary is

$$\frac{\Delta\gamma}{16}\left(\frac{\gamma_0}{16} - K_p\right) = \mu^2(C_1 \pm C_2) \qquad (118)$$

or in terms of the corner μ

$$\mu_1^2, \mu_2^2 = \frac{\frac{\Delta\gamma}{16}\left(\frac{\gamma_0}{16} - K_p\right)}{C_1 \pm C_2} \tag{119}$$

This is the usual form, with now

$$C_1 = -\frac{1}{2}\left(\frac{\gamma_0}{12}\right)^2 - \left(\frac{\gamma_0}{6}\right)^2 \frac{\nu^2 - \frac{\gamma_0}{8}K_p + 4K_p^2}{24} + K_p \frac{\gamma_0}{16} \tag{120}$$

$$C_2 = \frac{\gamma_0}{32}\sqrt{1 + K_p^2} \tag{121}$$

C_2, which gives the width of the critical region on the $\gamma - \mu$ plane, is the same as for the teetering rotor; hence, the width is, in general, smaller than for the individual blade, except for $\nu = 1$, in which case the widths are equal. C_1, which gives the offset of the region, is similar to the individual blade result. The first term is new, however, corresponding to the new order μ^2 shift in the $\pm i$ frequency of the roots away from the critical region (eq. (104)); and the second term has half the magnitude, corresponding to the second order μ^2 term in the radicand of equation (104). The eigenvalue of the low frequency mode is now

$$\lambda = -\frac{\gamma_0}{16} - \mu^2\frac{\gamma_2}{16} - \mu^2\left(\frac{\gamma_0}{12}\right)^2\left(-\frac{\gamma_0}{16} + 2K_p\right) \pm i\mu^2 D$$

$$= -\frac{\gamma}{16}\left[1 - \mu^2\frac{8}{9}(\nu^2 - 1)\right] \pm i\frac{\Delta\gamma}{16}\left(\frac{\gamma_0}{16} - 2K_p\right)\sqrt{\left(1 - \frac{\mu^2}{\mu_1^2}\right)\left(1 - \frac{\mu^2}{\mu_2^2}\right)} \tag{122}$$

So the eigenvalue also has a new term, an order μ^2 damping change, corresponding to the third order μ^2 term in the radicand of equation (104). For $K_p = 0$, the criterion for $\mathrm{Im}\lambda_0 = 1$ reduces to $\gamma_0/16 = \sqrt{\nu^2 - 1}$, equations (120) and (121) become

$$C_1 = -\frac{1}{2}\left(\frac{\gamma_0}{12}\right)^2 - \left(\frac{\gamma_0}{6}\right)^2\frac{\nu^2}{24} = -\frac{8}{27}(\nu^2 - 1)(\nu^2 + 3) \tag{123}$$

$$C_2 = \frac{\gamma_0}{32} = \frac{1}{2}\sqrt{\nu^2 - 1} \tag{124}$$

so the boundary reduces to

$$\mu_1^2, \mu_2^2 = \frac{\frac{\Delta\gamma}{16}}{-\frac{8}{27}\sqrt{\nu^2 - 1}\,(\nu^2 + 3) \pm \frac{1}{2}} \tag{125}$$

and the eigenvalues to

$$\lambda = -\frac{\gamma}{16}\left[1 - \mu^2\,\frac{8}{9}\,(\nu^2 - 1)\right] \pm i\,\frac{\Delta\gamma}{16}\sqrt{\nu^2 - 1}\sqrt{\left(1 - \frac{\mu^2}{\mu_1^2}\right)\left(1 - \frac{\mu^2}{\mu_2^2}\right)} \tag{126}$$

Compared to the individual blade result, the boundaries are identical if $\nu = 1$, but if $\nu > 1$ this boundary is offset more, with a smaller width. Compared to the teetering rotor, the width is the same but the teetering rotor is not offset even when $\nu > 1$.

Summary

For the hover limit, $\mu = 0$, the four eigenvalues of the three-bladed gimballed rotor are

$$\lambda = \pm i - \frac{\gamma}{16} + i\sqrt{\nu^2 + \frac{\gamma}{8}\,Kp - \left(\frac{\gamma}{16}\right)^2} \tag{127}$$

and their conjugates. For the hover frequency away from ½/rev or 1/rev (rotating), the roots to order μ are the same as the hover roots, and to order μ^2, they are given by equation (104) above. The influence of forward flight consists of: an order μ^2 frequency change, similar to the individual blade but with reduced magnitude; an order μ^2 change in the $\pm i$ frequency shift due to the transformation to the nonrotating frame; and a $\pm$ order μ^2 change in the damping of complex roots of the frequency for real roots. The latter change has the effect of pulling apart the real root intersection of the locus (at ±1/rev frequency nonrotating), so that the root loci only pass close when $\mu > 0$ rather than actually intersecting (the separation is order μ). The criterion for divergence stability is, in this case

$$(1 + \mu^2)\,\frac{\gamma}{8}\,Kp > -\nu^2\left[1 + \mu^2\,\frac{8}{9}\,\frac{\left(\frac{\gamma}{16}\right)^2 + \frac{\nu^2}{2}}{\left(\frac{\gamma}{16}\right)^2 + \frac{1}{4}}\right] \tag{128}$$

The ½/rev critical region is identical to that of the individual blades. Only the high frequency mode, at 3/2/rev nonrotating frequency, participates in this region, however. The low frequency mode, at ½/rev, has the same behavior as it does away from the critical region - that is, no forward flight influence at all to order μ.

If $\Delta\gamma = \gamma - \gamma_0$ is order μ^2 small, where γ_0 is the value required for $\mathrm{Im}\lambda_0 = 1$, that is, $\gamma_0/16 = K_p + \sqrt{\nu^2 + K_p^2} - 1$; then the low frequency mode, at 0/rev nonrotating frequency, encounters the 1/rev critical region. The high frequency mode does not participate in the critical region behavior; its roots are given by the same expression as away from the critical region, that is, equation (104). The low frequency roots are given by

$$\lambda = -\frac{\gamma}{16}\left[1 - \mu^2\,\frac{8}{9}\,(\nu^2 - 1)\right] \pm i\,\frac{\Delta\gamma}{16}\left(\frac{\gamma_0}{16} - 2K_p\right)\sqrt{\left(1 - \frac{\mu^2}{\mu_1^2}\right)\left(1 - \frac{\mu^2}{\mu_2^2}\right)} \tag{129}$$

where the corner μ^2 are

$$\mu_1^2, \mu_2^2 = \frac{\frac{\Delta\gamma}{16}\left(\frac{\gamma_0}{16} - K_p\right)}{C_1 \pm C_2} \tag{130}$$

with C_1 and C_2 given by equations (120) and (121) above. The behavior of the loci in the critical region is similar to what has been seen before with the individual blades and the teetering rotor. There are now, however, order μ^2 changes in the frequency and damping (in C_1, and explicitly in $\mathrm{Re}\lambda$ above) corresponding to the changes seen away from the critical region, as well as some changes in the magnitude of the forward flight influence.

The $\gamma - \mu$ plane boundary for the two real root region (±1/rev intersection nonrotating), writing $\gamma = \gamma_0 + \Delta\gamma$, is

$$\frac{\Delta\gamma}{16} = \mu^2\,\frac{\gamma_0}{16}\,\frac{\frac{8}{9}\,\nu^2\left(-K_p + \sqrt{\nu^2 + K_p^2}\right) + K_p}{\sqrt{\nu^2 + K_p^2}} \tag{131}$$

where $\gamma_0/16 = K_p + \sqrt{\nu^2 + K_p^2}$. This is only a soft boundary, however, the point of closest approach of the branches when $\mu > 0$. The ½/rev critical region boundaries (3/2/rev nonrotating) are

$$\frac{\Delta\gamma}{16} = \pm\mu\,\frac{\frac{\gamma_0}{24}\sqrt{\nu^2 - \frac{\gamma_0}{8}K_p + 4K_p^2}}{\frac{\gamma_0}{16} - K_p} \tag{132}$$

where $\gamma_0/16 = K_p + \sqrt{\nu^2 + K_p^2 - (1/4)}$; and the 1/rev critical region boundaries (0/rev nonrotating) are

$$\frac{\Delta\gamma}{16} = \mu^2\,\frac{C_1 \pm C_2}{\frac{\gamma_0}{16} - K_p} \tag{133}$$

where $\gamma_0/16 = K_p + \sqrt{\nu^2 + K_p^2 - 1}$. For $K_p = 0$ these boundaries reduce to

$$\frac{\Delta\gamma}{16} = \mu^2 \frac{8}{9} \nu^3 \qquad \text{with} \quad \frac{\gamma_0}{16} = \nu \tag{134}$$

$$\frac{\Delta\gamma}{16} = \pm\mu \frac{2}{3} \nu \qquad \text{with} \quad \frac{\gamma_0}{16} = \sqrt{\nu^2 - \frac{1}{4}} \tag{135}$$

$$\frac{\Delta\gamma}{16} = \mu^2\left[-\frac{8}{27}\sqrt{\nu^2 - 1}\,(\nu^2 + 3) \pm \frac{1}{2}\right] \qquad \text{with} \quad \frac{\gamma_0}{16} = \sqrt{\nu^2 - 1} \tag{136}$$

respectively.

GIMBALLED ROTOR, FOUR BLADES

The equation of motion for a four-bladed gimballed rotor are

$$\begin{pmatrix}\beta_{1c}\\ \beta_{1s}\end{pmatrix}'' + \begin{bmatrix}\frac{\gamma}{8} & 2\\ -2 & \frac{\gamma}{8}\end{bmatrix}\begin{pmatrix}\beta_{1c}\\ \beta_{1s}\end{pmatrix}' + \begin{bmatrix}\nu^2 - 1 + \mu^2\frac{\gamma}{16}\sin 4\psi & \frac{\gamma}{8}\left(1 + \frac{\mu^2}{2} - \frac{\mu^2}{2}\cos 4\psi\right)\\ -\frac{\gamma}{8}\left(1 - \frac{\mu^2}{2} + \frac{\mu^2}{2}\cos 4\psi\right) & \nu^2 - 1 - \mu^2\frac{\gamma}{16}\sin 4\psi\end{bmatrix}\begin{pmatrix}\beta_{1c}\\ \beta_{1s}\end{pmatrix}$$

$$= \begin{bmatrix}\frac{\gamma}{8}\left(1 + \frac{\mu^2}{2} - \frac{\mu^2}{2}\cos 4\psi\right) & -\mu^2\frac{\gamma}{16}\sin 4\psi\\ -\mu^2\frac{\gamma}{16}\sin 4\psi & \frac{\gamma}{8}\left(1 + \frac{3}{2}\mu^2 + \frac{\mu^2}{2}\cos 4\psi\right)\end{bmatrix}\begin{pmatrix}\theta_{1c} - K_p\beta_{1c}\\ \theta_{1s} - K_p\beta_{1s}\end{pmatrix} \tag{137}$$

The only forward flight effects remaining are order μ^2, the order μ moment cancelling internally at the hub as they did for the teetering rotor. The only periodic coefficients remaining are order μ^2, hence, only a 1/rev critical region is expected.

The hover result is identical to that of the $N = 3$ case; that result, in fact, holds for all $N \geq 3$. Only order μ^2 terms appear in the equations of motion, so an expansion in μ^2 is used:

$$\frac{\partial}{\partial\psi} = \frac{\partial}{\partial\psi_0} + \mu^2 \frac{\partial}{\partial\psi_2} + \ldots$$

$$\vec{\beta} = \vec{\beta}_0 + \mu^2\vec{\beta}_2 + \ldots$$

$$\gamma = \gamma_0 + \mu^2\gamma_2 + \ldots$$

The order 1 solution is the hover limit again, so is the same as the N = 3 result. The solution for $\vec{\beta}_0$ is

$$\vec{\beta}_0 = \mathrm{Re}\left[\beta_{02+}(\psi_2,\ldots)\begin{pmatrix} i \\ 1 \end{pmatrix} e^{(\lambda_0+i)\psi_0} + \beta_{02-}(\psi_2,\ldots)\begin{pmatrix} -i \\ 1 \end{pmatrix} e^{(\lambda_0-i)\psi_0}\right] \tag{138}$$

Order μ^2 Results

The order μ^2 equation is

$$-\left\{\frac{\partial^2\vec{\beta}_2}{\partial\psi_0^2} + \begin{bmatrix} \frac{\gamma_0}{8} & 2 \\ -2 & \frac{\gamma_0}{8} \end{bmatrix}\frac{\partial\vec{\beta}_2}{\partial\psi_0} + \begin{bmatrix} \nu^2 - 1 + K_p\frac{\gamma_0}{8} & \frac{\gamma_0}{8} \\ -\frac{\gamma_0}{8} & \nu^2 - 1 + K_p\frac{\gamma_0}{8} \end{bmatrix}\vec{\beta}_2\right\}$$

$$= 2\frac{\partial^2\vec{\beta}_0}{\partial\psi_0\,\partial\psi_2} + \begin{bmatrix} \frac{\gamma_0}{8} & 2 \\ -2 & \frac{\gamma_0}{8} \end{bmatrix}\frac{\partial\vec{\beta}_0}{\partial\psi_2} + \frac{\gamma_2}{8}\frac{\partial\vec{\beta}_0}{\partial\psi_0} + \begin{bmatrix} K_p\frac{\gamma_2}{8} + K_p\frac{\gamma_0}{16} & \frac{\gamma_2}{8} + \frac{\gamma_0}{16} \\ -\frac{\gamma_2}{8} + \frac{\gamma_0}{16} & K_p\frac{\gamma_2}{8} + K_p 3\frac{\gamma_0}{16} \end{bmatrix}\vec{\beta}_0$$

$$+ \begin{bmatrix} \frac{\gamma_0}{16}\sin 4\psi_0 - K_p\frac{\gamma_0}{16}\cos 4\psi_0 & -\frac{\gamma_0}{16}\cos 4\psi_0 - K_p\frac{\gamma_0}{16}\sin 4\psi_0 \\ -\frac{\gamma_0}{16}\cos 4\psi_0 - K_p\frac{\gamma_0}{16}\sin 4\psi_0 & -\frac{\gamma_0}{16}\sin 4\psi_0 + K_p\frac{\gamma_0}{16}\cos 4\psi_0 \end{bmatrix}\vec{\beta}_0$$

$$= \left\{\left(2\lambda_0 + \frac{\gamma_0}{8}\right)\frac{\partial \beta_{02+}}{\partial \psi_2} + \left[\frac{\gamma_2}{8}(\lambda_0 + K_p) + \frac{\gamma_0}{8}K_p\right]\beta_{02+}\right\}\begin{pmatrix} i \\ 1 \end{pmatrix} e^{(\lambda_0+i)\psi_0}$$

$$+ \left[\frac{\gamma_0}{16}(i + K_p)\beta_{02+}\right]\begin{pmatrix} -i \\ 1 \end{pmatrix} e^{(\lambda_0+i)\psi_0} + \left[\frac{\gamma_0}{16}(-i + K_p)\beta_{02+}\right]\begin{pmatrix} -i \\ 1 \end{pmatrix} e^{(\lambda_0-3i)\psi_0}$$

$$+ \left\{\left(2\lambda_0 + \frac{\gamma_0}{8}\right)\frac{\partial \beta_{02-}}{\partial \psi_2} + \left[\frac{\gamma_2}{8}(\lambda_0 + K_p) + \frac{\gamma_0}{8}K_p\right]\beta_{02-}\right\}\begin{pmatrix} -i \\ 1 \end{pmatrix} e^{(\lambda_0-i)\psi_0}$$

$$+ \left[\frac{\gamma_0}{16}(-i + K_p)\beta_{02-}\right]\begin{pmatrix} i \\ 1 \end{pmatrix} e^{(\lambda_0-i)\psi_0} + \left[\frac{\gamma_0}{16}(i + K_p)\beta_{02-}\right]\begin{pmatrix} i \\ 1 \end{pmatrix} e^{(\lambda_0+3i)\psi_0}$$

$$+ \text{conjugate} \tag{139}$$

Assuming that $\mathrm{Im}\lambda_0 \neq 1$, the secular term is

$$\frac{\partial \beta_{02\pm}}{\partial \psi_2} - \lambda_2 \beta_{02\pm} = 0 \tag{140}$$

where

$$\lambda_2 = -\frac{\frac{\gamma_2}{8}(\lambda_0 + K_p) + \frac{\gamma_0}{8}K_p}{2i\mathrm{Im}\lambda_0}$$

The solution is $\beta_{02\pm} = \beta_{04\pm}(\psi_4, \ldots)e^{\lambda_2\psi_2}$. Hence, the eigenvalues to order μ^2 are

$$\lambda = \lambda_0 + \mu^2\lambda_2 \pm i$$

$$= \pm i - \frac{\gamma}{16} + i\sqrt{\nu^2 + (1 + \mu^2)\frac{\gamma}{8}K_p - \left(\frac{\gamma}{16}\right)^2} \tag{141}$$

and the conjugates. This is the same result as for the teetering rotor roots away from the 1/rev critical region. It follows then that the real root boundary (at ±1/rev nonrotating) and the divergence stability criterion are the same as for the teetering rotor.

Near 1/rev Frequency

If the hover roots are order μ^2 from 1/rev frequency (rotating) - that is, $\mathrm{Im}\lambda_0 = 1$ - then, the periodic coefficients contribute to the order μ^2 secular terms:

$$\frac{\partial \beta_{02\pm}}{\partial \psi_2} - \lambda_2 \beta_{02\pm} - i \frac{\gamma_0}{32} (i + Kp) \bar{\beta}_{02\pm} = 0 \qquad (142)$$

Comparing this with the teetering rotor 1/rev secular equation, it follows that the four-bladed gimballed rotor has identical expressions for the roots and boundaries of the 1/rev critical region.

Summary

The behavior of the four-bladed gimballed rotor is the same as that of the teetering rotor flap stability - except, of course, that the gimballed rotor has four roots, in the nonrotating frame, hence, shifted by $\pm i$ from the teetering rotor roots (rotating). As for the teetering rotor, it also follows here that the constant coefficient approximation to the equations of motion, even in the rotating frame so the only forward flight influence retained is the factor of $(1 + \mu^2)$ in the mean of M_θ, gives exactly the correct eigenvalues except near the 1/rev critical region.

Away from the critical region, the eigenvalues of the four-bladed gimballed rotor are

$$\lambda = \pm i - \frac{\gamma}{16} + i \sqrt{\nu^2 + (1 + \mu^2) \frac{\gamma}{8} Kp - \left(\frac{\gamma}{16}\right)^2} \qquad (143)$$

and their conjugates. There is no ½/rev critical region. The 1/rev critical region is the same as for the teetering rotor; both the high frequency and low frequency modes (at 2/rev and 0/rev nonrotating) participate in the critical region behavior. The $\gamma - \mu$ plane boundaries are the same as given for the teetering rotor.

GIMBALLED ROTOR, FIVE OR MORE BLADES

For a gimballed rotor with five or more blades, the equation of motion is

$$\begin{pmatrix} \beta_{1c} \\ \beta_{1s} \end{pmatrix}'' + \begin{bmatrix} \frac{\gamma}{8} & 2 \\ -2 & \frac{\gamma}{8} \end{bmatrix} \begin{pmatrix} \beta_{1c} \\ \beta_{1s} \end{pmatrix}' + \begin{bmatrix} \nu^2 - 1 & \frac{\gamma}{8}\left(1 + \frac{\mu^2}{2}\right) \\ -\frac{\gamma}{8}\left(1 - \frac{\mu^2}{2}\right) & \nu^2 - 1 \end{bmatrix} \begin{pmatrix} \beta_{1c} \\ \beta_{1s} \end{pmatrix}$$

$$= \begin{bmatrix} \frac{\gamma}{8}\left(1 + \frac{\mu^2}{2}\right) & 0 \\ 0 & \frac{\gamma}{8}\left(1 + \frac{3}{2}\mu^2\right) \end{bmatrix} \begin{pmatrix} \theta_{1c} - Kp\beta_{1c} \\ \theta_{1s} - Kp\beta_{1s} \end{pmatrix} \qquad (144)$$

So to order μ^2 there are no periodic coefficients when $N \geq 5$. All the periodic flap moments cancel internally at the rotor hub, and do not contribute to the net pitch and roll moments on the rotor disk. The result is a constant coefficient differential equation for the gimballed rotor with five or more blades. The eigenvalues of this rotor are given by the roots of the characteristic equation of

$$\begin{bmatrix} \lambda^2 + \frac{\gamma}{8}\lambda + \nu^2 - 1 + K_p \frac{\gamma}{8}\left(1 + \frac{\mu^2}{2}\right) & 2\lambda + \frac{\gamma}{8}\left(1 + \frac{\mu^2}{2}\right) \\ -2\lambda - \frac{\gamma}{8}\left(1 - \frac{\mu^2}{2}\right) & \lambda^2 + \frac{\gamma}{8}\lambda + \nu^2 - 1 + K_p \frac{\gamma}{8}\left(1 + \frac{3}{2}\mu^2\right) \end{bmatrix} \begin{pmatrix} \beta_{1c} \\ \beta_{1s} \end{pmatrix} = 0$$

or

$$\left[\lambda^2 + \frac{\gamma}{8}\lambda + \nu^2 - 1 + K_p \frac{\gamma}{8}(1 + \mu^2)\right]^2 + \left(2\lambda + \frac{\gamma}{8}\right)^2 - \mu^4\left(\frac{\gamma}{16}\right)^2(1 + K_p^2) = 0 \tag{145}$$

As a constant coefficient equation, the eigenvalues are simply the roots of a polynomial, although in this case it is a fourth-order polynomial, which may, in general, only be solved numerically. Since the roots for the limit $\mu = 0$ are known, however, - that is, the hover roots - a perturbation technique may be used to obtain explicitly expressions for λ including the influence of forward flight.

Only order μ^2 and μ^4 terms appear in the characteristic equation, so an expansion in μ^2 is used. Write $\lambda = \lambda_0 \pm i + \mu^2\lambda_2 + \ldots$ and the conjugates, where λ_0 is the rotating hover root as usual:

$$\lambda_0 = -\frac{\gamma_0}{16} + i\sqrt{\nu^2 + \frac{\gamma_0}{8}K_p - \left(\frac{\gamma_0}{16}\right)^2} \tag{146}$$

The Lock number is also expanded as a series in μ: $\gamma = \gamma_0 + \mu^2\gamma_2 \ldots$. The order 1 characteristic equation then has just the solutions $\lambda = \lambda_0 \pm i$, $\bar{\lambda}_0 \pm i$. That is, the order 1 term in the expansion of λ above is indeed the correct hover limit.

Order μ^2 Results

The order μ^2 terms of the characteristic equation are

$$\left[(\lambda_0 \pm i)^2 + \frac{\gamma_0}{8}(\lambda_0 \pm i) + \nu^2 - 1 + K_p \frac{\gamma_0}{8}\right]\left[2(\lambda_0 \pm i)\lambda_2 + \frac{\gamma_0}{8}\lambda_2 + \frac{\gamma_2}{8}(\lambda_0 \pm i) + K_p \frac{\gamma_0}{8} + K_p \frac{\gamma_2}{8}\right] + \left[2(\lambda_0 \pm i) + \frac{\gamma_0}{8}\right]\left(2\lambda_2 + \frac{\gamma_2}{8}\right) = 0$$

or

$$(\mathrm{Im}\lambda_0 \pm 1)\left[(2i\mathrm{Im}\lambda_0)\,\lambda_2 + K_P\,\frac{\gamma_c}{8} + \frac{\gamma_2}{8}\,(\lambda_0 + K_P)\right] = 0 \tag{147}$$

Assuming that $\mathrm{Im}\lambda_0 \neq 1$ when the lower frequency root $\lambda_0 - i$ is being considered, so $\mathrm{Im}\lambda_0 - 1 \neq 0$, then the solution is

$$\lambda_2 = i\,\frac{\frac{\gamma_2}{8}\,(\lambda_0 + K_P) + \frac{\gamma_0}{8}\,K_P}{2\mathrm{Im}\lambda_0} \tag{148}$$

It follows then that the eigenvalues to order μ^2 are

$$\lambda = \pm i - \frac{\gamma}{16} + i\sqrt{\nu^2 + (1 + \mu^2)\,\frac{\gamma}{8}\,K_P - \left(\frac{\gamma}{16}\right)^2} \tag{149}$$

and the conjugates. The real root boundary and the divergence criterion are the same as given for the teetering rotor.

Notice that this is the same result as would have been obtained if a constant coefficient approximation were made in the rotating frame before finding the net pitch and roll moments. Actually, the expansion of λ as a series in μ^2 is not really necessary, for to order μ^2 the last term in the characteristic equation (the μ^4 term in eq. (145)) drops and λ may be found directly, exactly as for the hover case. However, such a procedure does not show that the solution is not valid for the low frequency mode near 1/rev (rotating frequency).

Near 1/rev Frequency

This is where the critical region is encountered when the equations have periodic coefficients, that is, when $\mathrm{Im}\lambda_0 = 1$. The high frequency mode is at 2/rev nonrotating frequency, and the roots must remain complex conjugates since this is a constant coefficient equation. Hence, the 1/rev critical region behavior cannot be encountered for this mode. Indeed, the order μ^2 result obtained above holds for the $\lambda_0 + i$ root, even when $\mathrm{Im}\lambda_0 = 1$ (the upper sign is used in eq. (147), so the first factor has the value 2). The low frequency mode, however, is at 0/rev nonrotating frequency, so these roots are able to meet and proceed in opposite directions along the real axis. This is the 1/rev critical region behavior which is allowed for this constant coefficient equation because the transformation to the nonrotating frame puts these roots near the real axis instead of 1/rev.

Consider the low frequency mode when $\mathrm{Im}\lambda_0 = 1$; that is, $\lambda = -(\gamma_0/16) + \mu^2\lambda_2 + \ldots$. The order μ^2 characteristic equation is

identially zero then (eq. (147), using the lower sign so the first factor has the value 0 when $\mathrm{Im}\lambda_0 = 1$), and it is necessary to go to order μ^4 to find λ_2. The order μ^4 terms in the characteristic equation are for this case

$$\left[\frac{\gamma_2}{8}\left(-\frac{\gamma_0}{16}+K_p\right)+K_p\frac{\gamma_0}{8}\right]^2+\left(2\lambda_0+\frac{\gamma_2}{8}\right)^2-\left(\frac{\gamma_0}{16}\right)^2(1+K_p^2)=0$$

or

$$\left(\lambda_2+\frac{\gamma_2}{16}\right)^2=-D^2 \tag{150}$$

where

$$D^2=\left[\frac{\gamma_2}{16}\left(-\frac{\gamma_0}{16}+K_p\right)+K_p\frac{\gamma_0}{16}\right]^2-\left(\frac{\gamma_0}{32}\right)^2(1+K_p^2)$$

Setting $D^2 = 0$ gives $\lambda_2 = -\gamma_2/16$, so $\lambda = -\gamma/16$ to order μ^2. Hence, $D^2 = 0$ is the boundary for two real roots in the nonrotating frame, or the 1/rev boundary in the rotating frame. In general, the root is

$$\lambda=-\frac{\gamma_0}{16}+\mu^2\left(-\frac{\gamma_2}{16}\pm iD\right)=-\frac{\gamma}{16}\pm\mu^2 iD \tag{151}$$

The expressions for λ and D are identical to the corresponding ones for the teetering rotor, or for the four-bladed gimballed rotor, near the 1/rev critical region. Thus, the gimballed rotor with five or more blades encounters a 1/rev critical region, although only the lower frequency mode (near the real axis nonrotating) participates in the critical region behavior. The boundary of the region, and the solution for λ, are the same as were given for the teetering rotor (-i to get to the low frequency nonrotating mode).

Summary

The gimballed rotor with five or more blades is described by constant coefficient differential equations. The behavior of the roots is, however, nearly identical to that of a teetering rotor or a four-bladed gimballed rotor; the latter is perhaps a better comparison since it is also a case with nonrotating degrees of freedom. Away from 1/rev rotating frequency, the roots are given by

$$\lambda=\pm i-\frac{\gamma}{16}+i\sqrt{\nu^2+(1+\mu^2)\frac{\gamma}{8}K_p-\left(\frac{\gamma}{16}\right)^2} \tag{152}$$

and the conjugates. The real root boundary (±1/rev nonrotating) and the divergence criterion are the same as for the teetering rotor.

A critical region is encountered by this rotor, when the rotating frequency is near 1/rev. The expressions for the boundary and the roots near the critical region are the same as for the teetering rotor. Only the lower frequency mode participates in the 1/rev critical region, however, for it is the fact that this mode is near the real axis (nonrotating) that allows the critical region behavior to occur with a system described by constant coefficient differential equations. The high frequency modes are near 2/rev for this case, and so are still given by equation (152), that is, have the same behavior as away from the critical region.

The equations of motion for the gimballed rotor with $N \geq 5$ are identical to the constant coefficient approximation of the equations for the three or four-bladed gimballed rotors (i.e., eq. (87) or (137) with the periodic terms dropped). Hence, the solution for $N \geq 5$ may be considered as a constant coefficient approximation to the dynamics of the $N = 3$ or 4 cases.

As a constant coefficient approximation to the $N = 4$ case, this present solution gives exactly the correct roots with the exception of the high frequency mode near the 1/rev critical region. These roots for the $N = 4$ case encounter the critical region along with the lower frequency roots; but for the constant coefficient approximation such behavior is not allowed for the high frequency roots if they are to remain complex conjugates. The behavior of the low frequency roots is given correctly everywhere, including the 1/rev critical region, because in the nonrotating frame that behavior occurs on the real axis. Away from the 1/rev critical region, it is, in fact, possible to make the constant coefficient approximation in the rotating frame, before finding the net pitch and roll moments, and still obtain the correct expressions for the roots of the four-bladed gimballed rotor.

As a constant coefficient approximation to the $N = 3$ case, this present solution is not really good anywhere. The errors are not even order μ^2 only, because the three-bladed gimballed rotor encounters the ½/rev critical region where there are order μ effects of forward flight. The order μ^2 effects on the roots, both away from and near the 1/rev critical region, are, in addition, quite different for the $N = 3$ case.

EQUATIONS OF MOTION IN THE NONROTATING FRAME

Consider a rotor with N independent blades, each with rotating natural frequency ν. The flap motion of the entire rotor is described by the N degrees of freedom $\beta^{(m)}$, and the N rotating equations of motion given above (eq. (57)), in contrast to the gimballed rotor, which is described by only two degrees of freedom and equations for all $N \geq 3$. As for the gimballed rotor, however, the motion of the rotor with independently flapping blades may also be described in the nonrotating frame. The following new degrees of freedom are introduced:

$$\left.\begin{aligned}
\beta_0 &= \frac{1}{N}\sum_{m=1}^{N} \beta^{(m)} \\
\beta_{nc} &= \frac{2}{N}\sum_{m=1}^{N} \beta^{(m)} \cos n\psi_m \\
\beta_{ns} &= \frac{2}{N}\sum_{m=1}^{N} \beta^{(m)} \sin n\psi_m \\
\beta_{N/2} &= \frac{1}{N}\sum_{m=1}^{N} \beta^{(m)}(-1)^m
\end{aligned}\right\} \qquad (153)$$

where $\psi_m = \psi + m\Delta\psi$ is the azimuth location of the mth blade and $\Delta\psi = 2\pi/N$ is the interval between the blades. The flap motion of the mth blade is then given by

$$\beta^{(m)} = \beta_0 + \sum (\beta_{nc} \cos n\psi_m + \beta_{ns} \sin n\psi_m) + \beta_{N/2}(-1)^m \qquad (154)$$

where the sum over n goes from 1 to (N - 1)/2 for N odd, and from 1 to (N - 2)/2 for N even. The $\beta_{N/2}$ degree of freedom only appears if N is even.

This is a Fourier coordinate transformation from the N degrees of freedom $\beta^{(m)}$ describing the rotor motion in the rotating frame to the N degrees of freedom β_0, β_{nc}, β_{ns}, $\beta_{N/2}$ describing the rotor motion in the nonrotating frame (for further discussion, see, i.e., ref. 13). The β_0 variable is the rotor coning motion; β_{1c} and β_{1s} are the tip path plane longitudinal and lateral tilt degrees of freedom as for the gimballed rotor. The $\beta_{N/2}$ motion is similar to the coning except that the blades alternate in up and down motion. This coordinate transformation must be accompanied by a conversion of the equations of motion from the rotating frame (eq. (57)) to the nonrotating frame. This is accomplished by operating on the equations of motion with the following summation operators:

$$\frac{1}{N}\sum_m (\ldots), \quad \frac{2}{N}\sum_m (\ldots)\cos n\psi_m, \quad \frac{2}{N}\sum_m (\ldots)\sin n\psi_m, \quad \frac{1}{N}\sum_m (\ldots)(-1)^m \qquad (155)$$

The summations combine the equations for flap moment equilibrium into the rotor moment equilibrium appropriate to the nonrotating degrees of freedom. For example, for the coning motion, the first operator finds the coning moment; and for the β_{1c} and β_{1s} motion, the operators find the net pitch and roll

moments on the disk as was done for the gimballed rotor. The resulting N equations in the nonrotating frame are coupled, even for the case of a shaft fixed rotor as here in contrast to the rotating equations, which are not coupled at all (eq. (57)).

The result of the summation operators depends on the number of blades (N) where, as here, the equations have periodic coefficients. Hence, the set of N nonrotating equations depend on N. The complete sets of differential equations describing the rotor flap motion of N independent blades excited by blade pitch inputs only are given below for the cases N = 3 and N = 4.

$$N = 3$$

$$\begin{pmatrix} \beta_0 \\ \beta_{1c} \\ \beta_{1s} \end{pmatrix}^{\cdot\cdot} + \begin{bmatrix} \frac{\gamma}{8} & 0 & \mu\frac{\gamma}{12} \\ 0 & \frac{\gamma}{8} + \mu\frac{\gamma}{12}\sin 3\psi & 2 - \mu\frac{\gamma}{12}\cos 3\psi \\ \mu\frac{\gamma}{6} & -2 - \mu\frac{\gamma}{12}\cos 3\psi & \frac{\gamma}{8} - \mu\frac{\gamma}{12}\sin 3\psi \end{bmatrix} \begin{pmatrix} \beta_0 \\ \beta_{1c} \\ \beta_{1s} \end{pmatrix}^{\cdot}$$

$$+ \begin{bmatrix} \nu^2 & \mu^2\frac{\gamma}{16}\sin 3\psi & -\mu^2\frac{\gamma}{16}\cos 3\psi \\ \mu\frac{\gamma}{6} + \mu^2\frac{\gamma}{8}\sin 3\psi & \nu^2 - 1 + \mu\frac{\gamma}{6}\cos 3\psi & \frac{\gamma}{8}\left(1+\frac{\mu^2}{2}\right) + \mu\frac{\gamma}{6}\sin 3\psi \\ -\mu^2\frac{\gamma}{8}\cos 3\psi & -\frac{\gamma}{8}\left(1-\frac{\mu^2}{2}\right) + \mu\frac{\gamma}{6}\sin 3\psi & \nu^2 - 1 - \mu\frac{\gamma}{6}\cos 3\psi \end{bmatrix} \begin{pmatrix} \beta_0 \\ \beta_{1c} \\ \beta_{1s} \end{pmatrix}$$

$$= \begin{bmatrix} \frac{\gamma}{8}(1+\mu^2) & -\mu^2\frac{\gamma}{16}\cos 3\psi & \mu\frac{\gamma}{6} - \mu^2\frac{\gamma}{16}\sin 3\psi \\ -\mu^2\frac{\gamma}{8}\cos 3\psi & \frac{\gamma}{8}\left(1+\frac{\mu^2}{2}\right) + \mu\frac{\gamma}{6}\sin 3\psi & -\mu\frac{\gamma}{6}\cos 3\psi \\ \mu\frac{\gamma}{3} - \mu^2\frac{\gamma}{8}\sin 3\psi & -\mu\frac{\gamma}{6}\cos 3\psi & \frac{\gamma}{8}\left(I + \frac{3}{2}\mu^2\right) - \mu\frac{\gamma}{6}\sin 3\psi \end{bmatrix} \begin{pmatrix} \theta_0 - K_p\beta_0 \\ \theta_{1c} - K_p\beta_{1c} \\ \theta_{1s} - K_p\beta_{1s} \end{pmatrix}$$

(156)

$$\begin{pmatrix}\beta_0\\ \beta_{1c}\\ \beta_{1s}\\ \beta_2\end{pmatrix}^{\cdot\cdot} + \begin{bmatrix}\frac{\gamma}{8} & 0 & \mu\frac{\gamma}{12} & 0\\ 0 & \frac{\gamma}{8} & 2 & \mu\frac{\gamma}{6}\sin 2\psi\\ \mu\frac{\gamma}{6} & -2 & \frac{\gamma}{8} & -\mu\frac{\gamma}{6}\cos 2\psi\\ 0 & \mu\frac{\gamma}{12}\sin 2\psi & -\mu\frac{\gamma}{12}\cos 2\psi & \frac{\gamma}{8}\end{bmatrix}\begin{pmatrix}\beta_0\\ \beta_{1c}\\ \beta_{1s}\\ \beta_2\end{pmatrix}^{\cdot}$$

$$+\begin{bmatrix}\nu^2 & 0 & 0 & \mu^2\frac{\gamma}{8}\sin 2\psi\\ \mu\frac{\gamma}{6} & \nu^2-1+\mu^2\frac{\gamma}{16}\sin 4\psi & \frac{\gamma}{8}\left(1+\frac{\mu^2}{2}\right)-\frac{\gamma}{16}\mu^2\cos 4\psi & \mu\frac{\gamma}{6}\cos 2\psi\\ 0 & -\frac{\gamma}{8}\left(1-\frac{\mu^2}{2}\right)-\frac{\gamma}{16}\mu^2\cos 4\psi & \nu^2-1-\mu^2\frac{\gamma}{16}\sin 4\psi & \mu\frac{\gamma}{6}\sin 2\psi\\ \mu^2\frac{\gamma}{8}\sin 2\psi & \mu\frac{\gamma}{6}\cos 2\psi & \mu\frac{\gamma}{6}\sin 2\psi & \nu^2\end{bmatrix}\begin{pmatrix}\beta_0\\ \beta_{1c}\\ \beta_{1s}\\ \beta_2\end{pmatrix}$$

$$=\begin{bmatrix}\frac{\gamma}{8}(1+\mu^2) & 0 & \mu\frac{\gamma}{6} & -\mu^2\frac{\gamma}{8}\cos 2\psi\\ 0 & \frac{\gamma}{8}\left(1+\frac{\mu^2}{2}\right)-\frac{\gamma}{16}\mu^2\cos 4\psi & -\mu^2\frac{\gamma}{16}\sin 4\psi & \mu\frac{\gamma}{3}\sin 2\psi\\ \mu\frac{\gamma}{3} & -\mu^2\frac{\gamma}{16}\sin 4\psi & \frac{\gamma}{8}\left(1+\frac{3}{2}\mu^2\right)+\frac{\gamma}{16}\mu^2\cos 4\psi & -\mu\frac{\gamma}{3}\cos 2\psi\\ -\mu^2\frac{\gamma}{8}\cos 2\psi & \mu\frac{\gamma}{6}\sin 2\psi & -\mu\frac{\gamma}{6}\cos 2\psi & \frac{\gamma}{8}(1+\mu^2)\end{bmatrix}\begin{pmatrix}\theta_0-K_p\beta_0\\ \theta_{1c}-K_p\beta_{1c}\\ \theta_{1s}-K_p\beta_{1s}\\ \theta_2-K_p\beta_2\end{pmatrix}$$

(157)

N = 4

The derivation and discussions of these equations may be found in the literature, for example in references 13 and 18.

The transformation to nonrotating degrees of freedom and equations of motion has the effect of sweeping the periodic coefficients from the lower degrees of freedom, especially as N increases. There are, however, always periodic coefficients in the nonrotating equations where $\mu > 0$, just as there are in the rotating equations, for the same system is being described and a constant coefficient set of equations could never give the behavior that has been found with the periodic coefficients.

The flap dynamics described by these sets of differential equations is nothing new. This is still a set of N independent blades and simply observing the motion in the nonrotating frame does not change the nature of the system. Hence, the eigenvalues must still be as calculated above for the case of a single independent blade; the only change is a $\pm ni$ for the β_{nc}/β_{ns} modes, that is, a $\pm n$/rev shift in the frequency to account for the transformation from rotating to nonrotating frames. The perturbation solution for these equations, including the influence of the periodic coefficients in forward flight, has already been obtained then. The value of the description of the rotor by these nonrotating degrees of freedom and equations lies in its use for dynamics involving the helicopter body or shaft motion, aerodynamic gust, or any other excitation from the nonrotating frame. The rotor responds to such excitation as a whole, in nonrotating modes of motion, so this description of the rotor motion and moment equilibrium is appropriate for studying such problems. For the current investigation, the use of these nonrotating equations is that they provide a basis for a constant coefficient approximation for the rotor flap dynamics.

CONSTANT COEFFICIENT APPROXIMATION

As should be quite apparent by now, differential equations with periodic coefficients require considerably more analysis than constant coefficient equations, even to simply find the eigenvalues. Constant coefficient differential equations are much preferable for the studies of dynamic systems. Can the flap dynamics of a helicopter rotor in forward flight be adequately described by some constant coefficient approximation to the equations of motion? The constant coefficient approximations for the teetering and gimballed rotors were discussed along with their perturbation solutions including the periodic coefficients; this section will be concerned with the case of individually flapping blades.

Consider the rotating equation of motion for $\beta^{(m)}$ (eq. (57)). The constant coefficient approximation to that equation, that is, using only the mean values of the coefficients, is

$$\ddot{\beta} + \frac{\gamma}{8}\dot{\beta} + \left[\nu^2 + (1 + \mu^2)\frac{\gamma}{8}K_p\right]\beta = 0 \qquad (158)$$

The eigenvalues of which are

$$\lambda = -\frac{\gamma}{16} \pm i\sqrt{\nu^2 + (1 + \mu^2)\frac{\gamma}{8}K_P - \left(\frac{\gamma}{16}\right)^2} \qquad (159)$$

The only influence of forward flight is the order μ^2 increase in the mean of M_θ, so in the effectiveness of Kp. Consider this equation and its roots as a representation of the flap dynamics of an independent blade in forward flight. A correct estimate of the eigenvalues to order μ is obtained with such a representation, except near the ½/rev critical region, simply because neither this constant coefficient approximation nor the correct solution away from the ½/rev region show any order μ effects. To order μ^2, this approximation is not correct even away from the critical regions.

With the constant coefficient approximation made in the rotating equation, the result is virtually just the hover root; so the question of the applicability of that approximation is really whether the hover roots may be used as a measure of the flap dynamics in forward flight as well as in hover. This approximation misses the ½/rev and 1/rev critical regions entirely, and so provides no information at all about those effects. Away from the critical regions, however, the correct roots show only quite small influence of forward flight, as for example case (c) in figure 1. This constant coefficient approximation - that is, the hover root - may be considered a reasonable representation for such cases. It should be noticed, however, that the influence of the critical regions becomes greater as μ increases, so this approximation must eventually break down for every case.

The nonrotating equations of motion provide another source of a constant coefficient approximation to the flap dynamics of a rotor with N independent blades. The transformation to the nonrotating frame is accomplished first, and then the averaged coefficients are found. The harmonics of the coefficients of the rotating equation contribute to the constant coefficients in the nonrotating frame, hence, this procedure retains more of the influence of the periodic coefficients. For N = 3, the resulting equations of motion are

$$\begin{pmatrix}\beta_0\\ \beta_{1c}\\ \beta_{1s}\end{pmatrix}'' + \begin{bmatrix} -\gamma M_{\dot\beta}^{0} & 0 & -\frac{\gamma}{2} M_{\dot\beta}^{1s} \\ 0 & -\gamma M_{\dot\beta}^{0} - \frac{\gamma}{2} M_{\dot\beta}^{2c} & 2 \\ -\gamma M_{\dot\beta}^{1s} & -2 & -\gamma M_{\dot\beta}^{0} + \frac{\gamma}{2} M_{\dot\beta}^{2c} \end{bmatrix} \begin{pmatrix}\beta_0\\ \beta_{1c}\\ \beta_{1s}\end{pmatrix}'$$

$$+ \begin{bmatrix} \nu^2 & -\frac{\gamma}{2} M_{\beta}^{1c} + \frac{\gamma}{2} M_{\dot\beta}^{1s} & 0 \\ -\gamma M_{\beta}^{1c} & \nu^2 - 1 & -\frac{\gamma}{2} M_{\beta}^{2s} - \gamma M_{\dot\beta}^{0} - \frac{\gamma}{2} M_{\dot\beta}^{2c} \\ 0 & -\frac{\gamma}{2} M_{\beta}^{2c} + \gamma M_{\dot\beta}^{0} - \frac{\gamma}{2} M_{\dot\beta}^{2c} & \nu^2 - 1 \end{bmatrix} \begin{pmatrix}\beta_0\\ \beta_{1c}\\ \beta_{1s}\end{pmatrix}$$

$$= \begin{bmatrix} \gamma M_{\theta}^{0} & 0 & \frac{\gamma}{2} M_{\theta}^{1s} \\ 0 & \gamma M_{\theta}^{0} + \frac{\gamma}{2} M_{\theta}^{2c} & 0 \\ \gamma M_{\theta}^{1s} & 0 & \gamma M_{\theta}^{0} - \frac{\gamma}{2} M_{\theta}^{2c} \end{bmatrix} \begin{pmatrix}\theta_0 - Kp\beta_0\\ \theta_{1c} - Kp\beta_{1c}\\ \theta_{1s} - Kp\beta_{1s}\end{pmatrix} \qquad (160)$$

where use has been made of the following Fourier series representations of the flap moments in forward flight:

$$M_{\theta} = M_{\theta}^{0} + M_{\theta}^{1s} \sin\psi + M_{\theta}^{2c} \cos 2\psi + \ldots$$

$$M_{\dot\beta} = M_{\dot\beta}^{0} + M_{\dot\beta}^{1s} \sin\psi + M_{\dot\beta}^{2c} \cos 2\psi + \ldots$$

$$M_{\beta} = M_{\beta}^{1c} \cos\psi + M_{\beta}^{2s} \sin 2\psi + \ldots$$

The missing harmonics is a general result valid for all μ, even including the reverse flow region effects. Substituting for the harmonics of the flap moments from equation (2), that is, neglecting reverse flow as usual for the present order μ^2 analysis, the equations are

$$\begin{pmatrix}\beta_0\\ \beta_{1c}\\ \beta_{1s}\end{pmatrix}'' + \begin{bmatrix}\frac{\gamma}{8} & 0 & \mu\frac{\gamma}{12}\\ 0 & \frac{\gamma}{8} & 2\\ \mu\frac{\gamma}{6} & -2 & \frac{\gamma}{8}\end{bmatrix}\begin{pmatrix}\beta_0\\ \beta_{1c}\\ \beta_{1s}\end{pmatrix}'$$

$$+ \begin{bmatrix}\nu^2+(1+\mu^2)\frac{\gamma}{8}K_p & 0 & K_p\mu\frac{\gamma}{6}\\ \mu\frac{\gamma}{6} & \nu^2-1+\left(1+\frac{\mu^2}{2}\right)\frac{\gamma}{8}K_p & \frac{\gamma}{8}\left(1+\frac{\mu^2}{2}\right)\\ K_p\mu\frac{\gamma}{3} & -\frac{\gamma}{8}\left(1-\frac{\mu^2}{2}\right) & \nu^2-1+\left(1+\frac{3}{2}\mu^2\right)\frac{\gamma}{8}K_p\end{bmatrix}\begin{pmatrix}\beta_0\\ \beta_{1c}\\ \beta_{1s}\end{pmatrix} = 0 \qquad (161)$$

This is the constant coefficient approximation, in the nonrotating frame, for the flap dynamics of a rotor with three independent blades. It may also be obtained from equation (156), by dropping the 3/rev terms in the coefficients.

The approximate eigenvalues are then solutions of the characteristic equation

$$\left[\lambda^2+\frac{\gamma}{8}\lambda+\nu^2+K_p\frac{\gamma}{8}(1+\mu^2)\right]\left\{\left[\lambda^2+\frac{\gamma}{8}\lambda+\nu^2-1+K_p\frac{\gamma}{8}(1+\mu^2)\right]^2\right.$$

$$\left.+\left(2\lambda+\frac{\gamma}{8}\right)^2-\mu^4\left(\frac{\gamma}{16}\right)^2(1+K_p^2)\right\}-\mu^2\left(\frac{\gamma}{12}\right)^2 2(\lambda+2K_p)\left[2\lambda+\frac{\gamma}{8}\left(1-\frac{\mu^2}{2}\right)\right]$$

$$-\mu^2\left(\frac{\gamma}{12}\right)^2 2(\lambda+2K_p)^2\left[\lambda^2+\frac{\gamma}{8}\lambda+\nu^2-1+K_p\frac{\gamma}{8}\left(1+\frac{\mu^2}{2}\right)\right] = 0 \qquad (162)$$

Only μ^2 and μ^4 terms appear, so consider an expansion in μ^2: $\lambda = \lambda_0 + \mu^2\lambda_2 + \ldots$, or $\lambda = \lambda_0 \pm i + \mu^2\lambda_2 + \ldots$, and the conjugates, for the coning mode and β_{1c}/β_{1s} modes, respectively. The Lock number is also expanded as a series: $\gamma = \gamma_0 + \mu^2\gamma_2 + \ldots$; and λ_0 is the rotating hover root as usual:

$$\lambda_0 = -\frac{\gamma_0}{16} + i\sqrt{\nu^2+\frac{\gamma_0}{8}K_p-\left(\frac{\gamma_0}{16}\right)^2}$$

To order 1, the solution for the roots is just $\lambda = \lambda_0$, $\lambda_0 \pm i$ and their conjugates, verifying that the above expansion is correct for the hover limit.

Coning Modes

Consider the coning mode roots in forward flight, that is, the expansion $\lambda = \lambda_0 + \mu^2\lambda_2 + \ldots$. The order μ^2 terms in the characteristic equation give then

$$\left(2\lambda_0\lambda_2 + \frac{\gamma_0}{8}\lambda_2 + \frac{\gamma_2}{8}\lambda_0 + K_p\frac{\gamma_0}{8} + K_p\frac{\gamma_2}{8}\right)\left[1 + \left(2\lambda_0 + \frac{\gamma_0}{8}\right)^2\right]$$
$$- \left(\frac{\gamma_0}{12}\right)^2 2(\lambda_0 + 2K_p)\left(2\lambda_0 + \frac{\gamma_0}{8}\right) + \left(\frac{\gamma_0}{12}\right)^2 2(\lambda_0 + 2K_p)^2 = 0$$

or

$$[1 - (2Im\lambda_0)^2]\left[2iIm\lambda_0\left(\lambda_2 + \frac{\gamma_2}{16}\right) + \frac{\gamma_2}{8}\left(-\frac{\gamma_0}{16} + K_p\right) + \frac{\gamma_0}{8}K_p\right]$$
$$+ \left(\frac{\gamma_0}{12}\right)^2 2\left(\nu^2 - \frac{\gamma_0}{8}K_p + 4K_p^2\right) = 0 \qquad (163)$$

Assuming that $Im\lambda_0 \neq 1/2$, the root to order μ^2 is then

$$\lambda = -\frac{\gamma}{16} \pm i\sqrt{\nu^2 + (1+\mu^2)\frac{\gamma}{8}K_p - \left(\frac{\gamma}{16}\right)^2\left[1 + \mu^2\frac{8}{9}\frac{\nu^2 - \frac{\gamma}{8}K_p + 4K_p^2}{\nu^2 + \frac{\gamma}{8}K_p - \left(\frac{\gamma}{16}\right)^2 - \frac{1}{4}}\right]} \qquad (164)$$

This is exactly the correct result for the eigenvalues away from the critical regions, that is, equation (24). The real root boundary and divergence criterion for this root are also correct then. This expression also applies for the coning mode approximate root when $Im\lambda_0 = 1/rev$, however, so it misses the 1/rev critical region.

Now consider the coning mode root near $Im\lambda_0 = 1/2$, that is, to order 1 $\lambda_0 = -(\gamma_0/16) + i/2$. The order μ^2 expansion did not work there, so consider an order μ expansion: $\lambda = \lambda_0 + \mu\lambda_1 + \ldots$ and $\gamma = \gamma_0 + \mu\gamma_1 + \ldots$ The order μ term of the characteristic equation is identically zero then, and the order μ^2 term is

$$\left(2\lambda_0\lambda_1 + \frac{\gamma_0}{8}\lambda_1 + \frac{\gamma_1}{8}\lambda_0 + K_p\frac{\gamma_1}{8}\right)\left[-2\left(2\lambda_0\lambda_1 + \frac{\gamma_0}{8}\lambda_1 + \frac{\gamma_1}{8}\lambda_0 + K_p\frac{\gamma_1}{8}\right)\right.$$
$$\left. + 2\left(2\lambda_0 + \frac{\gamma_0}{8}\right)\left(2\lambda_1 + \frac{\gamma_1}{8}\right)\right] - \left(\frac{\gamma_0}{12}\right)^2 2(\lambda_0 + 2K_p)\left(\lambda_0 + \frac{\gamma_0}{8} - 2K_p\right) = 0$$

or

$$\left(\lambda_1 + \frac{\gamma_1}{16}\right)^2 = -\left[\frac{\gamma_1}{8}\left(\frac{\gamma_0}{16} - K_p\right)\right]^2 + \left(\frac{\gamma_0}{12}\right)^2\left(\nu^2 - \frac{\gamma_0}{8}K_p + 4K_p^2\right)$$
$$= -D^2 \qquad (165)$$

The root to order μ is then

$$\lambda = \lambda_0 + \mu\lambda_1 = -\frac{\gamma}{16} + \frac{i}{2} \pm i\mu D \tag{166}$$

These are exactly the same expressions for D and λ as were found for the ½/rev critical region by the perturbation analysis in the rotating frame, including the periodic coefficients. So the coning mode of this constant coefficient approximation encounters the ½/rev critical region, with the correct boundary and roots. Now the roots in a critical region have a plus and minus increment in the damping due to the periodic coefficients, that is, the roots are not complex conjugates. What is happening to allow the roots of a constant coefficient approximation to exhibit this critical region behavior is the following. The low frequency mode roots $\lambda_0 - i$ and the conjugate are also at ±½/rev when $\mathrm{Im}\lambda_0 = 1/2$. Hence, with the coning and low frequency mode roots there are a total of four roots, two at ½/rev and two at -½/rev, which must participate in this ½/rev critical region behavior. Hence, the critical region behavior can occur while the roots remain as complex conjugate pairs as is required for constant coefficient equations.

High and Low Frequency Modes

Consider the low frequency and high frequency rotor modes, that is, the expansion $\lambda = \lambda_0 \pm i + \mu^2\lambda_2 + \ldots$. Then the order μ^2 equation is

$$(\mathrm{Im}\lambda_0 \pm 1)\left\{(\mp 2\mathrm{Im}\lambda_0 - 1)\left[(2i\mathrm{Im}\lambda_0)\lambda_2 + \frac{\gamma_2}{8}(\lambda_0 + Kp) + \frac{\gamma_0}{8}Kp\right] - \left(\frac{\gamma_0}{12}\right)^2(\lambda_0 \pm i + 2Kp)(\lambda_0 + 2Kp)\right\} = 0 \tag{167}$$

Assume for now that $\mathrm{Im}\lambda_0 \neq 1/2$ or 1 for the low frequency rotor mode; then

$$\lambda_2 = -\frac{\gamma_2}{16} + \frac{i}{2\mathrm{Im}\lambda_0}\left[\frac{\gamma_2}{8}\left(-\frac{\gamma_0}{16} + Kp\right) + \frac{\gamma_0}{8}Kp - \left(\frac{\gamma_0}{12}\right)^2\frac{(\lambda_0 \pm i + 2Kp)(\lambda_0 + 2Kp)}{\mp 2\mathrm{Im}\lambda_0 - 1}\right] \tag{168}$$

The roots to order μ^2 are then

$$\lambda = \pm i\left\{1 - \mu^2\left(\frac{\gamma}{24}\right)^2\left[2 - \frac{\nu^2 - \frac{\gamma}{8}Kp + 4Kp^2}{\nu^2 + \frac{\gamma}{8}Kp - \left(\frac{\gamma}{16}\right)^2 - \frac{1}{4}}\right]\right\}$$

$$-\frac{\gamma}{16} + i\left\{\nu^2 + (1+\mu^2)\frac{\gamma}{8}Kp - \left(\frac{\gamma}{16}\right)^2\left[1 + \mu^2\frac{4}{9}\frac{\nu^2 - \frac{\gamma}{8}Kp + 4Kp^2}{\nu^2 + \frac{\gamma}{8}Kp - \left(\frac{\gamma}{16}\right)^2 - \frac{1}{4}}\right] \mp i\mu^2\left(\frac{\gamma}{12}\right)^2\left(\frac{\gamma}{16} - 2Kp\right)\right\}^{1/2} \tag{169}$$

and the conjugates. This result is similar to what was found for the three-bladed gimballed rotor away from critical regions, so the behavior is familiar from that discussion. The only change, in fact, is a reversal of the signs of the $\pm$ order μ^2 terms, hence, all the analysis of that case may be used here.

The main feature of the behavior is that when $\mu > 0$ the real root intersection of the γ loci - at ± 1/rev nonrotating - pulls apart. The order μ^2 changes in the frequency and damping are in the opposite direction from what is shown in figure 9(c). The closest approach of the two branches has an order μ width:

$$2|\Delta\lambda|_{min} = \mu\frac{8}{3}\sqrt{\frac{\gamma_0}{16}}\nu \tag{170}$$

where $\gamma_0/16 = Kp + \sqrt{\nu^2 + Kp^2}$ is the γ for the boundary when $\mu = 0$. Taking the point of closest approach as the real root boundary, it is then

$$\frac{\gamma}{16} = \frac{\gamma_0}{16}\left[1 + \mu^2\frac{\frac{8}{9}\nu^2(-Kp + \sqrt{\nu^2 + Kp^2}) + Kp}{\sqrt{\nu^2 + Kp^2}}\right] \tag{171}$$

The criterion for divergence stability for these four roots is

$$(1 + \mu^2)\frac{\gamma}{8}Kp > -\nu^2\left[1 + \mu^2\frac{8}{9}\frac{\left(\frac{\gamma}{16}\right)^2 + \frac{\nu^2}{2}}{\left(\frac{\gamma}{16}\right)^2 + \frac{1}{4}}\right] \tag{172}$$

There is this important difference from the case of the three-bladed gimballed rotor: this solution does not represent the behavior of any real system, but rather is being considered as an approximation to the rotor flap dynamics in forward flight. As such, it has then order μ^2 errors in both

the frequency and damping compared to the correct solution (eq. (24)). Away from critical regions, the correct solution shows only a small influence of forward flight anyway, so these errors are probably not large either.

This behavior of the roots near the real root boundary has been seen twice now: with the three-bladed gimballed rotor, and here for the constant coefficient approximation to the independent blade dynamics. The origin of this behavior is the order μ, 1/rev term in the flap damping M_{β}. That term gives the 3/rev periodic coefficients for the gimballed rotor which produce the term in the radicand of λ that gives this behavior. For the constant coefficient approximation, the flap damping harmonic M_{β}^{1s} gives terms coupling the β_{1c} and β_{1s} motion, producing the observed behavior. With independent blades observed in the rotating frame, the loci intersect at the real axis as is characteristic of root loci; observed in the nonrotating frame, the behavior is shifted by $\pm i$ so it occurs at ± 1/rev now, but the blades are still independent so the root loci still intersect. The root loci of coupled degrees of freedom do not show that behavior, however; rather they simply pass close to one another, the minimum separation being a measure of the magnitude of the coupling. The gimballed rotor couples the blades by requiring that the rotor move as a whole, in β_{1c} and β_{1s} motion only. The constant coefficient approximation couples the blades by dropping terms from the equations of motion describing the independent blades, creating a description of some new system with coupled degrees of freedom. (How closely the dynamics of this new system might represent the rotor with independent blades is what is being examined here.)

When $\mathrm{Im}\lambda_0 = 1/2$, that is, when the hover rotating frequency is near ½/rev, the low frequency rotor mode (at -½/rev nonrotating frequency) encounters the ½/rev critical region. It is not necessary to go looking for this solution, because the only way the coning mode could exhibit the critical region behavior with a constant coefficient equation is if the low frequency mode joins it, so the roots may remain complex conjugates even inside the critical region. The critical region behavior found is the same as that of the perturbation solution including the periodic coefficients. So the constant coefficient approximation gives the correct behavior of these four roots near the ½/rev critical region. The high frequency rotor mode (at 3/2/rev nonrotating frequency) does not, however, participate in this behavior. Indeed, the above result (eq. (169)) is still valid for the $\lambda_0 + i$ root even when $\mathrm{Im}\lambda_0 = 1/2$; the error in that root is then order μ.

Now consider the low frequency mode ($\lambda_0 - i$) when $\mathrm{Im}\lambda_0 = 1$; these roots are at 0/rev nonrotating frequency, that is, to order 1 $\lambda = -\gamma_0/16$. The high frequency mode gives no problems in the order μ^2 characteristic equation even when $\mathrm{Im}\lambda_0 = 1$, so equation (169) gives the roots there. For the low frequency mode, however, the order μ^2 characteristic equation (eq. (167)) is identically zero when $\mathrm{Im}\lambda_0 = 1$, so it is necessary to go to order μ^4 to find λ_2. The order μ^4 characteristic equation is, when $\mathrm{Im}\lambda_0 = 1$:

$$\left(\lambda_2 + \frac{\gamma_2}{16}\right)^2 + \left(\frac{\gamma_0}{12}\right)^2\left(\frac{\gamma_0}{16} - 2K_p\right)\left(\lambda_2 + \frac{\gamma_2}{16}\right) + \left[\frac{\gamma_2}{16}\left(-\frac{\gamma_0}{16} + K_p\right) + K_p\,\frac{\gamma_0}{16}\right]^2 - \left(\frac{\gamma_0}{32}\right)^2(1 + K_p^2)$$

$$- \left(\frac{\gamma_0}{12}\right)^2\left(\frac{\gamma_0}{16} - 2K_p\right)\frac{\gamma_0}{32} - \left(\frac{\gamma_0}{12}\right)^2\left(\frac{\gamma_0}{16} - 2K_p\right)^2\left[\frac{\gamma_2}{16}\left(-\frac{\gamma_0}{16} + K_p\right) + K_p\,\frac{\gamma_0}{32}\right] = 0$$

or

$$\lambda_2 + \frac{\gamma_2}{16} = -\frac{1}{2}\left(\frac{\gamma_0}{12}\right)^2\left(\frac{\gamma_0}{16} - 2K_p\right) \pm iD \tag{173}$$

where

$$D^2 = \left[\left(\frac{\gamma_0}{16} - K_p\right)\frac{\gamma_2}{16} + \left(\frac{\gamma_0}{6}\right)^2\frac{\nu^2 - \frac{\gamma_0}{8}K_p + 4K_p^2}{8} - \frac{1}{2}\left(\frac{\gamma_0}{12}\right)^2 - K_p\,\frac{\gamma_0}{16}\right]^2$$

$$- \left(\frac{\gamma_0}{32}\right)^2\left\{\left[1 + \frac{\gamma_0}{9}\left(\frac{\gamma_0}{16} - 2K_p\right)\right]^2 + \left[K_p - \frac{\gamma_0}{9}\left(\frac{\gamma_0}{16} - 2K_p\right)^2\right]^2\right\} \tag{174}$$

and the root to order μ^2 is

$$\lambda = -\frac{\gamma}{16}\left[1 + \mu^2\,\frac{\gamma_0}{18}\left(\frac{\gamma_0}{16} - 2K_p\right)\right] \pm i\mu^2 D \tag{175}$$

This is the critical region behavior again, possible with the constant coefficient equations because for this mode the nonrotating roots are at the real axis. The critical region boundary is given by $D^2 = 0$, or the corner μ:

$$\mu_1^2, \mu_2^2 = -\frac{\left(\frac{\gamma_0}{16} - K_p\right)\frac{\Delta\gamma}{16}}{C_1 \pm C_2} \tag{176}$$

where here

$$C_1 = -\left(\frac{\gamma_0}{6}\right)^2\frac{\nu^2 - \frac{\gamma_0}{8}K_p + 4K_p^2}{8} + \frac{1}{2}\left(\frac{\gamma_0}{12}\right)^2 + K_p\,\frac{\gamma_0}{16}$$

$$= -\frac{8}{9}(\nu^2 - 1)^2 + K_p\,\frac{\gamma_0}{16} \tag{177}$$

$$C_2 = \frac{\gamma_0}{32}\sqrt{\left[1 + \frac{\gamma_0}{9}\left(\frac{\gamma_0}{16} - 2K_p\right)\right]^2 + \left[K_p - \frac{\gamma_0}{9}\left(\frac{\gamma_0}{16} - 2K_p\right)^2\right]^2}$$

$$= \frac{\gamma_0}{32}\sqrt{\left[1 + \frac{16}{9}(\nu^2 - 1)\right]^2 + \left[K_p - \frac{16}{9}(\nu^2 - 1)\left(\frac{\gamma_0}{16} - 2K_p\right)\right]^2} \tag{178}$$

and $\gamma_0/16 = K_p + \sqrt{\nu^2 + K_p^2 - 1}$ for the 1/rev region as usual. The root may be written then

$$\lambda = -\frac{\gamma}{16}\left[1 + \mu^2\frac{8}{9}(\nu^2 - 1)\right] \pm i\frac{\Delta\gamma}{16}\left(\frac{\gamma_0}{16} - K_p\right)\sqrt{\left(1 - \frac{\mu^2}{\mu_1^2}\right)\left(1 - \frac{\mu^2}{\mu_2^2}\right)} \tag{179}$$

and the boundary on the $\gamma - \mu$ plane is

$$\frac{\Delta\gamma}{16} = \mu^2\frac{C_1 \pm C_2}{\frac{\gamma_0}{16} - K_p} \tag{180}$$

For $K_p = 0$, these reduce to $\gamma_0/16 = \sqrt{\nu^2 - 1}$,

$$C_1 = -\frac{8}{9}(\nu^2 - 1)^2 \tag{181}$$

$$C_2 = \frac{\gamma_0}{32}\sqrt{1 + \frac{32}{9}(\nu^2 - 1) + \frac{256}{81}\nu^2(\nu^2 - 1)^2} \tag{182}$$

and the 1/rev critical region boundary on the $\gamma - \mu$ plane becomes

$$\frac{\Delta\gamma}{16} = \mu^2\left[-\frac{8}{9}(\nu^2 - 1)^{3/2} \pm \frac{1}{2}\sqrt{1 + \frac{32}{9}(\nu^2 - 1) + \frac{256}{81}\nu^2(\nu^2 - 1)^2}\right] \tag{183}$$

The general behavior of the roots in this 1/rev critical region is correct but there are order μ^2 errors in both the frequency and damping compared to the exact solution. C_2, the width of the critical region, is exactly correct. There is an order μ^2 change in the damping (eq. (179)); and the offset of the critical region, C_1, is not correct, leading to an order μ^2 change in the frequency. These order μ^2 errors correspond to those in the expression for the roots away from the critical region (eq. (169)). For $\nu = 1$ the damping change goes to zero, and for $\nu = 1$ and $K_p = 0$ the offset

C_1 reduces to zero for both the correct solution and for this approximation; in general, however, there are small errors in the 1/rev critical region behavior as there were for the roots away from the critical region.

The coning mode (at 1/rev nonrotating frequency) and the high frequency mode (at 2/rev) do not participate at all in the 1/rev critical region. These roots are given still by their respective expressions for away from the critical regions (eqs. (164) and (169)).

Summary

The flapping dynamics of a rotor with three independent blades are described by a total of six eigenvalues. In the rotating frame, there are three independent equations; then the eigenvalues occur as two triple poles. In the nonrotating frame, the degrees of freedom and equations of motion are coupled. There are two eigenvalues at the rotating value for the coning mode, and four eigenvalues at the rotating values ±1/rev for the high and low frequency rotor modes. Thus, if λ_R is the rotating eigenvalue, the nonrotating roots are $\lambda_{NR} = \lambda_R$, $\lambda_R \pm i$ (for $N = 3$). The total number of eigenvalues in the nonrotating frame is still six for the three-bladed rotor. The constant coefficient approximation in the nonrotating frame gives results for all six eigenvalues at once (in general, for all $2N$ roots of the rotor flap motion). This approximation gives the following behavior for the roots.

Away from critical regions (i.e., the hover rotating frequency not near ½/rev or 1/rev) the two coning mode roots are given by equation (164), which is exactly the result obtained including the periodic coefficients. The four roots of the low frequency and high frequency modes are given by equation (169), which has order μ^2 errors in both the frequency and damping. The effects of forward flight away from the critical region are, in general, small, however, so these errors are not too significant.

The four coning and low frequency mode roots encounter the ½/rev critical region (at ±½/rev nonrotating frequency), with exactly the same behavior as the correct solution (to order μ at least). The two roots of the high frequency mode (at 3/2/rev) do not participate in this behavior, which means an order μ error.

The four coning and high frequency mode roots do not encounter the 1/rev critical region, which means order μ^2 errors for these roots. The two roots of the low frequency mode, at the real axis in the nonrotating frame do show the critical region behavior. There are, however, in general order μ^2 errors in both the frequency and damping compared to the correct solution, corresponding to the behavior of the roots of this mode away from the critical regions. The magnitude of these errors is discussed below in terms of the $\gamma - \mu$ plane.

Consider the $\gamma - \mu$ plane for $\nu = 1$ and $Kp = 0$ (fig. 2). The constant coefficient approximation has an identical 1/rev region boundary but only for the low frequency rotor mode, that is, two out of the six roots. It has the

same ½/rev region, but only for the coning and low frequency modes (four out of six). The real root boundary for the coning mode is the same but the boundary for the high and low frequency modes shows only half the influence of μ. The latter boundary is, in fact, only the point of closest approach of these two modes at ±1/rev nonrotating frequency, not an intersection at all.

For $\nu = 1.1$ and $K_P = 0$ (fig. 4), the $\gamma - \mu$ plane of the constant coefficient approximation has a 1/rev region boundary, but only for the low frequency mode again. The region has the same width for a given μ as the correct solution, but is offset higher. The error in the boundary is roughly $\Delta\gamma = 4\mu^2$, or about $\Delta\gamma = 1$ at $\mu = 0.5$ (compared to γ_0 about seven for the 1/rev region with $\nu = 1.1$, as shown in fig. 4). As a result, rotors with γ such that the hover frequency is above 1/rev will have a higher μ_{corner} by this approximation. For example, with case (b) above, $\nu = 1.1$ and $\gamma = 6$, the constant coefficient approximation gives $\mu_{corner} = 0.326$, compared to the correct solution of $\mu_{corner} = 0.286$. This error in the 1/rev region boundary - which corresponds to the frequency error away from the critical region, and so is a measure of the magnitude of that also - is not negligible, but is small in terms of the $\Delta\gamma$ shift of the boundary, or even in terms of the μ_{corner}, which is more sensitive to the boundary shifts. The comparisons of the ½/rev region and real root boundaries for this case follow exactly as for $\nu = 1$, discussed above.

The constant coefficient approximation to the rotor flap dynamics in forward flight produces differential equations that do not actually describe the real rotor any more, and must always give some erroneous results. As a representation of the actual rotor dynamics, however, the constant coefficient approximation (in the nonrotating frame) is actually remarkably good. The influence of forward flight on the roots is given rather well by this approximation, the primary error being that the roots of the high frequency rotor modes do not encounter the critical regions. For this case of $N = 3$, the ½/rev region is seen by the four roots at ±½/rev, but not by the two roots at ±3/2/rev; the 1/rev region is seen by the two roots at the real axis, but not by the four roots at ±1/rev and ±2/rev. This behavior is fundamental to the constant coefficient approximation; the roots from that approximation must always be complex conjugates, so the critical region behavior can only be exhibited by two roots on the real axis (as the 1/rev region here); or at a multiple of ½/rev when there are four roots to participate, two at the positive frequency and two at the negative frequency (as the ½/rev region here). With these restrictions, the constant coefficient approximation picks up the critical region behavior of the periodic system whenever possible. The constant coefficient approximation in the nonrotating frame is better than in the rotating frame because the transformation to the nonrotating frame shifts the frequency of the roots to allow such occurrences. At the least, these results suggest that the constant coefficient approximation is adequate for the low frequency dynamics of a rotor as for helicopter stability and control investigations.

Four-bladed Rotor

Comparing the constant coefficient approximation of equations (156) and (157) for the $N = 3$ and $N = 4$ cases, it follows that the four-bladed rotor only adds the β_2 degree of freedom and equation which are completely decoupled for the constant coefficient approximation. So, to equation (161) must be added the equation

$$\ddot{\beta}_2 + \frac{\gamma}{8}\dot{\beta}_2 + \left[\nu^2 + (1 + \mu^2)\frac{\gamma}{8}K_p\right]\beta_2 = 0 \tag{184}$$

for the four-bladed rotor. The roots for this mode are

$$\lambda = -\frac{\gamma}{16} \pm i\sqrt{\nu^2 + (1 + \mu^2)\frac{\gamma}{8}K_p - \left(\frac{\gamma}{16}\right)^2} \tag{185}$$

This is the same as the constant coefficient approximation in the rotating frame which is not very good. All the critical regions are missed and there are even order μ^2 errors away from the critical region. The solution for the other six roots is the same as for the $N = 3$ case.

Five or More Blades

As the number of blades increases, more and more modes are added to the nonrotating representation of the rotor. For example, $N = 5$ has degrees of freedom β_0, β_{1c}, β_{1s}, and

$$\beta_{2c} = \frac{2}{N}\sum_m \beta^{(m)} \cos 2\psi_m$$

$$\beta_{2s} = \frac{2}{N}\sum_m \beta^{(m)} \sin 2\psi_m$$

with corresponding roots $\lambda_{NR} = \lambda_R \pm 2i$. Consequently, more of the low frequency modes will be able to pick up the critical region behavior in the constant coefficient approximation. The highest frequency modes always do not encounter the critical regions, of course, so the constant coefficient approximation can never give completely correct behavior. This effect of increasing N parallels the effect on the differential equations. Increasing N tends to sweep the periodic coefficients from the lower frequency modes; there are always periodic coefficients present in the degrees of freedom and equations of the high frequency modes, however.

TRANSFER FUNCTIONS

The experimental determination of the eigenvalues, especially the small increments (order μ or even μ^2) found here, in the harsh aerodynamic environment of the helicopter in forward flight, is a difficult task to accomplish with accuracy. A more direct measurement - hence, fundamentally more accurate - is the transfer function, that is, the response of the blade flap motion due to sinusoidal excitation.

Consider the transfer function of the flap response to blade pitch control, particularly the influence of the periodic coefficients in forward flight, which has led to the special behavior of the eigenvalues. The equation of motion for an independent blade excited by pitch control inputs only, in the rotating frame, is

$$\ddot{\beta} + \left(\frac{\gamma}{8} + \frac{\gamma}{6}\mu \sin\psi\right)\dot{\beta}$$

$$+ \left\{\nu^2 + \frac{\gamma}{6}\mu\cos\psi + \frac{\gamma}{8}\mu^2 \sin 2\psi + K_p\left[\frac{\gamma}{8}(1+\mu^2) + \frac{\gamma}{3}\mu\sin\psi - \frac{\gamma}{8}\mu^2\cos 2\psi\right]\right\}\beta$$

$$= \left[\frac{\gamma}{8}(1+\mu^2) + \frac{\gamma}{3}\mu\sin\psi - \frac{\gamma}{8}\mu^2\cos 2\psi\right]\theta \qquad (186)$$

The transfer function is defined as the response to sinusoidal input $\theta = \bar{\theta}e^{i\omega\psi}$, where $\bar{\theta}$ is a complex constant. Taking only the real parts of both the input and the output is implied. With a constant coefficient differential equation, the output will also be a sinusoid at frequency ω, that is, $\beta = \bar{\beta}e^{i\omega\psi}$. The differential equation relates the output $\bar{\beta}$ to the input $\bar{\theta}$ by a single complex function $H(\omega)$, which is the transfer function:

$$\frac{\bar{\beta}}{\bar{\theta}} = H(\omega) \qquad (187)$$

With a periodic coefficient differential equation, the response to θ at frequency ω is not just β at frequency ω. The sinusoidal input at ω is multiplied by the coefficients which have terms that are also sinusoidal now with frequencies 1/rev, 2/rev, etc. (Ω, 2Ω, . . .). The product of two sinusoidal functions is a sum of sinusoids at the sum and difference of the frequencies. It follows then that for a periodic coefficient system an input at frequency ω leads to an output with terms at frequencies ω, $\omega \pm 1$/rev, $\omega \pm 2$/rev, etc. The output is then a sum of the form

$$\frac{\beta}{\bar{\theta}} = H_0(\omega)e^{i\omega\psi} + H_{+1}(\omega)e^{i(\omega+1)\psi} + H_{-1}(\omega)e^{i(\omega-1)\psi}$$

$$+ H_{+2}(\omega)e^{i(\omega+2)\psi} + H_{-2}(\omega)e^{i(\omega-2)\psi} + \ldots \qquad (188)$$

where H_0, $H_{\pm1}$, $H_{\pm2}$, . . . are all the transfer functions of the system. Notice this may be written as $\beta/\bar{\theta} = H(\omega, \psi)e^{i\omega\psi}$, where H_0, $H_{\pm1}$, $H_{\pm2}$, etc. are the harmonics of a Fourier series representation of a function $H(\omega, \psi)$, which is periodic in ψ ($H(\omega, \psi)$ is complex, however, so H_{+n} and H_{-n} are not conjugates). Equation (188) is a general result for periodic coefficient differential equations: the dynamic behavior is described by not a single transfer function, but rather a series of transfer functions. There is the direct response H_0, the output at the same frequency as the input; and there are also now sideband responses $H_{\pm n}$, output at the input frequency $\pm n$/rev. Since for the hover limit $\mu = 0$ the present differential equation reduces to constant coefficients, all the transfer functions but H_0 must be zero then. It will be found, in fact, that $H_{\pm n}$ are order μ^n.

Analysis

Assume the input is $\theta = \bar{\theta}e^{i\omega\psi}$. It is possible to simply substitute into equation (186) the expansion for β as in equation (188), collect like harmonics, and thus solve for the transfer functions. Following the rest of the present investigation, however, an expansion in μ will be used which makes the analysis more orderly. Expand the output as a series in μ: $\beta = \beta_0 + \mu\beta_1 + \mu^2\beta_2 + \ldots$. Since it is known that the output has only time behavior like $e^{i(\omega\pm n)\psi}$, there are no other time scales but ψ in this problem. This means there is no critical region behavior in this problem that is a feature of the eigenvalues only. The critical region behavior is replaced here by the sideband transfer functions which will be shown to carry equivalent information about the system dynamics. It is therefore also not necessary to expand γ as a series in μ.

To order 1 the differential equation is

$$\ddot{\beta}_0 + \frac{\gamma}{8}\dot{\beta}_0 + \left(\nu^2 + \frac{\gamma}{8}K_P\right)\beta_0 = \frac{\gamma}{8}\theta \qquad (189)$$

So $\theta = \bar{\theta}e^{i\omega\psi}$ gives $\beta_0 = \bar{\beta}_0 e^{i\omega\psi}$ with

$$\frac{\bar{\beta}_0}{\bar{\theta}} = \frac{\frac{\gamma}{8}}{\Delta(\omega)} \qquad (190)$$

where

$$\Delta(\omega) = -\omega^2 + \frac{\gamma}{8} i\omega + \nu^2 + K_p \frac{\gamma}{8} \tag{191}$$

The order 1 solution is the hover limit as usual; here it is the hover transfer function for the response of blade flapping to pitch input. The transfer function has the usual form for a second order system response, in this case a heavily damped system with natural frequency $\omega_n^2 = \nu^2 + (\gamma/8)K_p$. Notice that $\Delta(i\lambda)$ is the hover characteristic equation.

The order μ differential equation is

$$\ddot{\beta}_1 + \frac{\gamma}{8}\dot{\beta}_1 + \left(\nu^2 + K_p \frac{\gamma}{8}\right)\beta_1 = \frac{\gamma}{3}\sin\psi\theta - \left[\frac{\gamma}{8}\sin\psi\dot{\beta}_0 + \left(\frac{\gamma}{6}\cos\psi + K_p \frac{\gamma}{3}\sin\psi\right)\beta_0\right]$$

$$= \frac{\gamma}{12}\left[-2i\bar{\theta} - (\omega + 1 - 2ik_p)\bar{\beta}_0\right]e^{i(\omega+1)\psi}$$

$$+ \frac{\gamma}{12}\left[2i\bar{\theta} + (\omega - 1 - 2iK_p)\bar{\beta}_0\right]e^{i(\omega-1)\psi} \tag{192}$$

Hence, the solution is $\beta_1 = \bar{\beta}_{1+}e^{i(\omega+1)\psi} + \bar{\beta}_{1-}e^{i(\omega-1)\psi}$ with the transfer functions

$$\frac{\bar{\beta}_{1\pm}}{\bar{\theta}} = \frac{\frac{\gamma}{12}\left[-\frac{\gamma}{8} \pm 2i(\omega^2 - \nu^2)\right]}{\Delta(\omega \pm 1)\Delta(\omega)} \tag{193}$$

The order μ response is then just the $\omega \pm 1$/rev sideband functions. The forcing terms, the right-hand side of equation (192), are the same terms which gave the order μ, ½/rev critical region for the eigenvalues. That is, near ½/rev these terms contributed to the order μ secular equation. Hence, the order μ sideband transfer functions at $\omega \pm 1$/rev constitute behavior of the system equivalent to the ½/rev critical region of the eigenvalues.

The order μ^2 differential equation is

$$\ddot{\beta}_2 + \frac{\gamma}{8}\dot{\beta}_2 + \left(\nu^2 + \frac{\gamma}{8}K_p\right)\beta_2 = \frac{\gamma}{8}(1 - \cos 2\psi)\theta$$

$$- \left[\frac{\gamma}{6}\sin\psi\dot{\beta}_1 + \left(\frac{\gamma}{6}\cos\psi + K_p\frac{\gamma}{3}\sin\psi\right)\beta_1\right.$$

$$\left. + \left(\frac{\gamma}{8}\sin 2\psi + K_p\frac{\gamma}{8} - K_p\frac{\gamma}{8}\cos 2\psi\right)\beta_0\right] \tag{194}$$

Substituting for θ, β_0, and β_1, the solution is

$$\beta_2 = \bar{\beta}_2 e^{i\omega\psi} + \bar{\beta}_{2+} e^{i(\omega+2)\psi} + \bar{\beta}_{2-} e^{i(\omega-2)\psi} \tag{195}$$

with

$$\Delta(\omega)\frac{\bar{\beta}_2}{\bar{\theta}} = \frac{\gamma}{8} - K_p\frac{\left(\frac{\gamma}{8}\right)^2}{\Delta(\omega)} + \left(\frac{\gamma}{12}\right)^2\frac{(\omega - 2iK_p)4i\left[\nu^2 - \omega^2 + \frac{\gamma}{16}\left(\frac{\gamma}{8} + 2i\omega\right)\right]}{\Lambda(\omega)\Delta_1(\omega)} + \left(\frac{\gamma}{12}\right)^2\frac{(\omega - 2iK_p)4i(\omega^2 - \nu^2)}{\Lambda_1(\omega)} \tag{196}$$

where

$$\Delta_1(\omega) = \Delta(\omega + 1)\Delta(\omega - 1) = [\Delta(\omega) - 1]^2 + \left(2i\omega + \frac{\gamma}{8}\right)^2 \tag{197}$$

Notice that $\Delta_1(i\lambda)$ is just the characteristic equation for the β_{1c}/β_{1s} hover roots. The direct response to order μ^2 is then

$$\frac{\bar{\beta}_0 + \mu^2\bar{\beta}_2}{\bar{\theta}} = \left[\frac{\gamma}{8}(1 + \mu^2) + \mu^2\left(\frac{\gamma}{12}\right)^2\frac{(4i\omega + 8K_p)(\omega^2 - \nu^2)}{\Delta_1}\right] \div \left\{-\omega^2 + \frac{\gamma}{8}i\omega + \nu^2 + (1 + \mu^2)\frac{\gamma}{8}K_p + \mu^2\left(\frac{\gamma}{12}\right)^2\frac{(4i\omega + 8K_p)\left[\omega^2 - \nu^2 - \frac{\gamma}{16}\left(\frac{\gamma}{8} + 2i\omega\right)\right]}{\Delta_1}\right\} \tag{198}$$

So the order μ^2 response contributes to the direct transfer function much as it does to the eigenvalues away from the critical regions. The order μ^2 correction for the mean of M_θ is recognizable as usual, and there are other order μ^2 effects due to the periodic coefficients. The $\omega \pm 2$/rev sideband transfer functions are

$$\frac{\bar{\beta}_{2\pm}}{\bar{\theta}} = \frac{1}{\Delta(\omega \pm 2)} \left\{ -\frac{\gamma}{16} + \frac{2\left(\frac{\gamma}{16}\right)^2 (\pm i + Kp)}{\Delta(\omega)} \mp \left(\frac{\gamma}{12}\right)^2 \frac{(\omega \pm 2 - 2iKp)\left[-\frac{\gamma}{8} \pm 2i(\omega^2 - \nu^2)\right]}{\Delta(\omega)\Delta(\omega \pm 1)} \right\} \tag{199}$$

Summary

The transfer functions describing the response of the blade flap motion to pitch excitation are

$$\left.\begin{aligned} H_0 &= \frac{\bar{\beta}_0 + \mu^2 \bar{\beta}_2}{\bar{\theta}} \\ H_{\pm 1} &= \mu \frac{\bar{\beta}_{1\pm}}{\bar{\theta}} \\ H_{\pm 2} &= \mu^2 \frac{\bar{\beta}_{2\pm}}{\bar{\theta}} \end{aligned}\right\} \tag{200}$$

By measuring the response to a sinusoidal input, it is then possible to verify the equation representing the flap dynamics. Specifically, it is possible to verify the periodic coefficients which produce the critical region behavior of the eigenvalues. There is not, however, any critical region behavior for the transfer functions, that is, specific ranges of the parameters where there is more critical behavior of the response. That is replaced by the sideband transfer functions. Hence, the transfer function measurement does not provide experimental demonstration of the critical region behavior, although it does equivalent information, verifying the equation which produces the critical region for the eigenvalues.

A Point About Experimental Technique

Since the response of a periodic system to input at frequency ω is output at $\omega \pm n$/rev, for all integers n (although the magnitude of the response decreases with n), it follows that the random excitation technique for measuring the transfer function of a constant coefficient system is not directly applicable to periodic coefficient systems. A random input has all frequencies at once, hence, the output is also composed of all frequencies. For constant coefficient systems the knowledge that the response at ω came only from the input at ω can be used to determine the transfer function when the input is random - the entire function at once, in fact. With a periodic coefficient system, however, the output at ω has contributions from inputs at $\omega \pm n$/rev for all n, so not enough information is available to determine the transfer function.

An input at a single frequency ω must be used then and the output at all harmonics $\omega \pm n/\text{rev}$ measured; this task is performed for the range of ω required. This technique is slower than with the random excitation; in addition, the noise filtering feature of the random input is lost, that is, accuracy of the measurements is lost.

The problem is that there is not a single transfer function to measure but rather several. For example, the rotor flap response up to $\mu = 0.5$ or so would require the measurement of H_0, $H_{\pm 1}$, and $H_{\pm 2}$ at least. It is probably possible to extend the random excitation techniques to periodic systems. It would be necessary, however, to use a number of inputs with independent spectra so that enough independent measurements are made at each frequency to determine the required number of transfer functions. In any case, the periodic system will require more experimental effort than the constant coefficient system.

Nonrotating Response

For the dynamics of the helicopter as a whole, it is the response of the rotor in the nonrotating frame that is of interest, that is, the response of the β_0, β_{1c}, β_{1s}, etc. degrees of freedom. Similarly, the inputs usually available for the rotor are collective and cyclic pitch control: θ_0, θ_{1c} θ_{1s}. Here, the transfer functions in the nonrotating frame may be examined, in addition to the rotating response given above. The analysis proceeds much as above. It is straightforward since there are no critical regions to be concerned with or any other singular behavior; it is convenient to use vectors of the input and output variables and matrices of the transfer functions ($\vec{\beta}$ due to $\vec{\theta}$). The analysis and results are not very illuminating, however, because of their complexity.

DISCUSSION OF PREVIOUS WORK

Horvay (ref. 1) considered the flap dynamics of a rotor with $\nu = 1$, $K_p = 0$, and no reverse flow effects. By the substitution

$$\beta = y e^{-\frac{\gamma}{16}\psi + \frac{\gamma}{12}\mu \cos\psi}$$

he transformed the flap equation to the standard form of Hill's equation:

$$\ddot{y} + f(\psi)y = 0$$

where f is a periodic function. This equation he solved by the infinite determinant method of classical theory. The solution produced numerical

results presented as constant $Re\lambda$ lines on the $\gamma - \mu$ plane. The boundaries found were essentially those given in figure 7 although he did not investigate small enough γ to find the 1/rev region. Horvay used the notation $n = \gamma/8$, since this is the coefficient of the flap damping in hover. Then, in hover and outside the critical regions, $Re\lambda = -\gamma/16 = -n/2$. Hence, he introduced the "apparent damping coefficient" $n_{app} = -2Re\lambda$. Then $n_{app}/n = -Re\lambda/(\gamma/16)$ takes the values 1 outside the critical regions, 1 to 0 in the stable portions of the critical regions, and less than 0 in the unstable portions of the critical regions. The use of the notation n_{app}/n and the parameter n_{app} for $Re\lambda$ is found in much of the literature on rotor flap stability. Horvay found approximate solutions at high μ (to $\mu = 8$) for several equations which are not true descriptions of the flap dynamics but do illustrate some of the high μ behavior of the real rotor.

Horvay and Yuan (ref. 2) considered blade flap stability for the case of $\nu = 1$ and no reverse flow but including $K_P = 0$. The roots were found from the transient solution for β, using the results of Floquet theory (as outlined in Appendix A here). Much of the literature uses this approach, the real differences being the method used to find the transient solution for β. Horvay and Yuan used the ripple method to integrate the differential equation. They presented the numerical results on the $\gamma - \mu$ plane for $\nu = 1$ and $K_P = 0$, $-\sqrt{3}/12$, and $\sqrt{3}/4$ (these values of K_P were chosen because they place exactly at $\gamma/8 = \sqrt{3}$ the ½/rev region, the real root, and the 1/rev region boundaries, respectively, when $\mu = 0$). A large azimuth interval was used in the ripple method but the results compare fairly well with the solution of Horvay (ref. 1), at least at small μ.

Parkus (ref. 3) considered the flap stability for $\nu = 1$, no reverse flow but $K_P \neq 0$ (with the notation $k = -K_P$). He found the roots from the Floquet result using an expansion of β as a series in μ to find the transient solution. The expansion is the same as is used here away from the critical regions since the multiple time scales and expansion of γ are not needed there. Parkus left his result in the form of a quadratic equation for $\sigma = e^{2\pi[\lambda+(\gamma/16)]}$; since it is only an order μ^2 solution, however it is possible to solve explicitly for λ. The result is exactly the same as obtained here for the roots away from the critical regions (eq. (24), with $\nu = 1$). Parkus did not recognize, however, that this solution is not valid for $Im\lambda$ near 1/rev or ½/rev. The assumption that the β_n in the expansion of β are all the same order is violated near the critical regions. Parkus calculated the roots for varying μ, for $\gamma = 12$ and 14; the behavior of the roots looks like that in critical regions but really the expression for the roots away from the critical regions is breaking down as the roots approach the ½/rev region. When $Im\lambda_0$ is near ½, the order μ^2 term in the radicand of λ (eq. (24) here) is large, so for large enough μ the radicand is negative. The result is two real roots and an order μ^2 effect which is far from the correct ½/rev region behavior.

Gessow and Crim (ref. 19) considered the flap stability at high μ numerically integrating the equations of motion to find the transient behavior of β. Reverse flow was included, as well as the effects of stall, compressibility, and large angles. They found the flap motion to be stable at $\mu = 1$

for $\gamma = 2.4$ to 14.9, at $\mu = 2.2$ for $\gamma = 2.4$ to 7.1, and at $\mu = 3$ for $\gamma = 0.6$ to 2.4. The motion was unstable at $\mu = 3$ for $\gamma = 14.9$.

Shulman (ref. 4) considered the flap stability for $\nu = 1$, $K_p = 0$, and no reverse flow. He added, however, a second degree of freedom, the first elastic flapwise bending mode of the articulated blade. His principal solution method was simply to numerically integrate the equation of motion. He found a significant effect of the second degree of freedom for high advance ratio, $\mu = 1.0$ say, but small influence for μ up to 0.5. The equations were solved for $\mu = 1$ and 1.2, but with the neglect of reverse flow the true flap dynamics are no longer represented at that μ. His conclusion that the flap instability occurs at $\mu = 1.5$ to 1.8 is not correct then; but the importance of the second degree of freedom at high μ is probably qualitatively correct.

Perisho (ref. 5) considered the stability of the flap and pitch dynamics of the blade at high μ, for an articulated rotor, $K_p \neq 0$, and including reverse flow aerodynamics. He solved the equations by numerical integration for the case $\nu = 1.05$, $\gamma = 5$, and a pitch natural frequency of 10/rev. For just the rigid flap degree of freedom, he found the instability boundary at $\mu = 2.2$ with $K_p = 0$, and at $\mu = 2.45$ with $K_p = 2$, in the 1/rev region for both cases. Adding the torsion degree of freedom reduced the μ for instability to $\mu = 1.8$ for $K_p = 0$; and to $\mu = 1.65$ for $K_p = 2$, in the ½/rev region now. Adding flapwise bending, that is, three degrees of freedom, reduced the speed for instability still farther to $\mu = 1.43$ for $K_p = 2$. The reduction in the stability at high μ due to the torsion degree of freedom appeared to be largely a torsion divergence in the reverse flow region.

Shutler and Jones (ref. 6) considered the flap stability for $\nu = 1$ and $K_p = 0$, with no reverse flow. They solved for the eigenvalues and for β by a perturbation solution based on the Floquet theory result that the solution of a periodic coefficient differential equation may be written in the form

$$\beta = C_1 e^{\lambda_1 \psi} u_1(\psi) + C_2 e^{\lambda_2 \psi} u_2(\psi)$$

where the eigenvectors u_1 and u_2 are periodic (Appendix A). The substitution $\beta = e^{\lambda\psi} u$ is made into the flap equation and then λ and u expanded as series in μ. The requirement that all the functions in the expansion of $u(\psi)$ must be periodic is equivalent to the requirement in the method of multiple time scales that the successive functions grow no faster than the earlier ones (the order 1 term of $u(\psi)$ is the hover limit, so it is constant; then requiring successive terms in the expansion grow no faster means they can at most be periodic); the result has the same secular terms as obtained here. This is basically the method used by Shutler and Jones, although the details differed considerably. To treat the critical regions it is necessary to quantify the requirement that the frequency be near a multiple of ½/rev. The present investigation used an expansion of γ to do this, while Shutler and Jones essentially expanded $\mathrm{Im}\lambda$ itself (their eq. (25); with the present notation for λ). So contrary to their statement, this expansion (eq. (25)) does have physical significance, namely, what "close" to a critical region means. Similarly, their parameter σ also has physical significance: it

gives contours of constant $Re\lambda$ in the critical regions; for example, the critical region boundary is such a contour. They found the eigenvalues and β for the cases of the ½/rev region, the 1/rev region, and away from the critical region to order μ^2 everywhere, including in the ½/rev region. Their results may be shown to be equivalent to those obtained here, for $\nu = 1$ and $K_p = 0$; except that here the ½/rev region is only carried to order μ. Their result for the ½/rev region boundary to order μ^2 has been given above (eq. (55a)) and illustrated in figure 7. They did not, however, take advantage of the fact they had a perturbation solution to put together explicit analytic expressions for the eigenvalues.

Lowis (ref. 7) considered the flap stability for $\nu = 1$ and $K_p = 0$, at high μ particularly, first without and then with reverse flow effects. He solved for the roots by the results of Floquet theory, after numerically integrating the equation to find β. Without reverse flow he found an instability at about $\mu = 1.42$ in the 1/rev region. With reverse flow, the instability occurred at about $\mu = 2.3$, still in the 1/rev region. The representation of the reverse flow aerodynamics used was only approximately correct, however: he did not account for the azimuth range where the blade is partly in normal flow and partly in reverse flow. This model has the correct limit for very large μ but it is not good at all below $\mu = 1$. The behavior of the solution around $\mu = 2$, that is, including the flap instability, is probably correct but neither of the solutions (without and with reverse flow) he obtained is good in the range $\mu = 0.5$ to $\mu = 1.5$ or so.

Wilde, Bramwell, and Summerscales (ref. 20) considered flap stability at high μ, including the effects of reverse flow, and presenting results mainly for $\nu = 1$ and $K_p = 0$. They considered a teetering rotor also. The solution was obtained by use of an analog computer. They found a flapping instability at about $\mu = 2.25$ for $\gamma = 6$. The teetering rotor was stable to $\mu = 5$ at least.

Sissingh (ref. 8) considered the flap stability at high μ, including $\nu \geq 1$, $K_p \neq 0$, and reverse flow (with the notation $P = \nu$, $C_1 = -K_p$; and only $K_p = 0$ was used for the results). The aerodynamic coefficients of reverse flow were derived and discussed. The solution of the equation of motion was obtained by use of an analog computer. The results were presented as stability boundaries for several μ, on the $\gamma - \nu$ plane, with the emphasis on quite large ν, typical of a slowed or stopping rotor. For $\nu = 1$, he found $\mu = 2.2$ for instability at $\gamma \cong 8$ (higher for other values of γ).

Stammers (ref. 9) considered the influence of forward flight on the flutter of the helicopter rotor blade. He found a perturbation solution by methods similar to those of Shutler and Jones (ref. 6) rather than the methods used in the present work.

Hall (ref. 10) investigated the dynamics of the flap/lag/torsion motion of the blade. He used Floquet theory to obtain the roots from a numerical integration of the equations over one period. He discussed Floquet theory and its results for a multi-degree of freedom system. He also presented results for a single degree of freedom, that is, just rigid flap.

Sissingh and Kuczynski (ref. 11) extended the earlier work of Sissingh (ref. 8) to include the torsion degree of freedom; the emphasis again was on the results for very high μ. They showed a quite significant effect of torsion on the blade stability reducing the μ for instability considerably. For example, with $\gamma = 6$ the μ for instability was reduced to about 1.7 for a torsion frequency of 8/rev and to about $\mu = 1.35$ for a frequency of 5/rev. These boundaries were just a little below those for torsion only; the effect was largely due to torsional divergence in the reverse flow region where there is a negative aerodynamic spring and reduced aerodynamic damping on the pitch motion. Their results compared well with those of Perisho (ref. 5).

Peters and Hohenemser (ref. 12) considered the flap stability including $\nu \geq 1$, $K_p \neq 0$, and reverse flow aerodynamics. They used a continuous representation of the reverse flow aerodynamic coefficients as obtained by Sissingh (ref. 8). They solved for the roots by integrating over one period and then using Floquet theory. Their solution compared well with the analog computer solution of reference 8. They presented the numerical results on the γ - μ plane for $\nu = 1$ and $K_p = 0$, 0.1, -0.1, out to $\mu = 2.5$. They found approximately $\mu = 2.3$ for the flap instability in the 1/rev region (at $\gamma = 9$, higher for other values of γ); $K_p > 0$ increased the μ for instability. There were possibly some numerical problems with the 1/rev boundary at low μ (below 0.5), since the boundaries appear more like order μ than the correct order μ^2 behavior (their fig. 3). In addition, the $\mu = 0$ point of the 1/rev region really must shift for $K_p \neq 0$ and not remain always at $\gamma = 0$ as shown (their figs. 4 and 5).

Hohenemser and Yin (ref. 13) investigated the flap dynamics using the nonrotating degrees of freedom and equations including the periodic coefficients in forward flight. They gave the equations for the case of $N = 4$. They solved for the roots by the methods of reference 12. They discussed the constant coefficient approximation to the nonrotating equations in forward flight but only in the context of tip path plane tilt feedback control, however (at $\mu = 0.4$ with $N = 3$, and $\mu = 0.8$ with $N = 4$). They found the constant coefficient approximation was not bad at low gain, especially for the low frequency modes but for high gain it could be unconservative.

Johnson (ref. 14) considered rotor flap stability including $\nu \geq 1$, $K_p \neq 0$, and reverse flow. He obtained perturbation solutions for the cases of small and large μ and small and large γ. The small μ solution formed the basis for the analysis of the individual blade case in the present work. This report was summarized in reference 15, and reference 17 presented a synoptic of the small μ results.

Tong (ref. 16) considered the blade flap/lag dynamics. He obtained a solution by perturbation techniques to handle the nonlinear features of this problem (i.e., limit cycle instabilities), as well as the influence of forward flight.

Biggers (ref. 18) considered the flap dynamics for $K_p = 0$ and no reverse flow but including $\nu \geq 1$. He constructed μ root loci and γ - μ planes for several cases using a numerical calculation of the exact

eigenvalues by means of Floquet theory. He presented the nonrotating equations of motion including the periodic coefficients in forward flight for N = 3 and N = 4. Then, he considered the constant coefficient approximation in the nonrotating frame, solving the characteristic equation for the roots of the system numerically and comparing this constant coefficient approximation with the exact results (Floquet theory). He examined several cases out to $\mu = 0.5$. The results of this comparison of the exact and constant coefficient eigenvalues (both obtained by numerical techniques) are in agreement with the results of the comparison given here (of corresponding perturbation solutions).

CONCLUSIONS

This report has considered the influence of forward flight on the flapping stability of several helicopter rotor configurations. The eigenvalues of the motion have been obtained by a perturbation technique which gives analytic expressions for the roots. Comparison between numerical solutions for the exact roots and the present perturbation solutions indicates that the latter are quantitatively accurate to about $\mu = 0.5$. (An exception is near the ½/rev region, where the perturbation solution was carried to only order μ. It should evidently be extended to order μ^2 as was the rest of the solution.) In general, for this range of μ, the flap motion retains the high aerodynamic damping of hover and so remains very stable in forward flight. There exist, however, critical regions due to the periodic coefficients which are encountered if the hover root frequency is too near a multiple of ½/rev. The influence of the critical regions increases with μ as the periodic coefficients increase. For the usual values of ν, Kp, and γ, the critical regions of interest are the ½/rev and the 1/rev regions. In a critical region there is a plus and minus increment in the real part of the root from the hover value while the frequency remains fixed at a multiple of ½/rev. Hence, there is a decrement in the stability of the system when a critical region is encountered. However, the damping change is only order μ in the ½/rev region, and order μ^2 in the 1/rev region, so the stability decrease is small and the flap motion remains highly damped in forward flight.

For μ order 2 or so, that is, beyond the range of validity of the perturbation solutions obtained here, there can occur a sufficient stability degradation in a critical region (usually in the 1/rev region) so that a flap instability is encountered.

These conclusions about the flap stability may generally be found in the existing literature on this problem. What the present work adds is explicit analytic expressions for the eigenvalues of the flap motion, including the periodic coefficient influence in forward flight. Also, the behavior of cantilever ($\nu > 1$), teetering, and gimballed rotor configurations is examined in addition to that of an independent, articulated blade.

The transfer function of the flap response to blade pitch has been considered as an alternative to the eigenvalues for describing the dynamic characteristics of the system. The transfer function indeed is found to

represent equivalent information about the dynamics, but with quite different behavior. The critical region behavior of the eigenvalues is replaced by sideband transfer functions (response at frequency $\omega \pm n\Omega$ to input at frequency ω).

The constant coefficient approximation to the flap equations of motion in the nonrotating frame was investigated and the eigenvalues compared with the solutions including the periodic coefficients. Such an approximation cannot be entirely correct, of course, but it is remarkably good, especially for the lower frequency nonrotating modes of the rotor. This implies that for certain problems - such as the low frequency dynamics of the rotor involving the helicopter body motions - the constant coefficient approximation is an adequate representation of the system. The possibility of using the constant coefficient approximation involves a considerable reduction in the effort required to analyze and understand the rotor dynamics. It is suggested, therefore, that the first step in an investigation involving helicopter rotor forward flight dynamics should be to check the validity of the constant coefficient approximation by comparing with an exact solution (obtained by numerical techniques probably) for the particular problem. The periodic coefficients (in the nonrotating frame) may not even be needed. If they are required, then the methods of perturbation theory are very useful in examining the fundamental behavior.

APPENDIX A

PERIODIC SYSTEMS

The forward flight of the helicopter introduces periodic coefficients into the differential equations describing the flap motion due to the periodic variation of the free-stream velocity seen by the rotating blade. For large enough μ the periodic aerodynamic forces radically influence the behavior of the root loci, and the analysis techniques required to find the eigenvalues.

The root loci of a constant coefficient system characteristically exhibit behavior in which two roots start as complex conjugates, meet at the real axis, and then proceed in opposite directions along the real axis. The existence of periodic coefficients in the differential equations describing the motion generalizes this behavior so that it can occur at any frequency that is a multiple of ½/rev, that is, at $\mathrm{Im}\lambda$ = n/rev or n + ½/rev where n is an integer, not just at 0/rev (the real axis). The property of the solution that allows this behavior is the fact the eigenvectors are themselves periodic (instead of constant as for a constant coefficient system; see the mathematics below). The analysis which demonstrates that periodic systems show this behavior is called Floquet theory.

Thus, the following behavior of root loci is characteristic of periodic systems (refer to fig. 10). If the parameter being varied, for example, the advance ratio μ in the present problem, is such that at $\mu = 0$ the system is not periodic, then the roots start out as complex conjugates (point A on the loci in fig. 10). As μ increases, the periodic forces increase, and the roots move toward n/rev (or n + ½/rev) frequency, remaining complex conjugates. At some critical μ the loci reach $\mathrm{Im}\lambda$ = n/rev (point B on fig. 10), and then for still larger μ the frequency remains fixed at n/rev while the real part of one root is decreased and that of the other is increased. The root being destabilized may cross into the right half plane for some μ (point C on fig. 10), indicating that the system has become unstable due to the influence of the periodic coefficients.

A general system of differential equations with periodic coefficients may be reduced to a set of first-order equations, and may therefore be written (in matrix notation) as

$$\dot{\vec{x}} = A\vec{x} \tag{A1}$$

where $\vec{x}$ is the state vector of the system and $A(t)$ is a periodic matrix of coefficients: $A(t + T) = A(t)$. It may be shown that the solution to this differential equation can be obtained in the form

$$\vec{x}(t) = \sum_i q_i(0)e^{\lambda_i t}\vec{u}_i(t) \tag{A2}$$

The λ_i are the eigenvalues; the eigenvectors $\vec{u}_i$ are periodic: $\vec{u}_i(t + T) = \vec{u}_i(t)$; and the numbers $q_i(0)$ are constants obtained from the initial conditions. The theory that shows this is called Floquet theory. The solution in this form is a direct extension of the normal solution for a constant coefficient differential equation which is characterized by constant eigenvectors ($\vec{u}_i$ independent of time).

The eigenvalues λ_i may be obtained by the following procedure. The equation

$$\dot{\phi} = A\phi \tag{A3}$$

where $\phi(t)$ is a matrix, is integrated over one period, from $t = 0$ to $t = T$, with the initial conditions $\phi(0) = I$ (the unit matrix). Then, if λ_{c_i} are eigenvalues of the matrix $C = \phi(T)$, the roots λ_i are given by $\lambda_c = e^{\lambda T}$, or $\lambda = (\ln \lambda_c)/T$. While the roots λ_{c_i} (as eigenvalues of a real matrix C) must appear as real numbers or complex conjugate pairs, the eigenvalues λ_i are under no such restriction, leading to the behavior of the root loci as described above.

For a single degree of freedom, second-order system, let x_R be the solution obtained from integrating the equation with the initial conditions $\dot{x}(0) = 1$, $x(0) = 0$; and let x_P be the solution with initial conditions $\dot{x}(0) = 0$, $x(0) = 1$. Then, the roots λ_c are given by the quadratic equation:

$$\lambda_c^2 - [\dot{x}_R(T) + x_P(T)]\lambda_c + [\dot{x}_R(T)x_P(T) - x_R(T)\dot{x}_P(T)] = 0 \tag{A4}$$

APPENDIX B

METHOD OF MULTIPLE TIME SCALES

This appendix describes briefly the perturbation technique known as the method of multiple time scales. It should be used in parallel with the analysis of the flap equation, for many of the steps are more clearly expressed in the context of a specific example. More details of the method, and examples of its application may be found in reference 21 (and also ref. 14).

Fundamental to perturbation methods is the existence of a small parameter, here the advance ratio μ; and for the solution of periodic coefficient differential equations, that the periodic terms be functions of μ such that the equations reduce to constant coefficients when $\mu = 0$. For a study of the stability of a system, a solution is required that is uniformly valid over long time periods, so the long time behavior may be assessed. This leads to the use of the method of multiple time scales. Define a series of time scales $\psi_n = \mu^n \psi$. The time scales ψ_n are all assumed to be of the same order. Then for $\psi_1 = \mu\psi$ the actual time ψ must be order μ^{-1}, that is, very large compared to the basic scale $\psi_0 = \psi$. The behavior of the solution over several time scales ψ_n will be investigated, each implying successively longer time behavior. The derivative with respect to time becomes then

$$\frac{\partial}{\partial \psi} = \frac{\partial}{\partial \psi_0} + \mu \frac{\partial}{\partial \psi_1} + \mu^2 \frac{\partial}{\partial \psi_2} + \cdots$$

So the assumption of the time scales is equivalent to an expansion of $d/d\psi$ as a series in μ.

Next the dependent variable is also expanded as a series in μ:

$$\beta = \beta_0(\psi_0, \psi_1, \psi_2, \ldots) + \mu\beta_1(\psi_0, \psi_1, \ldots) + \cdots$$

The β_n now depend on all the time scales ψ_n. The β_n are all assumed to be of the same order, for all the long time scale behavior. This requirement is critical to obtaining the solution; it leads, for certain values of the free parameters, to critical regions in which there is a reduction in the stability of the system. In order to investigate the influence of the free parameters, they also are expanded as series in μ. In this case, for the Lock number γ have

$$\gamma = \gamma_0 + \mu\gamma_1 + \mu^2\gamma_2 + \cdots$$

where the γ_n are all of the same order. For certain critical values of γ_0 - that is, when γ is order μ or order μ^2 from certain critical values - there will occur a stability degradation due to the influence of the periodic coefficients.

So now β, $d/d\psi$, and the free parameters are all expanded as series in μ. These are substituted into the differential equation, and then all terms of like order in μ are collected and separately set to zero. Thus, differential equations are obtained for order 1, μ, μ^2, . . ., μ^n, ... With the expansion of $d/d\psi$, that is, the use of multiple time scales, these equations are now partial differential equations for β_n as functions of ψ_n. The order μ^n equation has the following form: it may be written as a differential equation for $\beta_n(\psi_0)$, forced by the lower order solutions. That is, on the right-hand side there are β_{n-1}, β_{n-2}, . . ., β_0 and their derivatives with respect to ψ_n, ψ_{n-1}, . . ., ψ_0. The set of partial differential equations is solved progressively, beginning with the lowest order equation (order 1), then order μ, etc.

It is the characteristic of this expansion in μ that the μ^n order equations, written as ordinary differential equations for $\beta_n(\psi_0)$, all have the same homogeneous solution. Since the equation for $\beta_n(\psi_0)$ is forced by the lower order solutions β_{n-1}, . . ., β_0, it follows then that when the known solutions for β_{n-1}, . . ., β_0 are substituted, the equation for β_n will be forced by its own homogeneous solution. This would give rise to solutions for β_n of the form ψ_0 times its homogeneous solution, that is, solutions for β_n of order $\psi_0\beta_{n-1}$, . . ., $\psi_0\beta_0$. Then β_n/β_{n-1}, . . ., β_n/β_0 would be order ψ_0, that is, would become arbitrarily large if ψ_0 is large enough. This violates the assumption that β_n is of the same order as β_{n-1}, . . ., β_0. The only way such a solution may be avoided is if the coefficient of the homogeneous solution on the right-hand side of the μ^n order equation for $\beta_n(\psi_0)$ is itself set to zero. This coefficient of the homogeneous solution forcing the equation for $\beta_n(\psi_0)$ is called the secular term. The secular term is set to zero so that the solution for β_n will be uniformly valid for all time, that is, for large ψ_0.

Now the right-hand side of the β_n equation itself involves derivatives of β_{n-1}, . . ., β_0 with respect to the time scales ψ_n, . . ., ψ_0. At this stage in the analysis, considering the μ^n order equation, some of the solution for β is known already. What is not known is the behavior of β_{n-1} with respect to ψ_1, ψ_2, . . ., the behavior of β_{n-2} with respect to ψ_2, . . ., and so on down to β_0 with respect to ψ_n. Hence, these combinations of the dependent and independent variables remain on the right-hand side of the $\beta_n(\psi_0)$ equation when the known solution is substituted. Specifically, these combinations will be in the coefficients of the homogeneous solution, that is, in the secular term. Then, setting the secular term to zero results in a differential equation, which may be written as an equation for $\beta_{n-1}(\psi_1)$, forced on the right-hand side by the lower order solutions. This equation will also be forced by its own homogeneous solution, and so its secular term must be set to zero in order to maintain the uniform validity of β_{n-1} over the ψ_1 time scale. The result is an equation for $\beta_{n-2}(\psi_2)$; this process is continued down to an equation for $\beta_0(\psi_n)$.

So the order μ^n equation produces a set of differential equations for $\beta_n(\psi_0)$, $\beta_{n-1}(\psi_1)$, $\beta_{n-2}(\psi_2)$, . . ., $\beta_0(\psi_n)$. This set of equations is then solved, for the behavior of β_n with respect to ψ_0, β_{n-1} with respect to ψ_1, and so on down to β_0 with respect to ψ_n, thus completing the solution to order μ^n. The analysis then proceeds to the order μ^{n+1} equation. For the stability of the system, it is the behavior of β_0 with respect to ψ_n that is of interest since that gives the eigenvalue to order μ^n. The nesting behavior of the differential equations makes each successive order solution more involved but the basic procedure remains the same.

APPENDIX C

SOLUTION OF THE SECULAR EQUATION

The application of the method of multiple time scales to periodic coefficient differential equations results in secular equations of the form

$$\frac{\partial \beta}{\partial \psi} + (a + id)\beta + (b + ic)\bar{\beta} = 0 \tag{C1}$$

where β is a complex quantity, and the constants a, b, c, and d are real. Writing

$$D^2 = d^2 - (b^2 + c^2) = d^2 - |b + ic|^2 \tag{C2}$$

$$D = \sqrt{|D^2|} \tag{C3}$$

it may be verified that the solution of this equation is, for $D^2 > 0$:

$$\beta = e^{-a\psi}\left\{A[d - D + i(b + ic)]e^{iD\psi} + \bar{A}[d + D + i(b + ic)]e^{-iD\psi}\right\} \tag{C4}$$

where A is a complex constant; for $D^2 = 0$:

$$\beta = e^{-a\psi}(A\{[d + i(b + ic)]\psi + i\} + B[d + i(b + ic)]) \tag{C5}$$

where A and B are real constants; and for $D^2 < 0$:

$$\beta = e^{-a\psi}\left\{A[d + iD + i(b + ic)]e^{D\psi} + B[d - iD + i(b + ic)]e^{-D\psi}\right\} \tag{C6}$$

where A and B are real constants. The limiting case $b = c = 0$ gives $D = d$, so the solution is

$$\beta = Ae^{-(a+id)\psi} \tag{C7}$$

where A is a complex constant.

The region of decreased stability - the critical region - is given by $D^2 < 0$. The boundary of the critical region is $D^2 = 0$. The behavior of the

solution of this equation when b or $c \neq 0$ is that described for periodic systems; indeed it will be found that the $\bar{\beta}$ term comes from the periodic coefficients.

15. Johnson, Wayne: A Perturbation Solution of Rotor Flapping Stability. AIAA Paper no. 72-955, AIAA 2nd Atmospheric Flight Mechanics Conference, Sept. 1972.

16. Tong, Pin: Nonlinear Instability of a Helicopter Blade. AIAA Paper no. 72-956, AIAA 2nd Atmospheric Flight Mechanics Conference, Sept. 1972.

17. Johnson, Wayne: A Perturbation Solution of Helicopter Rotor Flapping Stability. J. Aircraft Synoptic, vol. 10, no. 5, May 1973.

18. Biggers, James C.: Some Approximations to the Flapping Stability of Helicopter Rotors. AHS/NASA-Ames Specialists' Meeting on Rotorcraft Dynamics, Moffett Field, Calif., Feb. 13-15, 1974.

19. Gessow, Alfred; and Crim, Almer D.: A Method for Studying the Transient Blade-Flapping Behavior of Lifting Rotors at Extreme Operating Conditions. NACA TN-3366, Jan. 1955.

20. Wilde, E.; Bramwell, A. R. S.; and Summerscales, R.: The Flapping Behavior of a Helicopter Rotor at High Tip-Speed Ratios. Aeronautical Research Council C. P. no. 877, April 1965.

21. Cole, J. D.: Perturbation Methods in Applied Mathematics. Blaisdell Pub. Co., Waltham, Mass., 1968.

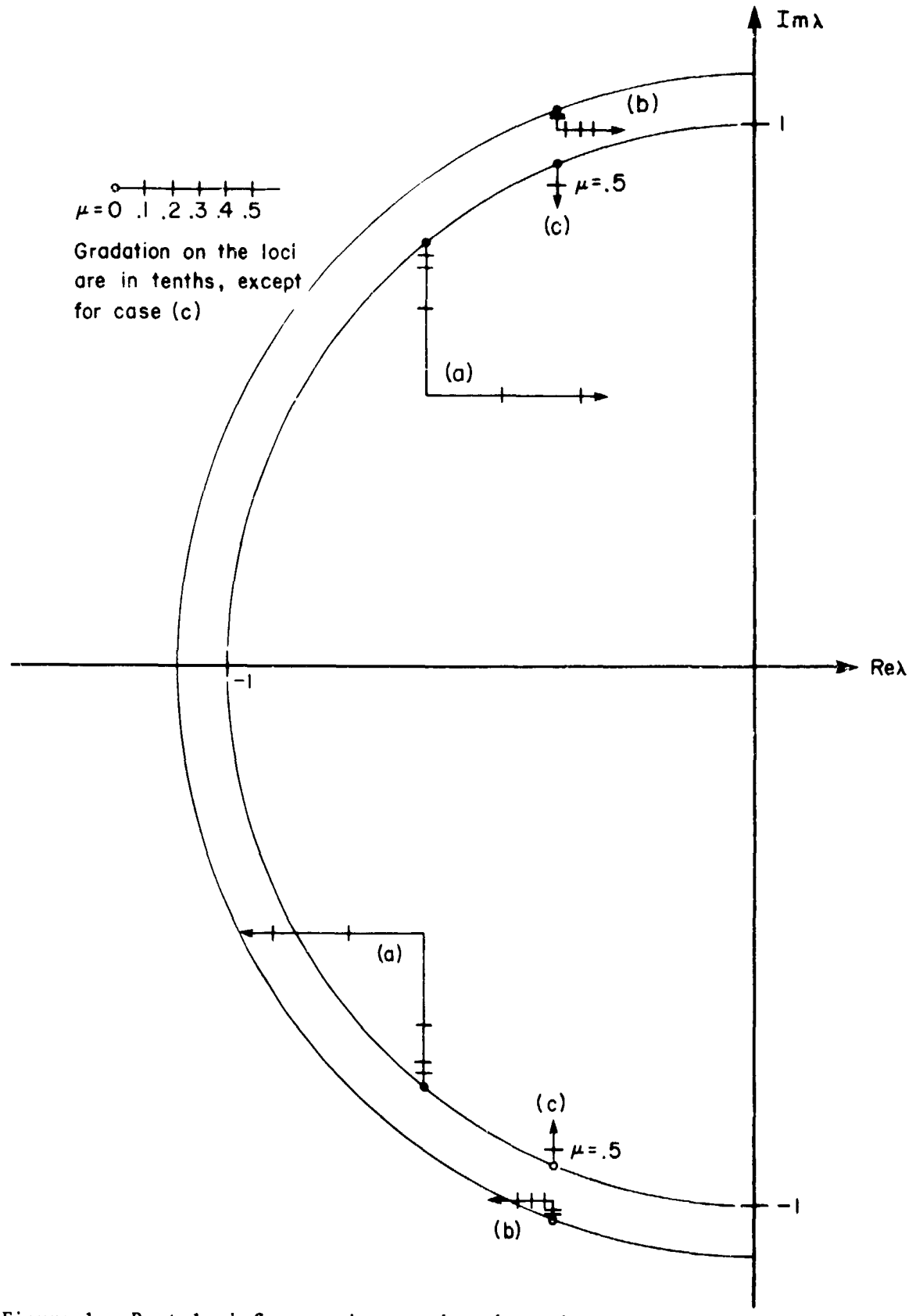

Figure 1.- Root loci for varying μ, based on the perturbation solution. The cases shown are (a) $\nu = 1$ and $\gamma = 10$, (b) $\nu = 1.1$ and $\gamma = 6$, and (c) $\nu = 1$ and $\gamma = 6$ ($K_p = 0$ for all three cases).

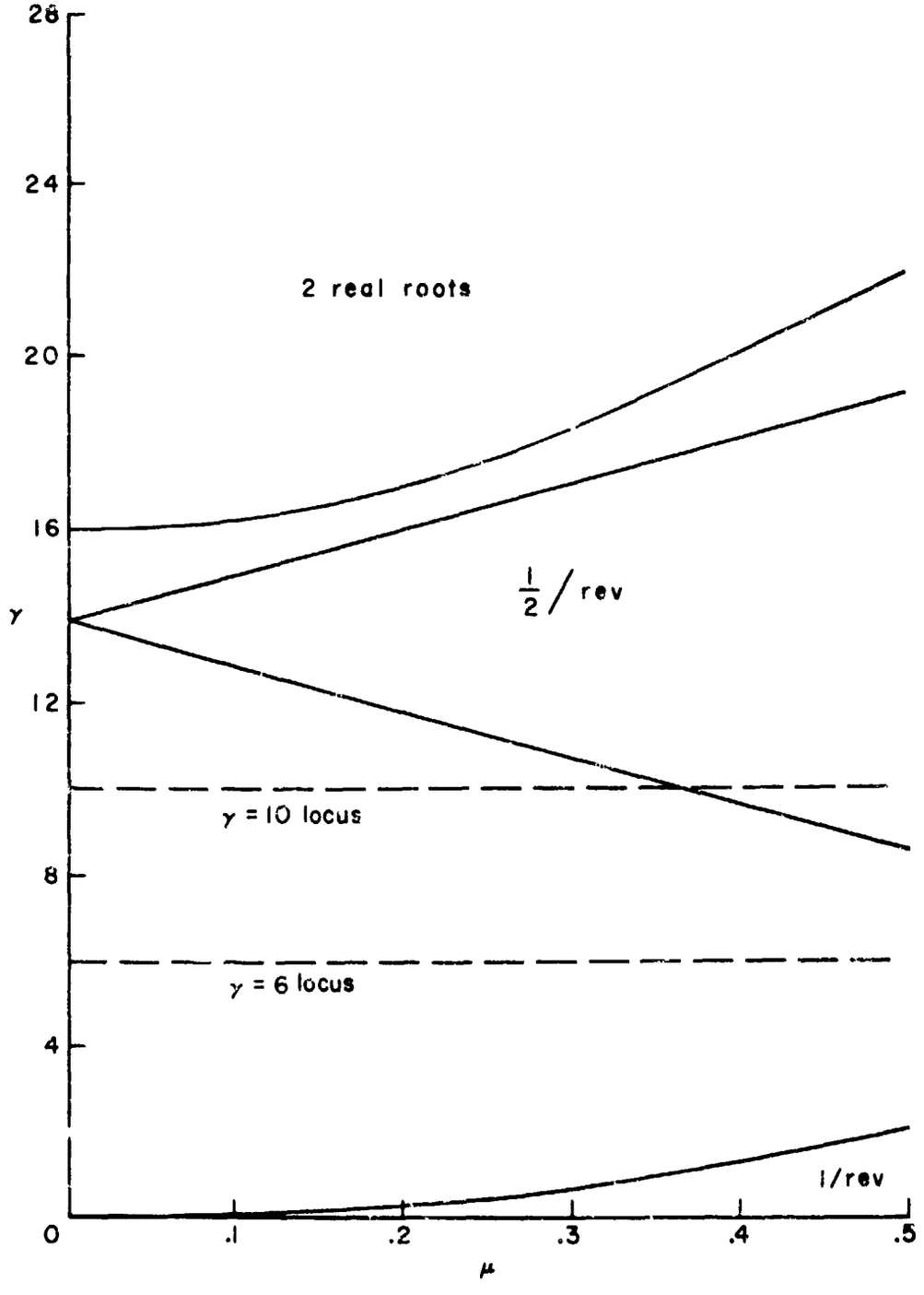

Figure 2.- Critical region and real root boundaries on the $\gamma - \mu$ plane for $\nu = 1$ and $K_p = 0$ (based on the perturbation solution).

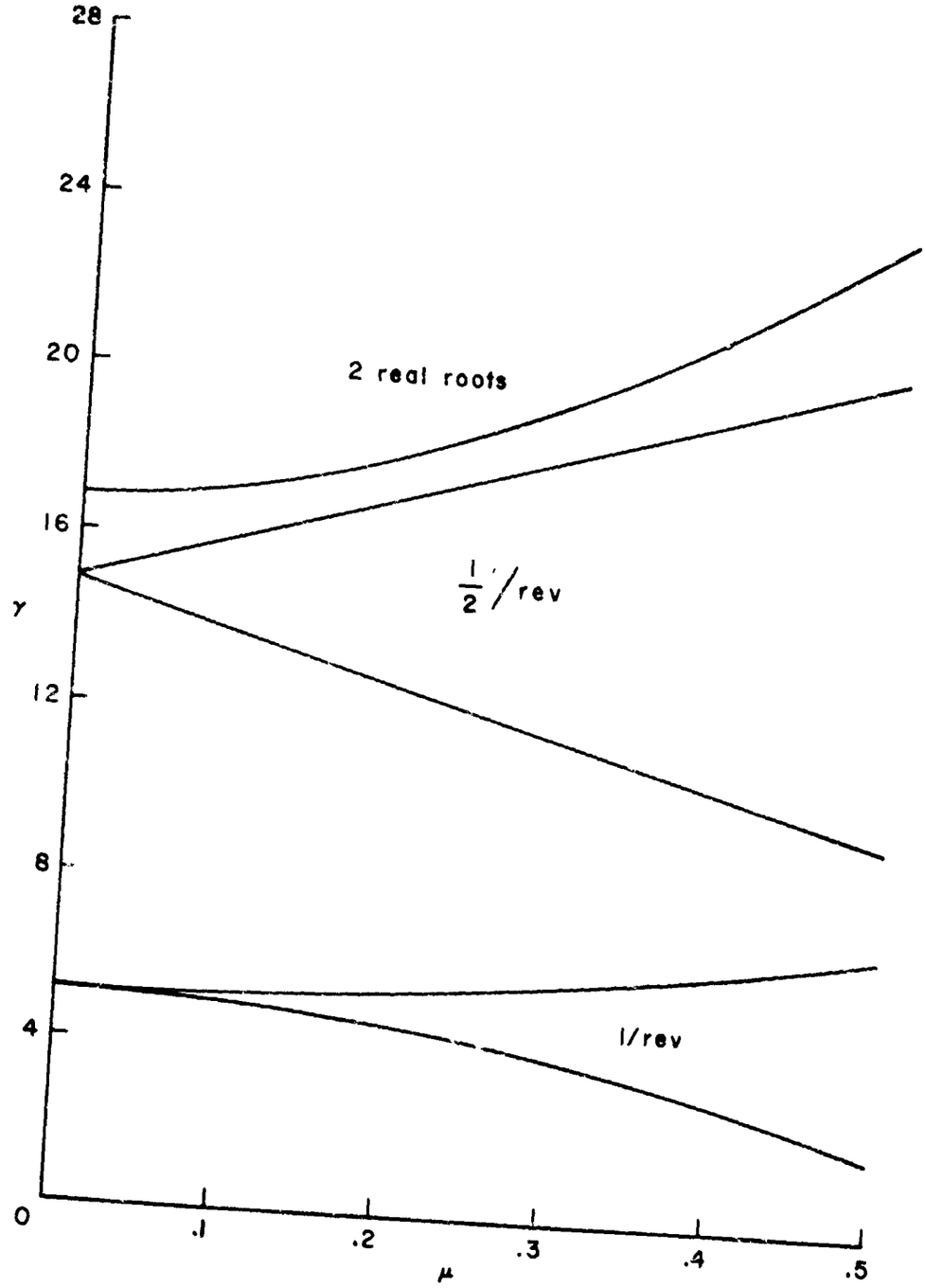

Figure 3.- Critical region and real root boundaries on the $\gamma - \mu$ plane for $\nu = 1.05$ and $Kp = 0$ (based on the perturbation solution).

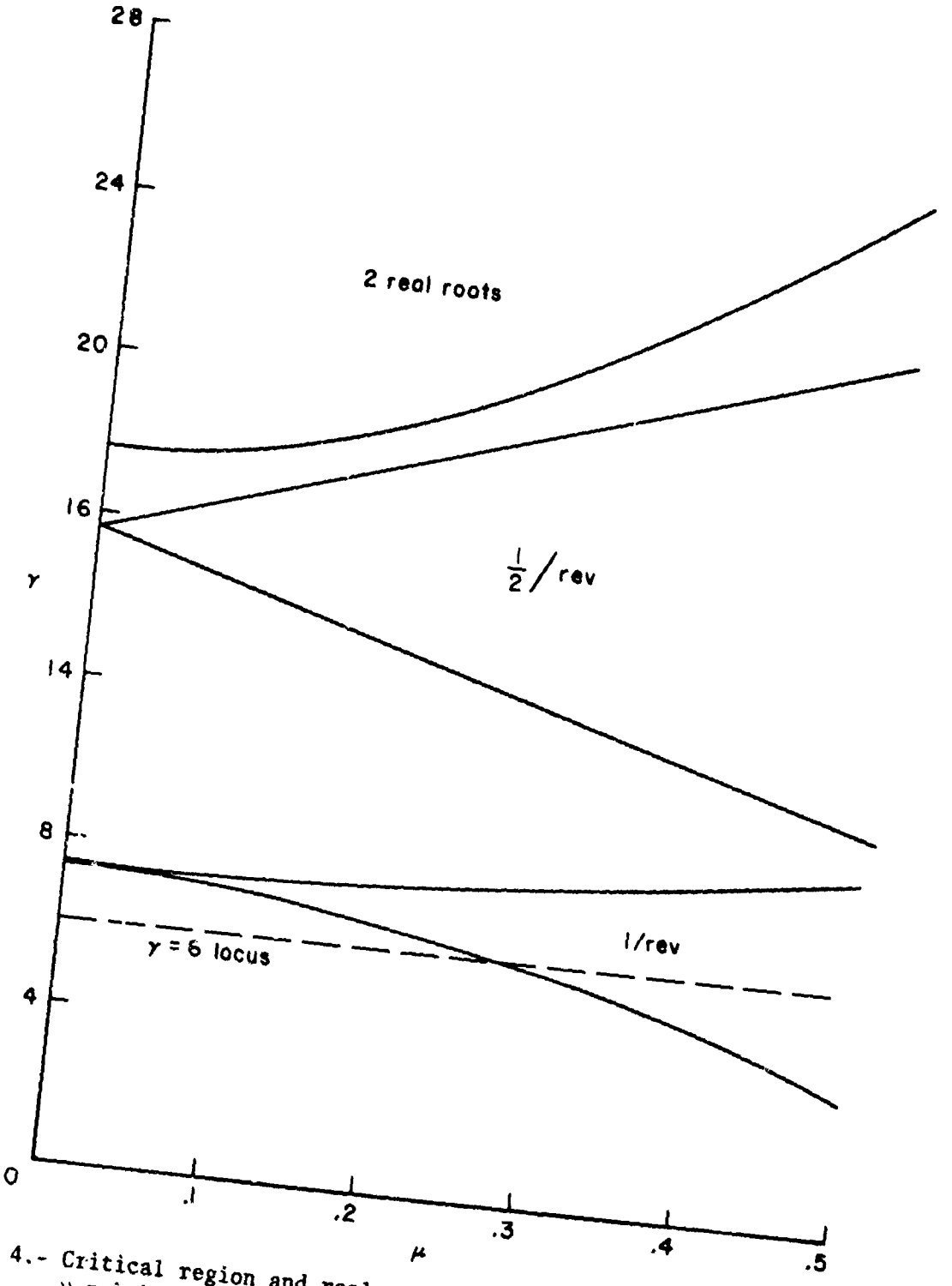

Figure 4.- Critical region and real root boundaries on the $\gamma - \mu$ plane for $\nu = 1.1$ and $K_p = 0$ (based on the perturbation solution).

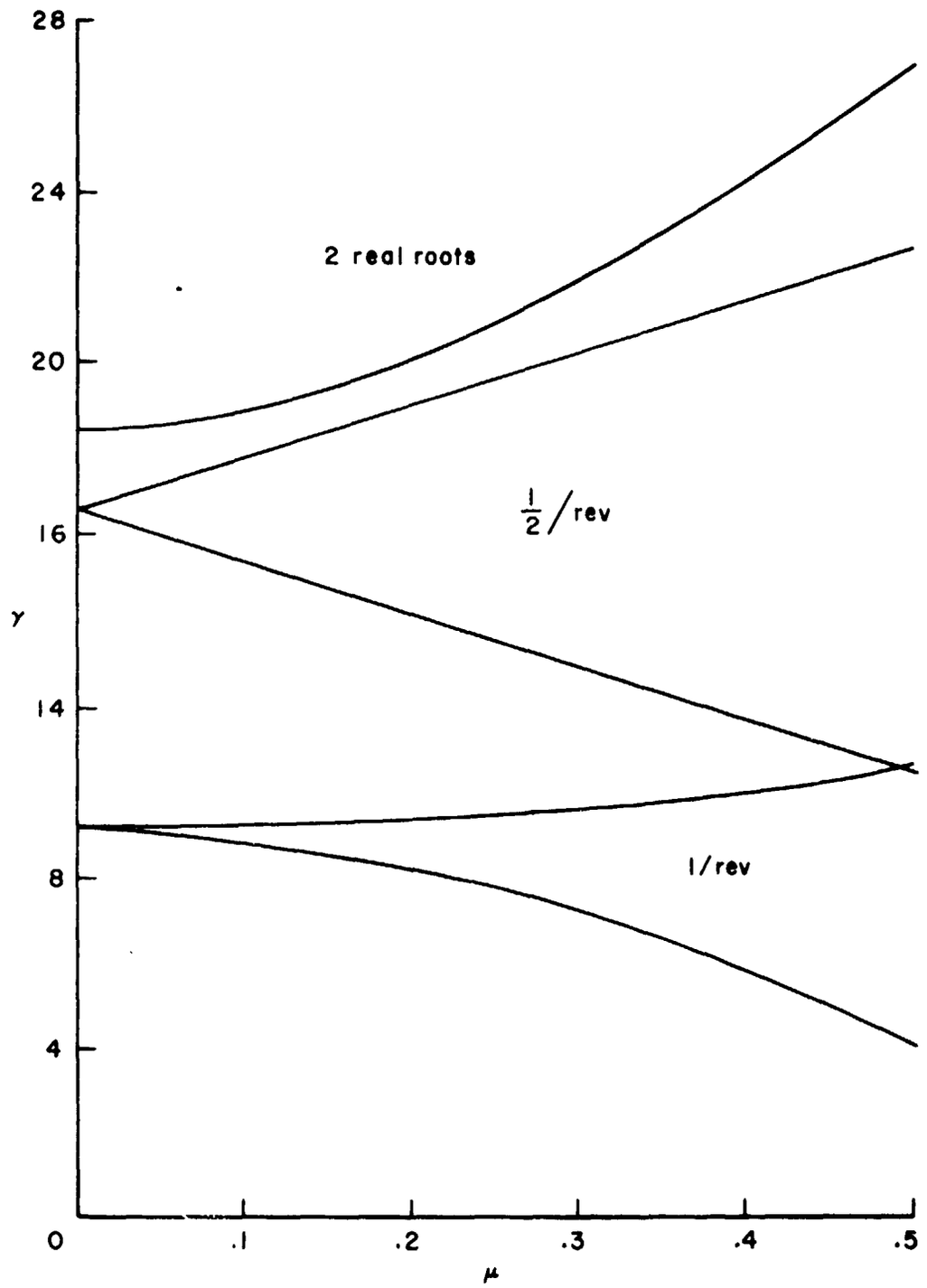

Figure 5.- Critical region and real root boundaries on the γ - μ plane for $\nu = 1.15$ and $K_p = 0$ (based on the perturbation solution).

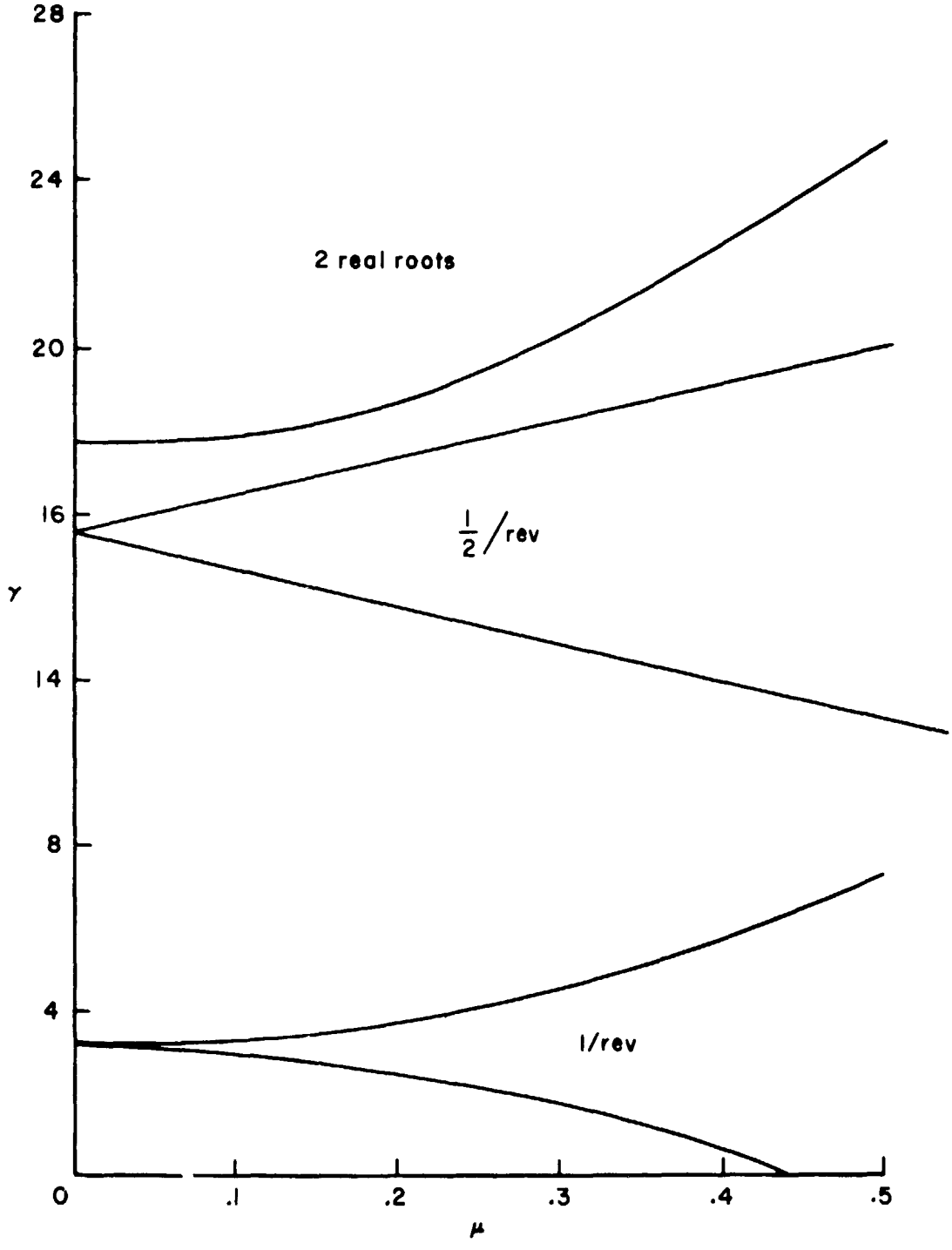

Figure 6.- Critical region and real root boundaries on the γ - μ plane for ν = 1 and Kp = 0.1 (based on the perturbation solution).

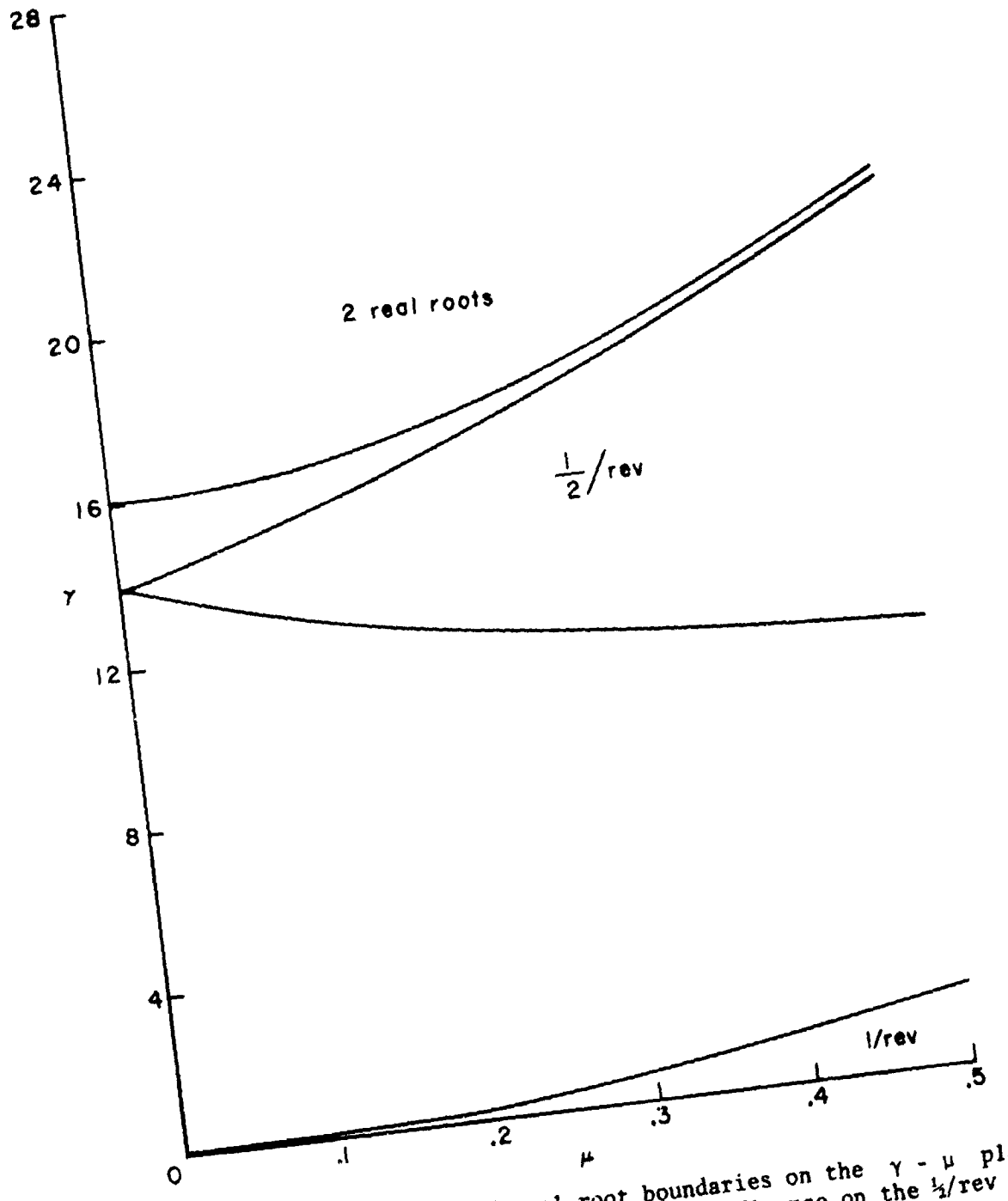

Figure 7.- Critical region and real root boundaries on the $\gamma - \mu$ plane for $\nu = 1$ and $Kp = 0$, including the order μ^2 influence on the ½/rev region boundary (from ref. 6).

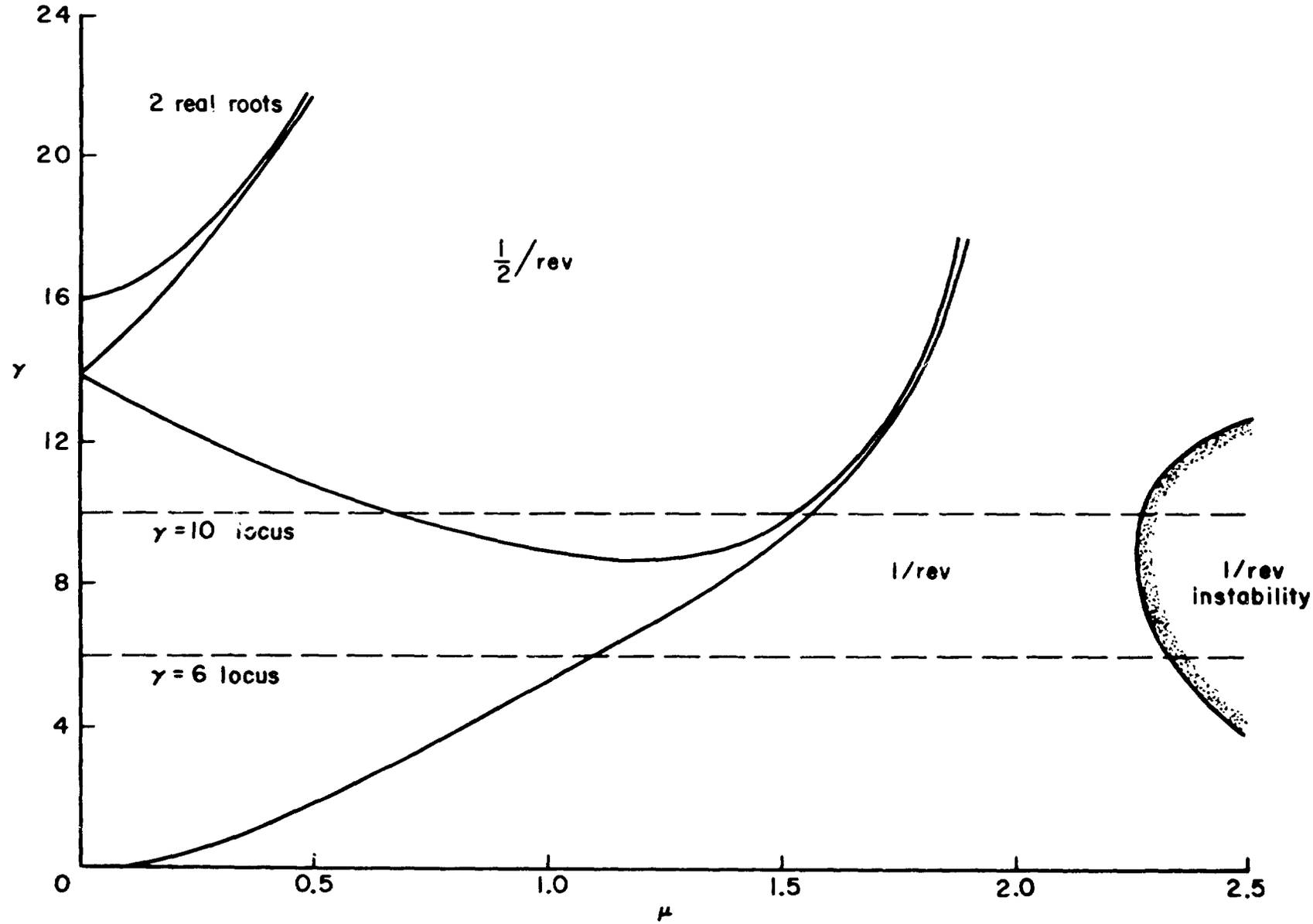

Figure 8.- Critical region, real root, and high μ instability boundaries on the γ - μ plane for $\nu = 1$ and $K_p = 0$, for μ = 0 to 2.5 (a composite plot based on the results of refs. 1 to 18).

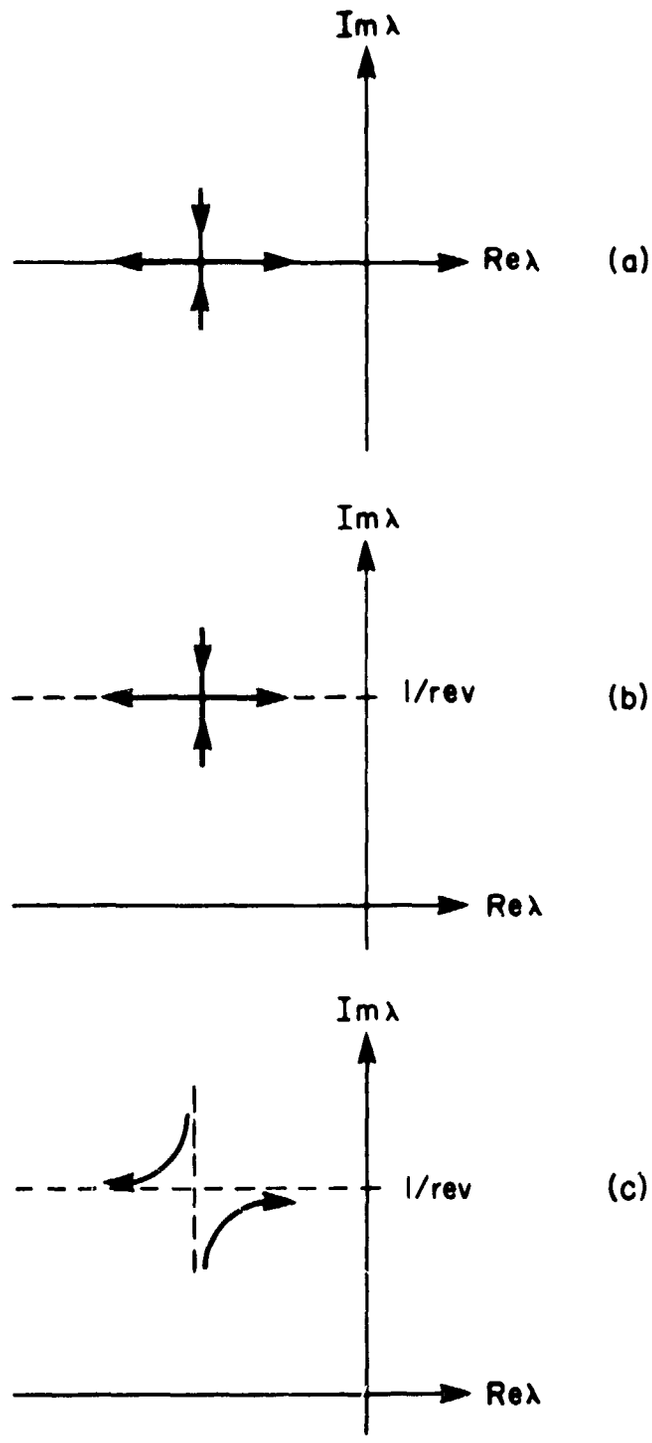

Figure 9.- Behavior of the γ root locus of the three-bladed gimballed rotor, near the two real root boundary. The three cases are discussed in the text.

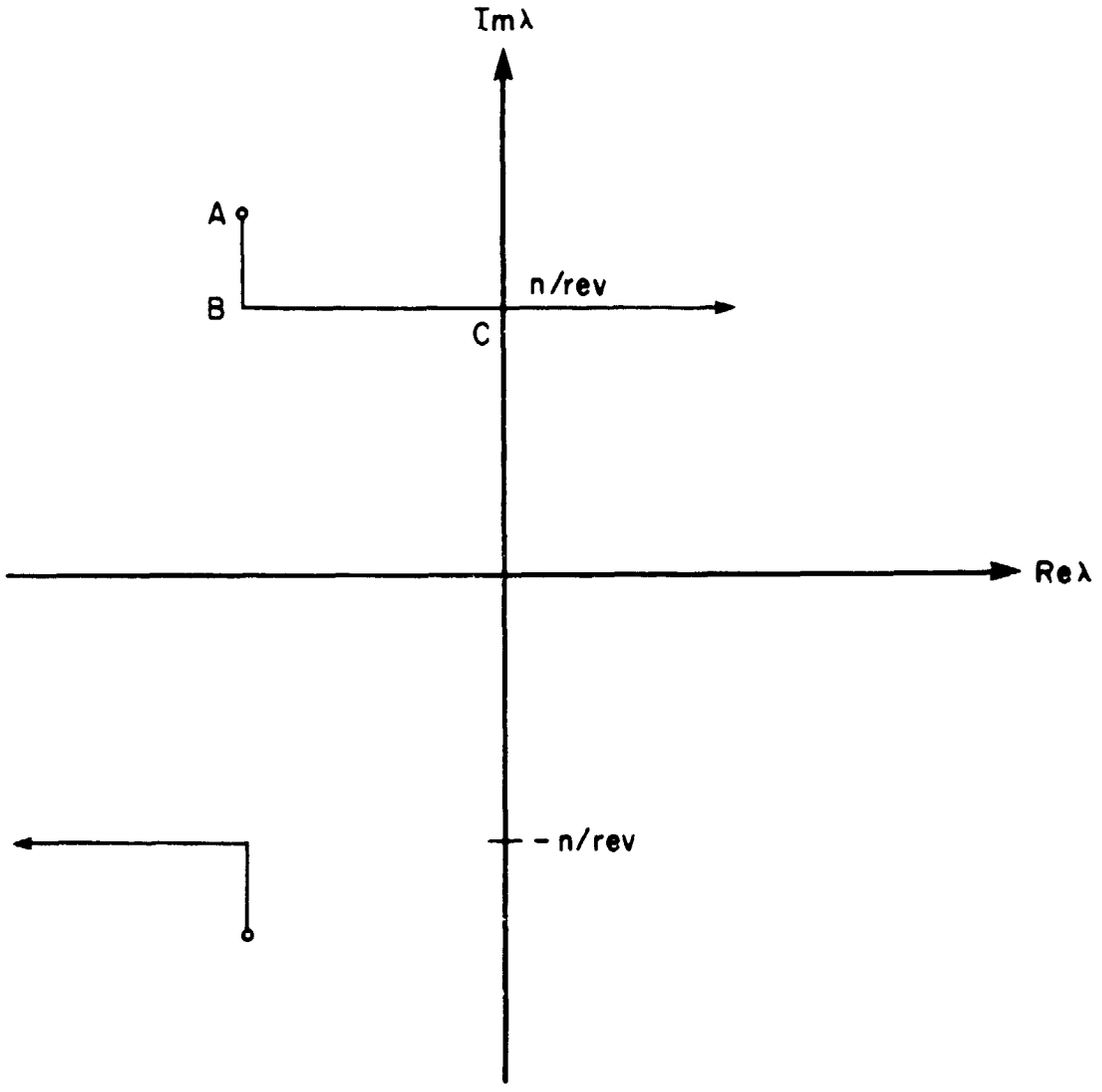

Figure 10.- Sketch of the characteristic behavior of root loci of periodic coefficient differential equations